Dissertation

Basic aspects of neuroinflammation

Submitted by

Arijit GHOSH,

for the Academic Degree of
Doctor of Philosophy
(Ph.D.)

at the

Medical University of Graz
Division of Endocrinology and Metabolism
Department of Internal Medicine

under the supervision of

Univ.-Prof. Dr. Thomas R PIEBER, M.D.

2014

Declaration

I hereby declare that this thesis is my original work and that I have fully acknowledged by name all of those individuals and organisations that have contributed to the research for this thesis. Due acknowledgement has been made in the text to all other materials used. Throughout this thesis and in all related publications I followed the guidelines of "Good Scientific Practice".

The cerebral open flow microperfusion (cOFM) probe used in this study was crafted and assembled in Joanneum Research GmbH, HEALTH – Institute for Biomedicine and Health Sciences. A patent regarding the cOFM technology is pending (PCT/EP2012/059192 "Catheter having a healing dummy").

Arijit Ghosh

Graz, 29th January 2014.

Acknowledgement

First and foremost, it is my great pleasure to express my gratitude and indebtedness towards my guide Prof. Thomas R. Pieber for his guidance and support for the successful completion of my Ph.D. dissertation. I am grateful to him for his encouragement throughout this project. I am really thankful to him for his valuable time to discuss the experimental plans and results of my research work. This thesis would never have been accomplished without Prof. Pieber's support and his passion to help Ph.D. students like me to go forward in my work.

I wish to express my sincere gratitude to Prof. Wolfgang Sattler and Prof. Andreas Zimmer for being the members of my Ph.D. thesis committee and for their timely and untimely help during my Ph.D. study. I would like to thank Prof. Sattler for his suggestions and comments, which helped me a lot to improve my work significantly.

I am grateful to Dr. Nandu Goswamy of Centre for Medical Physiology for his guidance and other mentors of Medical University of Graz for their help during my Ph.D. tenure.

I would like to thank Dipl.-Ing Thomas Birngruber for helping me from every possible facet throughout my stay in Austria in and out of laboratory. I am grateful to him for teaching me stereotaxic brain surgery on rat and many more things indispensable for the successful completion of my Ph.D. project. I am thankful for his valuable suggestions throughout my Ph.D. tenure. I would also like to thank him for his guidance and sparkling comments. I am glad that he always maintained positive attitude and persevered to bring the best out of me.

I am extremely thankful to Dr. Sonja Hochmeister for giving me time and for her valuable suggestions in histology study. I am grateful to Dr. Martin Asslaber and Prof. Gerald Höfler for giving me permission to work in the Institute of Pathology. I would like to thank Dr. Asslaber for his inputs in histology study.

I am thankful to Dr. Frank Sinner for his support and financial help during my extended Ph.D. tenure. I would like to thank Ms. Maria Ratzer, Ms. Agnes Prasch, Dr. Reingard Raml and the whole analytical team for providing supports, reagents and other necessary things. I am thankful to Ms. Alison Green and Ms. Selma Mautner for their help in paper

writing process and finalizing the manuscripts. I am grateful to Ms. Sophie Narath and Ms. Katharina Eberhard for their help in statistical analysis.

I am grateful to the whole staff at the animal care facility (Institute for Biomedical Research, Medical University of Graz, Austria) for providing proper animal care.

I would like to thank Prof. Andrea Olschewski, Prof. Barbara Obermayer-Pietsch and the entire faculty members of the Molecular Medicine Ph.D. programme for introducing me in this unique programme and helped to learn important aspects of medicine and natural sciences.

I shall always remain grateful to Ms. Karin Osibow and Ms. Claudia Sinner for helping in complicated administration process and for sending timely reminder for guest lectures and other important events in order to achieve credits required for successful completion of the degree. I am thankful to Ms. Karin Osibow for her help including arrangement of accommodation, guidance for VISA processes, organizing German classes for Ph.D. students and so on.

I would like to thank my entire group comprising of Barbara Prietl, Alexandra Harger, Mina Bashir, Katrin Kaineder, Rohksareh Rohban, Veronika Perez-Yarza, Günther Rauter, Brunhilde Bacher, Waltraud Schulter, Klug Ursula and other colleagues specially Thomas Kroath, Amra Ajsic and Mathias Tschaikner for providing me an excellent atmosphere to enjoy my work.

I am thankful to the Medical University of Graz and Zentrum für Grundlagenforschung (ZMF) for providing nice research atmosphere and friendly personnel for guiding and executing my research projects.

In this endeavour, I would like to thank my wife, my son and extend my deepest gratitude to my parents for their constant support and motivation. This thesis would never have been possible without their inspiration. Moreover, I would also like to thank the almighty for helping me.

Arijit Ghosh

TABLE OF CONTENTS.

Zusammenfassung

Die Entzündung des Gehringewebes ist eine schwerwiegende Krankheit, die normalerweise durch eine erhöhte Anzahl an proinflammatorischen Zytokinen im CNS, welche zu einer Änderung der Blut-Hirn Schranke als auch zu der Infiltration der Gehirnimmunzellen führen, charakterisiert ist. Studien haben gezeigt, dass die proinflammatorische Zytokine für eine ganze Reihe von Krankheiten, wie zum Beispiel Amyotrophe Lateralsklerose, Alzheimer-Krankheit, Multiple Sklerose, oder Parkinson-Krankheit, verantwortlich sind. Die Produktion der proinflammatorischen Zytokinen im Gehirn wird durch die Aktivierung der Mikroglia und der Astroglia ausgelöst. Diese Aktivierung wird wiederum durch verschiedene Stimuli wie Trauma, Toxine, Chemikalien, oder Pharmaka hervorgerufen und führt zu einer Entstehung von Narben im betroffenen Gehringewebe.

Um die Entzündungsprozesse im Gehirn beobachten zu können wurden bisher zahlreiche Methoden zur Verfolgung verschiedener chemischen Substanzen in der interzellularen Flüssigkeit des Gehirns entwickelt. Allerdings, sind die meisten dieser Methoden in ihrer Anwendung limitiert. Die Mikrodialyse, zum Beispiel, ist einer dieser Methoden die oft in medizinischen Studien und bei diagnostischen Patientenuntersuchungen eingesetzt wird. Auch diese Methode weist einige Nachteile auf: z. b. ist ihre Anwendungsdauer beschränkt, und auch die Größe der zu verfolgenden Moleküle ist ein limitierender Faktor. Außerdem, werden durch die Anwendung dieser Methode die schon erwähnten Narben im Gehirngewebe gebildet. Aus diesen Gründen haben wir eine innovative in vivo Technik, nämlich die, Cerebral Open Flow Microperfusion (cOFM) als eine Alternative zu der Mikrodialyse entwickelt. Die cOFM Sonde ist einzigartig da sie keine Membran benötigt und daher auch große Moleküle unabhängig ihres Molekulargewichtes und ihrer Lipophilität aus der interstitiellen Flüssigkeit des Gehirns entnehmen kann.

In dieser Studie verwendeten wir Albumin gebundenes Evans Blue, einen bekannten Marker mit großem Molekulargewicht der bei Permeabilitätsstudien eingesetzt wird, und zeigten, dass sich die BHS Integrität 11 Tage nach der cOFM-Sonden Implantation wieder erholt. Zusätzlich testeten wir die BHS Unversehrtheit während dem Sampling von interstitieller Hirnflüssigkeit mit dem niedermolekular-gewichtigem Marker

Natriumfluoreszein. Das Sampling wurde 15 Tage nach der Implantation der cOFM-Sonde begonnen und 5 Stunden lang durchgeführt. Es konnte gezeigt werden, dass sich die cOFM-Methode eignet um den Substanztransport über die intakte BHS zu messen. Zusätzlich konnte die Reaktion des Gewebes, das die cOFM-Sonde umgibt, beobachtet und evaluiert werden.

Kürzlich durchgeführte Mikrodialysestudien haben gezeigt, dass sich um eine implantierte Mikrodialyse-Sonde eine Narbe bildet. Diese Narbe stellt dann eine mechanische Barriere dar und reduziert im weiteren Verlauf die Effizienz der Sonde. Da der Hauptbestandteil von Narben im Gehirngewebe Mikroglia und Astroglia sind verwendeten wir Iba-1 und GFAP um diese beiden Zelltypen in dem Gewebe um die implantierte cOFM-Sonde zu detektieren.

Dabei fanden wir 15 Tage nach der Implantation eine signifikante Erhörung der Anzahl an Mikroglia Zellen in der näheren Umgebung der cOFM-Sonde. Diese Erhöhung ist wahrscheinlich auf das Implantationstrauma zurückzuführen. Weiteres konnte bei der 15-Tage Gruppe, im Gegensatz zur 30-Tage Gruppe, eine geringere Iba-1 Reaktion in der Umgebung der Sonde festgestellt werden. Die Ergebnisse der Gruppe, bei der die cOFM-Sonde nicht perfundiert wurde, wurden mit den Ergebnissen der Gruppe mit perfundierter cOFM-Sonde verglichen wodurch gezeigt werden konnte, dass wiederholtes Sampling auch in einem Tier möglich ist. Zusätzlich dazu entwickelte keines der Versuchstiere eine permanente Schicht GFAP positiver Hirnzellen um die cOFM-Sonde.

In einer anderen Studie untersuchten wir die Zeit abhängigen Änderungen der intrazerebralen Cytokin- (17-26 kDA) Konzentrationen wie auch die Änderungen der BHS Permeabilität.

Bei dieser Studie wurde ein LPS-induziertes Modell verwendet um systemischen Entzündungen in Verbindung mit Studien von Gehirnentzündungen zu untersuchen. Unsere Ergebnisse zeigten, dass das pro-inflammatorische cytokin TNF-aplpha eine wichtige Rolle bei der LPS induzierten Erhörung der BHS Permeabilität spielt was zu neuroinflammation führt. Daraus schlossen wir, dass cOFM angewendet werden kann um Substanzen mit großem Molekulargewicht, wie z.B. Signalproteine, aus der interstitiellen Hirnflüssigkeit zu entnehmen und zu detektieren.

Summary

Neuroinflammation is a devastating condition characterised by an increased level of pro-inflammatory cytokines in the CNS leading to an alteration of the blood-brain barrier (BBB) and an infiltration of the immune cells in the brain. Recently, it has been linked to many neurodegenerative diseases such as Amyotrophic lateral sclerosis, Alzheimer's disease, Multiple sclerosis and Parkinson's disease. The production of the pro-inflammatory cytokines in the brain is mainly caused by the activation of microglia and astroglia. The activation of the glial cells occurs in response to various stimuli such as trauma, toxins, chemicals and drugs.

So far, many techniques have been developed to track different chemical substances in the brain extracellular fluid with the purpose of monitoring disease processes such as brain inflammation, but their applications are mostly limited. For example, micro-dialysis is one of the techniques which are widely used in both experimental and clinical set-up. However, this particular technique has a number of drawbacks such as limited application time - it is also unsuitable for substances with a large molecular weight and causes glial scar formation. We, therefore, propose the cerebral Open Flow Microperfusion (cOFM), a novel in vivo technique, as an alternative to microdialysis. The design of the cOFM probe is unique in that it features no membrane and is, therefore, capable of recovering large molecules from the brain interstitial fluid regardless of the molecular weight and lipophilicity. In this present study, we utilized albumin bound Evans blue, a known large molecular weight marker used in permeability studies, and demonstrated that the BBB integrity re-establishes 11 d after the cOFM probe implantation. In addition, we also tested the BBB intactness during sampling of the brain interstitial fluid with a low molecular weight marker sodium fluorescein. We performed the sampling over a 5 h period 15 d after the implantation of the cOFM probe and showed that the cOFM is suitable for monitoring substance transport across the intact BBB. Here we also evaluated the tissue reaction surrounding the implanted cOFM probe.

Contemporary microdialysis studies have shown that a glial scar forms around the implanted microdialysis probe which then acts as a mechanical barrier and reduces probe efficiency over time. Since the main cellular components of glial scars are microglia and astroglia we used Iba-1 and GFAP to detect both cell types in the brain tissues surrounding the cOFM probe. On examination we found a significant increase in the number of microglia cells in the close vicinity of the cOFM probe track 15 d after the probe

implantation which was probably due to the implantation trauma. Furthermore, in contrast to the 15 d group, the 30 d group showed a minor Iba-1 reactivity surrounding the probe. The results obtained from the non-perfused group were comparable to those of the perfused group indicating that repeated sampling is possible in one individual animal. Moreover, none of the tested animals developed a continuous layer of GFAP positive glial cells surrounding the cOFM probe at any time point during the experiment.

In another study, we measured the time dependent changes in the intracerebral cytokine (17 – 26 kDa) concentration as well as changes in BBB permeability. Here we adopted a LPS induced model of systemic inflammation to study neuroinflammation. Our results showed that a pro-inflammatory cytokine TNF-alpha plays an important role in LPS induced increase in BBB permeability that results in neuroinflammation. Further, we demonstrated that the cOFM is suitable for detecting and recovering substances with a large molecular weight such as signalling proteins from the brain interstitial fluid.

Abbreviations

BBB	Blood-brain barrier
$CaCl_2$	Calcium chloride.
CNS	Central nervous system
cOFM	Cerebral Open Flow Microperfusion
EB	Evan's blue
ECF	Extra-cellular fluid
FEP	Fluorinated ethylene propylene
FMD	Fentanyl Midazolam Domitor
GFAP	Glial fibrilary acidic protein
Iba-1	Ionized calcium binding adaptor molecule 1
IL-6	Interleukin 6
IL-10	Interleukin 10
kDa	Kilo Dalton
KH_2PO_4	Potassium dihydrogen phosphate
LH	Left hemisphere
LPS	Lipopolysaccharide
MD	Microdialysis
$MgCl_2$	Magnesium chloride
mRNA	Messenger ribonucleic acid
NaCl	Sodium chloride
NaF	Sodium Fluorescein
Na_2HPO_4	Disodium hydrogen phosphate
OFM	Open Flow Microperfusion
PBS	Phosphate buffered saline

PD	Pharmacodynamics
PK	Pharmacokinetics
RH	Right hemisphere
ROI	Region of interest
TNFα	Tumour necrosis factor alpha

Introduction…

The concept of blood-brain barrier

Paul Ehrlich (14th March 1854 – 20th August 1915) was a german scientist, a Nobel laureate, had great interest in staining microscopic tissue structures since childhood. He kept the interest during his studies at the Universities of Wroclaw (Breslau), Strasbourg, Freiburg im Breisgau and Leipzig. During his experiments, Ehrlich reported all the organs were stained except brains and spinal cord after injection of water soluble dyes in the circulatory system of some animals (Ehrlich, 1885). He explained it as lack of affinity of nervous tissue to the dye (Ehrlich, 1904).

However, later in 1913, one of Ehrlich's students Edwin Goldmann direct injection of trypan blue into the cerebrospinal fluid stains the cells in brain but the stain failed to penetrate peripheral tissues (Goldmann, 1913). At that time, it was believed that some sort of compartmentalization exists between the body and brain of an animal and probably the blood vessels were responsible for the barrier. Lewandowsky was the first to coin the term "*bluthirnschranke"* (blood-brain barrier) while investigating the limited penetration of potassium ferrocyanate into the brain (Lewandowsky, 1900).

The concept of blood-brain barrier was termed as hematoencephalic barrier by Lina Stern in 1921. Although Goldmann's work indicated the existence of a physical barrier between the central nervous system and the peripheral circulation, indeed its existence was criticised in the 1960s. One of the major criticisms of Goldmann's experiment was the difference in composition of blood and Cerebrospinal fluid which influenced the diffusibility and affinity of dyes for nervous tissue. Therefore it was unsuitable to compare injections into the bloodstream with injections into the cerebrospinal fluid. The situation became more complicated when basic aniline dyes crossed the so called BBB and stained the brain, while acidic aniline dyes did not. Friedemann postulated substance with a positive or no charge are permeable to CNS capillaries at blood pH whereas substance with a negative charge are impermeable to them (Friedmann, 1942).

This hypothesis could not provide adequate explanation when the exchange rates for more solutes were measured between the blood and CNS (Tschirgi, 1962). Another controversy was whether BBB was formed only by the capillary endothelium cells and / or the glial limitans that ensheathe the capillaries or the basal lamina. The close contact of astrocytic

processes to capillaries certainly indicated that astrocytes were one of the major constituents involved in the BBB formation. Actually, a certain number of experiments were performed which also supported this fact (de Robertis et al., 1961). However, electron microscopy by Reese and Karnovsky (1967) at a resolution of 100,000X, could demonstrate a space between the capillary lumen and the end-feet/basal lamina and outer wall of the capillary. Furthermore, the presence of "tight junctions" was reported in the interendothelial cleft and it was proposed that the capillary lumen bridged by tight junction formed a continuous, impermeable barrier that constituted the primary component of the BBB (Reese et al., 1967).

Anatomical description of blood-brain barrier

The BBB works as a selective permeability barrier for substance transport. It is unique in structure due to the presence of tight junctions present between the brain endothelial cells, pericytes, basal lamina, astrocytes and neurons. Altogether form a neurovascular unit. The brain endothelial cells are different from the periphery in terms of mitochondrial content (Oldendorf et al., 1977), lack of fenestrations (Fenstermacher et al., 1988), low pinocytotic activity (Sedlakova et al., 1999) and the presence of tight junction (Kniesel et al., 2000). Pericytes are irregularly attached to the opposite side of the lumen of endothelial cells. Pericytes were divided into granular and filamentous subtypes (Tagami et al., 1990). Pericytes and endothelial cells are surrounded by the basal lamina (30 to 40-nm thick) composed of structural proteins, specialized proteins and proteoglycans (Farkas et al., 2001; Adibhatla et al., 2008; Wolburg et al., 2009). The basal lamina is indifferent with the plasma membranes of astrocytic processes, which surround the cerebral capillaries.

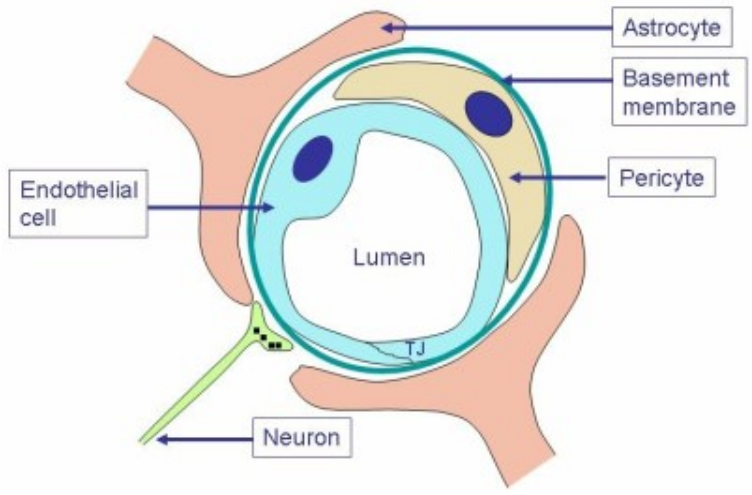

Fig. 1 – Diagrammatic representation of a cerebral capillary. Capillary lumen is surrounded by a single

endothelial cell and tight junction molecules seal the opposing membranes. Pericytes are attached to the abluminal side of the endothelial cells and these two cell types are surrounded by the basement membrane, which is continuous with the plasma membranes of astrocytic end feet (image taken from Google Image Search, originally from Laboratory of Molecular Neurobiology Brain Endothelial Research, BRC, Hungary).

Role of brain endothelial cells in BBB – Brain microvascular endothelial cells play the crucial role in the maintenance, stability and proper functioning of BBB. It is reported that brain microvascular endothelial cells are 50 to 100 times closer than periphery and restricts the diffusion of hydrophilic molecules (Abbott, 2002). The volume and number of mitochondria in brain endothelial cells are more, in order to generate more ATP for enzymes to break down compounds and to transport substances actively (de Boer et al., 2006). Further the surface of the brain endothelial cells is negatively charged that repulses compounds of same charge (Cardoso et al., 2006). Brain endothelial cells express adhesion molecules that attach them with the basal lamina and in turn influence tight junction molecules and BBB integrity. Brain endothelial cells expresses specific receptors and transporters that help in substance transport such as nutrients, hormones and actively regulate the concentration of ions, metabolites and xenobiotics in brain (Zhen, 2003; Weksler, 2005; Zlokovic, 2008).

Role of pericytes in BBB – Pericytes are also known as rouget cells after its discovery by a French scientist. They are present in the pre-capillary arterioles, capillaries and post-capillary venules (Dore-Duffy et al., 2008). The exact function and mechanism of pericytes involvement in BBB is not very clear. It is reported that pericytes synthesizes proteoglycans and laminal proteins (Cardoso et al., 2010). In addition, pericytes regulate BBB related gene expression pattern in brain endothelial cells and induces polarization of astrocytic processes surrounding brain blood vessels (Armulik et al., 2010).

Role of basal lamina in BBB – It is an important part of BBB. Basal lamina keeps the cells in position and provides mechanical stability. It is composed of different classes of molecules including Collagen, elastin, fibronectin, laminin, proteoglycans (Adibhatla et al., 2008; Wolburg et al., 2009). The basal lamina also contains cell adhesion molecules and signalling molecules which gives it a complex nature (Carvey et al., 2009). Disruption of basal lamina as witnessed in some pathological conditions, leading to alteration of cytoskeleton, affecting tight junction molecules associated with increased BBB permeability (Hawkins et al., 2005; Carvey et al., 2009; Zlokovic et al., 2008).

Role of astrocytes in BBB – Astrocytes are the most abundant cell types present in brain. They are identified by their typical star shaped appearance. Astrocytes are often called astroglia and also present in spinal cord. They are one of the major components for BBB formation. Astrocytic processes closely ensheath the brain blood vessels from the abluminal side of the endothelium (Abbott et al., 2002). It has been reported that astrocytes stimulate synthesis of proteoglycan and thereby helps in BBB function (Yamagata et al., 1997, Bernourd et al., 1998). The close proximity of astrocytes, neurons and blood vessels indicates an interrelationship for proper functioning of neurovascular unit (Persidsky et al., 2006). It is also reported that astrocytes can confer BBB like features in blood vessels those are lacking astrocytic foot processes (Abbott et al., 2002). It is reported that astrocytes maintain ion balance in extracellular space and signal to neurons through calcium dependent release of glutamate (Fiacco et al., 2009).

It is also claimed that astrocytes play a protective role in traumatic brain injury by sequestering the injured area with a scar formation (Kawano et al., 2012). During injury to the brain hematogenous cells such as red blood cells, leukocytes along with platelets enter the injured area in brain and the leukocytes start secreting cytokines, chemokines etc. These inflammatory substances in turn activate inflammatory reaction leading to inflammation, damage of neural tissues and activate residential microglia and astrocytes to form glial scar around the lesion and ultimately help in BBB re-establishment. It was also reported that leakage of fibrinogen in the brain after BBB breakdown induces astroglial scar formation by TGF-beta / Smad pathway (Schachtrup et al., 2010).

Role of neurons in BBB – The direct role of neurons in BBB development and / or maintenance is not very clear. However, neurones can modulate the function of blood vessels depending on the metabolic requirement (Persisdsky et al., 2006). The brain endothelial cells are also innervated by non-adrenergic, cholinergic, serotonergic and GABA neurons. Moreover, being a crucial component of neurovascular unit, neurons interact with other non-neuronal cells.

Transport of substances across blood-brain barrier and molecular involvement

The Blood-brain barrier (BBB) is a structural and functional unit helps in selective transport of substances present in plasma and restricts the passage of harmful constituents into the brain (Zlokovic et al., 2008). Transport of substances across BBB is tightly

regulated. There are basically two pathways: (1) paracellular and (2) transcellular. Paracellular pathway is guarded by the presence of a junctional complex comprises of tight junctions (Kniesel et al., 2000; Wolburg et al., 2002; Vorbrodt et al., 2003), adherens junctions (Schulze et al. 1993) and possibly gap junctions (Tao-Cheng et al., 1987; Braet et al., 2001; Kojima et al., 2003; Simard et al., 2003) to mediate intercellular communication. The transmembrane components of the tight junction consists of junctional adhesion molecule (JAM)-1 (Del Maschio et al., 1999), occludin, and claudins. JAM-1 has molecular weight of 40-kDa and a member of the IgG superfamily forms the early attachment of adjacent endothelial cell membranes (Dejana et al., 2000). JAM-2 and JAM-3 are other members of this group present in endothelial tissues and lymphatic cells (Bauer et al., 2004). JAMs are believed to regulate the transendothelial migration of leukocytes (Del Maschio et al., 1999) but their function in the mature BBB is still unclear.

Occludin is a 65-kDa integral protein of plasma membrane highly expressed in a distinct, continuous pattern along the cell membrane in cerebral endothelial cells (Lippoldt et al., 2000; Hawkins et al., 2004), while it is sporadically distributed in non-neuronal endothelial cells (Hirase et al., 1997). Being an integral protein, it passes four times the plasma membrane of the endothelial cells and the extracellular loops are thought to regulate paracellular permeability. Surprisingly, several knockout and knockdown experiments indicated occludin is not an essential component for the tight junction. Nevertheless, decreased expression of occludin is associated with compromised BBB function in several diseases (Bolton et al., 1998; Huber et al., 2002; Brown et al., 2005).

Claudins are the most important components of the tight junction and have similar membrane topography to occludin (Furuse et al., 1998). Claudins are small with a molecular weight of 20- to 24-kDa. At least 24 isoform of claudins have been identified in mammals (Bauer et al., 2004). All the isoforms have similar structural homology and folding among themselves (Heiskala et al., 2001). The N- terminal and C-terminal end remains towards cytosol and the extracellular loops of claudins show highest degree of conservation. They interact with each other by homophilic and heterophilic interactions (Furuse et al., 1999). It is hypothesized that the extracellular loops of claudins form the primary “seal” of the tight junction and occludin gives additional support. The expression pattern of claudins varies in different tissues. Claudin-1, -3, and -5 have been detected in the cerebral endothelium, whereas the expression of claudin-1 in cerebrovascular

endothelia has not yet confirmed (Morcos et al., 2001; Nitta et al., 2003; Witt et al., 2003; Wolburg et al., 2003; Hawkins et al., 2004).

In addition to the extracellular components of the tight junction, several accessory proteins are attached structurally and functionally with the transmembrane proteins in the cytosolic side. These include membrane-associated guanylate kinase-like (MAGUK) homolog family. MAGUK proteins are characterized by multiple postsynaptic density protein-95 / discs-large / ZO-1 binding domains, a Src homolog-3 domain, and a guanylate kinase-like domain. These domains allow multiple protein-protein interactions (Shin et al., 2000). MAGUK proteins seem to coordinate and form cluster of protein complexes in the establishment of specialized domains within the endothelial cell membrane (Gonzalez-Mariscal et al., 2000). So far, three MAGUK proteins have been identified: ZO-1, ZO-2, and ZO-3.

ZO-1 is associated with the tight junction (Stevenson et al., 1986). It has a molecular weight of 220-kDa and expressed in endothelial cells as well as in many other cell types those do not even possess tight junction (Howarth et al., 1992). It was reported, ZO-1 is also associated with adhesion junction (Itoh et al., 1993) and gap junction (Toyofuku et al., 1998) proteins. ZO-1 attaches transmembrane proteins of tight junction to the actin cytoskeleton (Fanning et al., 1998). This interaction is critical for the stability and function of the tight junction because dissociation of ZO-1 from the junctional complex is associated with increased BBB permeability (Abbruscato et al., 2002; Fischer et al., 2002; Mark et al., 2002).

ZO-2 is a 160-kDa phosphoprotein and strongly resembles with the amino acid sequences of ZO-1 (Gumbiner et al., 1991). The function of ZO-2 is not very clear; it appears to bind to the structural components of the tight junction and signaling molecules such as transcription factors (Betanzos et al., 2004). It is reported that ZO-2 localizes in the nucleus during stress condition (Islas et al., 2002; Traweger et al., 2002). ZO-3 is another homolog having molecular weight of 130-kDa has been found in association with tight junctions in some tissues. It has also been reported that accessory proteins such as cingulin, AF-6, and 7H6 are associated with BBB. Cingulin is a 140- to 160-kDa protein and associates with tight junction components (Citi et al., 1989). AF-6 is a 180-kDa protein containing two Ras-associated domains believed to reacts with ZO-1. The function of 7H6

protein is unknown but it has been found that 7H6 (155-kDa) reversibly dissociates from tight junction complex during ATP depletion (Zhong et al., 1994).

It is reported that adherens junction components are responsible to initiate and maintain cell to cell contact between endothelial cells (Stamatovic et al., 2008). Vascular endothelial cadherin is the main component of brain microvascular endothelial cells. The cytoplasmic component includes catenin protein family and p120 (Bezzoni et al., 2000; Nagafuchi, 2001). It was demonstrated that beta and gamma catenin helps cadherin to bind with alpha catenin which ultimately couple with the actin filaments of cytoskeleton. Recently catenin p120 has been discovered, although the function of the protein is not yet known but it is believed that p120 binds to vascular endothelial cadherin to regulate BBB permeability (Hatzfeld, 2005).

The transcellular pathway combines several modes of transport including passive diffusion, facilitated diffusion or carrier mediated endocytosis, simple diffusion through an aqueous channel and active transport. Astroglial limitans tightly ensheath the vessel wall in the brain and plays a major role in substance transport transcellularly and helps in maintenance of the blood brain barrier properties and function. Because of these properties, the BBB allows entry of small lipophilic molecules by passive diffusion. Compounds that are not lipid soluble such as glucose, several amino acids and nucleic acid precursors cross BBB via specific transporters called facilitated diffusion. The transporters work unidirectional (symport) and opposite direction (antiport). Members of facilitated diffusion include multidrug resistance proteins, P-glycoprotein and organic anion transporting polypeptides. These are expressed at brain capillary endothelial cells and / or astrocytic end feet that confer the unique permeability properties to the BBB. Most of these multidrug resistance proteins belong to the family of ATP-binding cassette transporters. P-glycoprotein is of particular interest because it has broad substrate specificity which includes a variety of structurally different drugs in clinical practice (Fromm, 2003; Lin, 2004; Sun et al., 2003). Furthermore, P-glycoprotein is expressed in tissues with excretory function, blood–brain barrier, blood–testis barrier and placenta. Therefore regulates drug entry and promoting drug elimination into bile and urine, and limiting drug penetration into sensitive organs like brain (Fromm, 2004; Lin, 2004). Apart from ATP-binding cassette transporters, different members of the organic anion transporting-polypeptide family and the organic anion transporter-family are expressed in the brain. It has been reported that

they play a significant role in drug efflux at the BBB and blood–CSF barrier (Gao et al., 2001; Lee et al., 2001; Kim et al., 2003; Sun et al., 2003; Hagenbuch et al., 2004). Organic anion transporters and organic anion transporting-polypeptides generally function as exchangers. The exact localization of most organic anion transporters and organic anion transporting-polypeptides in the brain is not very clear (Lee et al., 2001; Sun et al., 2003; Fricker et al., 2004).

Techniques used to monitor blood brain barrier functionality

Different techniques are available to monitor the alteration of blood-brain barrier functionality. These comprise of biopsy, push-pull perfusion, microelectrode arrays, magnetic resonance imaging (MRI), positron emission tomography (PET), magnetic resonance spectroscopy (MRS), and microdialysis.

Biopsy is a clinical test commonly performed by the surgeons involving extraction of cells and / or tissues for microscopical examination by a pathologist and / or chemical analysis. This technique is often used in experimental set up for research to study the structural and functional changes in brain which combines microscopical examination, chemical analysis, and genetic study. The major advantage of this technique is, a combinatorial approach can be adopted as well as the properties of substances for permeability study do not influence measurement and the results are quite reproducible. However, the technique is associated with potential drawbacks. It is an end-point technique or doesn't allow continuous monitoring of BBB function. It consumes a lot of animals to achieve the reproducibility. Further, in clinical set up, it is often associated with cognitive impairment in the subject.

Push pull perfusion was among the first techniques developed in 1960s for monitoring concentration of different neurotransmitters and chemical substances present in the extracellular fluid in brain. The technique has greatly abandoned due to high flow rate > 10 microliter / min which could result in greater extent of tissue damage near a push-pull sample region (Myres, 1986). With the invention of microdialysis in 1980s, push-pull perfusion gradually lost its popularity and applicability. It has gained its importance again in 2002 with the use of microfluidics and invention of miniaturized probes. Low-flow-push-pull perfusion was also reported to cause less tissue damage than other contemporary techniques (Kottegoda et al., 2002).

Microelectrode arrays are used to record neural signals from the brain. However, the use of microelectrodes is limited due to the materials used for their fabrication. Another major concern for using microelectrodes is unproven chronic biocompatibility (McCarthy et al., 2009).

Some studies utilized electrochemical sensors which provide information with a high temporal and spatial resolution but sensitivity often remains restricted to one neurochemical (Burmeister et al., 2001).

Magnetic resonance imaging (MRI), magnetic resonance spectroscopy (MRS), and computer tomography are cutting edge technologies available to find out abnormalities in the body but these techniques are very expensive in order to implement in experimental set up for research.

Microdialysis is a widely used and popular technique in neuroscience and pharmaceutical research (Stahl et al., 2002). It allows the investigator to monitor chemistry of different substances present in the extracellular fluid of brain and other organs (Helmy et al., 2007). However, the recovery of substances depends on the physiochemical properties of the target molecules (Bungay et al., 1990). Small hydrophilic molecules recovered more efficiently by microdialysis than higher molecular weight and hydrophobic substances. To resolve this issue, high molecular weight cut-off microdialysis membranes were introduced to improve the relative recovery of high molecular weight molecules such as signalling peptides. Use of large pore size microdialysis membrane caused loss of microdialysate in the interstitial space leading to low fluid recovery which ultimately influenced the surrounding tissue. To prevent fluid loss, colloids such as dextran, albumin was added in the preparation of microdialysate (Hillman et al., 2005) but addition of colloids potentially dehydrates the extracellular space. Moreover, microdialysis has certain limitations. **1**). It has limited timeframe for application (Hascup et al., 2009), **2**). Existing literatures suggest microdialysis over estimates substances because BBB re-establishment takes hours to days (König et al., 2001), **3**). High molecular weight, lipophilicity and polarity of a substance potentially diminish extraction capacity of microdialysis (Bungay et al., 1990), **4**). Recovery measurement decreases from hours to days (Rosenbloom et al., 2005; Rosenbloom et al., 2006), **5**). Biofouling associated with formation of trauma layer due to extensive reactive gliosis surrounding the microdialysis membrane acts like a mechanical

barrier between microdialysis membrane and healthy brain tissue (Wisniewski et al., 2001; Polikov et al., 2005; Winslow et al. 2012).

Tissue reactions induced by neural probes

Implantation of neural probe causes tissue damage and perturbs local blood flow due to physical damage to the blood vessels (Mitala et al. 2008; Morgan et al., 1996). On histological examination, these reactions appear as a core of activated microglia or macrophages along with fibroblast and meningeal cells and / or foreign body giant cells surrounded by reactive hypertrophied astroglia (Winslow et al., 2010). Several studies done over few decades have indicated that brain tissue reaction is influenced by several factors including probe design, chemical properties of probe materials, flexibility, fixation method etc. The influence of implant size on brain tissue reaction was specially addressed by stice et al. It was demonstrated that sizes of neural implants have minimal influence on brain tissue reaction after 2 weeks. However, larger size neural implants impart significant changes after 4 weeks (Stice et al., 2007). Another study focused on the chemical properties of neural probe material and brain tissue reactions (Stensaas et al., 1978). Implantation of stiff neural implants causes inflammation and more tissue damage near the implantation site (Karumbaiah et al., 2012). It was reported that the mismatch between neural probe and surrounding brain tissue is particularly responsible for the damage (Harris et al., 2011). The situation further aggravates, when the probes are transcranially implanted. It was demonstrated that transcranially implanted probes produce larger glial response than intraparenchymally implanted probes (Thelin et al., 2011; Seymour et al., 2007). A study demonstrated the span of reactive astroglia stained with GFAP was 500 – 600 μm after 2 weeks of silicon electrode implantation (Turner et al., 1999). Another group showed a denser sheath of GFAP+ astroglia formed by 6 weeks extending only 50 – 100 μm (Szarowski et al., 2003). Such a compact nature of the scar tissue hampers substance transport and increase resistance or impedance therefore influence the performance of implanted probes (Pollikov et al., 2005).

CHAPTER – I

cOFM: a new in vivo technique for continuous monitoring of substance transport across intact blood-brain barrier.

Introduction…

Brain is a specialised structure remains protected from outside by skull box and from inside by blood-brain barrier. The main function of BBB is to maintain the internal environment and restricts entry of harmful substances but it also impedes therapeutic substances from entering the brain (Pardridge, 2005; Miller, 2002). This special arrangement complicates the development of drugs that specifically target the brain. It has been shown that CNS-active drugs are under represented in spite of prevalence of CNS diseases (Upton, 2007; Pardridge, 2005). There is a need of methods that provide information on chemical and metabolic composition of fluids and tissues in the CNS. Since two decades microdialysis is extensively used in research but it features a membrane which diminishes the loss of perfusion fluid but excludes high molecular weight and lipophilic substances from analyses (Rosenbloom et al., 2005; Rosenbloom et al., 2006). To access the high molecular weight substances, large pore microdialysis membranes are introduced but it leads to fluid loss. Moreover, to prevent fluid loss, colloids such as dextran, albumin was added to the perfusate. Addition of colloids diminished fluid loss but dehydrate the extracellular space. Further, the microdialysis membrane is subject to occlusion due to cell process migration and protein deposition. The phenomenon is known as biofouling. It has also been reported that neural probes including microdialysis membrane produces astroglial scar surrounding the implanted probe (Benveniste 1987). The compact nature of the astroglial scar hinders transport of substances which ultimately responsible for the poor performance of the probe (Polikov et al., 2005). Studies performed to address these problems, suggested that although biofouling and tissue encapsulation by glial scar both contribute to the reduction of dialysis efficiency, the relative contribution of tissue encapsulation is likely to be greater (Stenken et al., 2010). It has been shown that formation of glial scar has 3 to 5 times more influence on substance transport than biofouling (Winslow et al., 2010). All probe based techniques are invasive procedures requiring probe implantation into the brain area of interest and are consecutively associated with implantation stress such as tissue damage and rupture of the BBB (Biran et al., 2005; Winslow et al., 2010). BBB rupture facilitates infiltration of erythrocytes, leucocytes and platelets from the blood, whereas rupture of meninges helps intrusion of fibroblastic cells (Berry et al., 1983; Maxwell et al., 1990). Perfusion probes such as microdialysis and push-pull cannula have additional stress factors caused by chemical composition of the perfusate and mechanical forces due to flow of perfusate (Meyers, 1986; Chefers et al., 2009).

Herein, we propose cerebral Open Flow Microperfusion (cOFM) for continuous monitoring of substance transport across intact BBB. cOFM is the latest development combining push-pull perfusion and Open Flow Microperfusion (OFM). OFM is a relatively new technique that has been utilised to assess organ specific pharmacokinetic and phamacodynamic study in the dermis (dOFM) and adipose tissues (aOFM). The main advantage of OFM is that it can be employed for sampling a wide range of substances including small ions, hydrophilic substances, lipophilic substances, antibodies and even entire cells (Holmgaard et al., 2012; Bodenlenz et al., 2012; Bodenlenz et al., 2005; Schaupp et al., 1999; Ellmerer et al., 1998; Trajanoski et al., 1997). In contrast to microdialysis, cOFM features no membrane, allows direct access to brain interstitial fluid and potentially eliminates limitations of microdialysis which arises from size, shape and lipophilicity. Moreover the sampling performance doesn't deteriorate over time, since there is no membrane occlusion and biofouling. BBB intactness can also be monitored in each animal and in each cOFM sample. cOFM is a minimally invasive probe based sampling technique. All materials used in the fabrication of cOFM probe are biologically inert in order to minimise adverse tissue reactions and glial scar formation. Moreover avoiding a membrane in cOFM probe design minimises adhesion of cells and substances on probe surface which ultimately decreases continuous irritations of surrounding brain tissues due to a rough or uneven surface of the probe (Dahlin et al., 2012; Scopelliti et al., 2010).

Aim…

Like all other invasive catheter techniques, implantation of cOFM probe causes trauma and rupture of blood vessels which ultimately leads to disruption of BBB. Two different markers are used in this study to assess BBB intactness. Albumin bound Evans blue (Mol. Wt. ~ 67 kDa) was used to follow the course and extent of BBB leakage after cOFM probe implantation over a period of 15 days. Sodium Fluorescein (Mol wt ~ 376 Da) was used to detect variability in BBB intactness during continuous measurement. The purpose of the present study is: (i) to determine the duration of BBB re-establishment after cOFM probe implantation, (ii) to demonstrate the ability of cOFM technique to sample interstitial fluid of brain tissue with intact BBB.

Moreover, we aimed: (iii) to evaluate the effect of the materials and design used in cOFM probe for long term implantation in respect to brain tissue reaction. We compared the histology of brain tissue surrounding the cOFM probe with native frontal lobe tissue of the contralateral hemisphere and (iv) studied the effects of probe perfusion.

Materials and Methods…

Experiment – 1: Re-establishment of BBB after cOFM probe implantation.

1.1. Animals

The study was approved by the Austrian Ministry for Science and Research Ref II / 10b Vienna (Permit Number: BMWF-66.010/0003-0024II/3b/2011). A total of 34 adult male Sprague Dawley rats (Harlan Laboratories, Udine, Italy) weighing approximately 250 – 400 g were used for the study. The animals were housed in a 12 h light / dark cycle with food and water being available ad libitum. Animals were allowed at least 1 week to acclimatize to the environment prior to any surgical procedure. Appropriate animal care such as cleaning of cage, bedding etc. was provided by the resource staffs at the animal care facility centre (Institute for Biomedical Research, Medical University of Graz). There were no procedures involving undue discomfort to the animal.

1.2. cOFM Probe

The cOFM probe consists of a 20 Ga guide tubing (Perfluorethylenpropylen –FEP) and two 25 Ga inflow/outflow tubing with a low adhesion surface (Polytetrafluorethylen-PTFE). In this experiment, during the healing period a healing dummy made of stainless steel was placed in the guide tube to allow tissue regeneration and prevent tissue migration into guide tube (Fig.2).

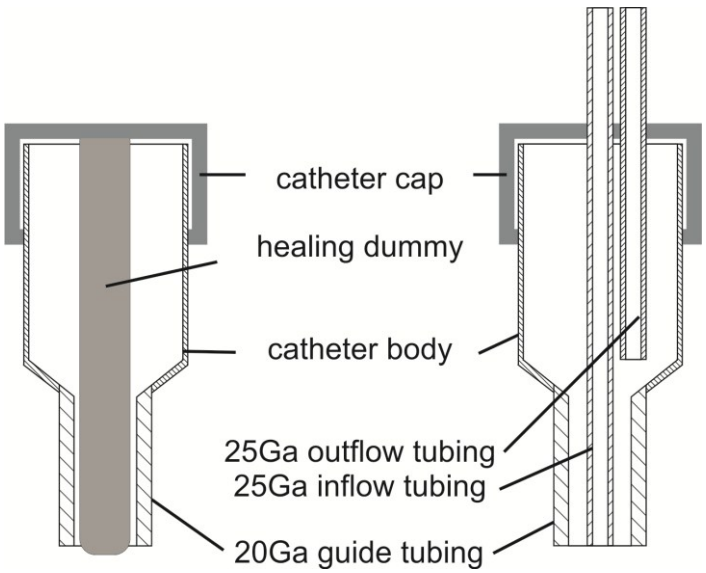

Fig. 2 – Diagrammatic representation of cOFM probe with healing dummy (left) and inflow-outflow tubing (right).

1.3. Surgery

For cOFM probe implantation, the rats were anaesthetised with a combination (2:2:1) of Fentanyl (0.05 mg/ml; Janssen-Cilag Pharma), Midazolam (5 mg/ml; Janssen-Cilag Pharma) and Domitor (0.1 mg/ml, Pfizer Corporation, Austria) (0.15 ml/100 g of body weight) and prepared for surgery by shaving the head and placed in a stereotaxic frame (KOPF Instruments, USA). The surgical area of the scalp was disinfected using 70% ethanol and a 2 cm midline incision was made to expose the skull. Thereafter, the tissue attached to the skull was removed with the help of a scalpel and bleeding was stopped holding gauze against the skull bone with gentle pressure. Then, a fine hole (1 mm) was made 2 mm lateral to the bregma on the left side with the help of a drill machnine to expose the dura mater. The dura mater was pricked cautiously with the help of a sharp head forceps. The cOFM probe (with healing dummy) was inserted slowly into the left frontal lobe to a depth of 2 mm. cOFM probe was fixed to the skull bone with 2 anchor screws and dental cement (iCEM Self Adhesive; Heraeus).

After surgery, the animals received a mixture of Anexate (0.1 mg/ml; Roche Austria GmbH) and Antisedan (0.5 mg/ml; Pfizer Corporation, Austria) (5: 0.5, same as the volume used for anaesthesia) serves as an antidote. Subsequently the animals received subcutaneous injection of Cefotaxim 5 mg/100 g (Sanofi-aventis GmbH, Wien) and Rimadyl 0.5 mg in 0.5 ml normal saline (carprofen 50 mg/ml; Pfizer Corporation, Austria) and continued for 2 more days after surgery. The surgical procedure was completed within 30 min after initial induction with Isoflurane for each rat. Following surgery, rats were individually housed in specially designed cages under same conditions.

1.4. Preparation of Albumin bound Evans Blue (EB)

10 mg of Evans Blue was mixed with albumin solution (7 ml Albunorm 200 g/L; Octapharma, Austria) and the final volume was made 10 ml with 3 ml saline (0.9 M NaCl; Fresenius Kabi, Austria). The solution was incubated overnight at room temperature for efficient binding. Thereafter the solution was stored at 2° - 8° C. From the final solution 1 ml was injected to each rat for the experiments. Before injection, the solution was brought down to room temperature.

1.5. Determination of re-establishment of BBB for high molecular weight substance with albumin bound evans blue (EB)

BBB permeability was assessed by albumin bound EB fluorescence intensity measurement in intact brain tissue. EB do not cross intact blood-brain barrier but stains brain tissues when BBB is compromised after cOFM probe implantation. EB solution was injected i.v. (tail vein) at different time points (5, 7, 9, 11, 15 days) after cOFM probe implantation. Two hours after EB injection (1 mg of EB) blood was flushed from brain vessels via transcardial perfusion with phosphate buffered saline (50 mmHg for 15 min) so that only EB that crossed the BBB remained in brain tissue. To determine the extent of EB staining, whole brains were extracted and the tissue was fixed in 4% paraformaldehyde. EB fluorescence was measured with Maestro™ In-vivo Imaging System (CRI) and images were analyzed with Image J software.

Thirty four rats were divided in three groups as follows: 6 rats were implanted cOFM probe but nothing was injected and considered as negative control, 6 rats were implanted cOFM probe and EB solution was injected immediately considered as positive control, the rest of the rats were implanted cOFM probe and EB solution was injected at different time point from 5 – 15 days. Two rats each were used for 5 and 7 days healing period and 6 rats each were used for 9, 11 and 15 days.

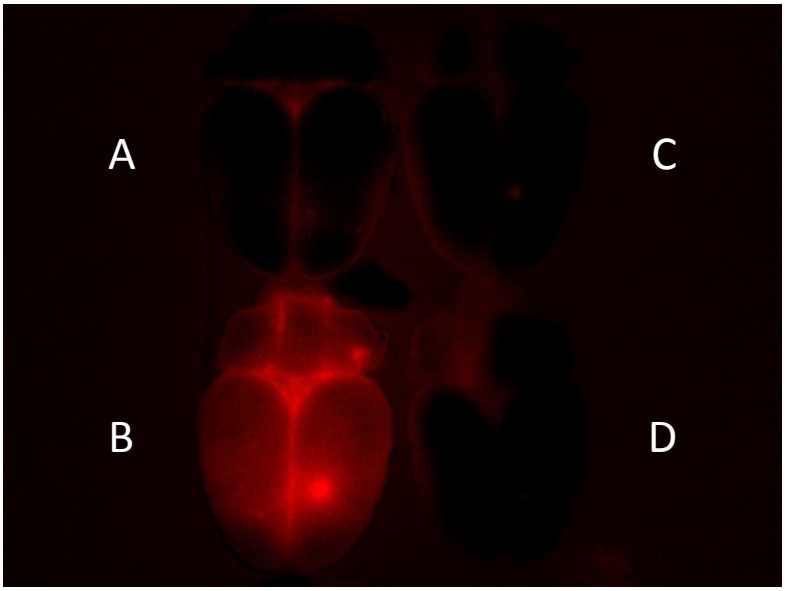

Fig. 3 – Representation of rat brains in Maestro Imaging Chamber. A and B represents negative and positive control respectively. C and D represents the test group after different healing period.

Spectral fluorescence images were obtained using the Maestro™ In-vivo Imaging System (CRI) with appropriate filters for EB (excitation = 445-490 nm, emission = 515 nm). In order to monitor measurement accuracy two test samples were always compared with negative and positive control (Fig.3). Images were analyzed with Image J (Abramoff et al., 2004) by comparing a ROI (circular; ø 2.5 mm) around the probe position from different groups.

1.6. Statistical Analysis

The two-sample Wilcoxon rank test was used to examine the differences in mean EB fluorescence values between the test group and the negative control group. Statistical analyses were performed with R version 2.13.1 and differences were considered significantly different at $p < 0.05$.

Experiment – 2: Testing BBB intactness during cOFM sampling procedures

2.1. Reagents used

All reagents were purchased from Sigma Aldrich, Austria (purity ≥ 99%) unless stated otherwise.

- Standard cOFM perfusate: cOFM standard perfusate was composed to match brain extracellular fluid in order to avoid chemical stress for the BBB (modified following McNay et al., 2004). Perfusate composition: NaCl 123 mM, $MgCl_2$ 0.4 mM (purity ≥ 98%), $CaCl_2$ 0.7 mM (purity ≥ 93%), KCl 4.3 mM, NaH_2PO_4 1.3 mM, Na_2HPO_4 21 mM, Glucose 4 mM. All reagents were dissolved in sterile water (Aqua bidest, Fresenius Kabi, Austria). In order to remove possible bacterial contamination the perfusate was filtered through a 0.22 µm sterile filter (Thermo Fisher Scientific, Germany). All steps were carried out under sterile conditions.

- cOFM perfusate with hyperosmolar mannitol: cOFM perfusate with hyperosmolar mannitol was prepared as for standard cOFM perfusate except that glucose was exchanged with 1000 mM mannitol (purity ≥ 98%).

- Sodium Fluorescein (NaF): NaF marker was prepared by dissolving NaF (7.5 mg) in saline (1 ml; 0.9 M, Fresenius Kabi, Austria).

- Phosphate buffered saline (PBS): Na_2HPO_4 x $2H_20$ 151.29 mg, KH_2PO_4 20.41 mg, NaCl 850 mg dissolved in 100 ml deionized water. PBS was sterilized at 120 °C, 30 min; pH 7.2 – 7.3.

2.2. cOFM probe implantation

Rats were anaesthetized with a mixture of Fentanyl, Midazolam and Domitor and a cOFM dummy probe was implanted in the left frontal lobe following the same procedure as mentioned in section 1.3.

2.3. cOFM working principle

The cOFM probe was implanted into the frontal lobe of the left hemisphere. The probe consists of the probe body with a 20 Ga guide cannula that extends into brain tissue and a probe cap to fix the two cartridge elements:

- The healing dummy provides mechanical stability during probe insertion allows tissue regeneration and prevents tissue migration into guide tube (Fig.4).
- The inflow/outflow tubing was exchanged with the healing dummy before sampling; and perfusion fluid was then pushed into brain tissue and withdrawn at the same flow rate.

The outflow and the inflow tubing were connected to a Hamilton syringe and 1 ml standard syringe (BBraun, Austria) respectively. Both were operated with a syringe pump (Aladdin, World Precision Instruments, Germany) at a flow rate of 1 µl/min. The inflow and the guide tube were arranged concentrically to provide a constant flow through the cOFM probe with minimal geometric dimensions.

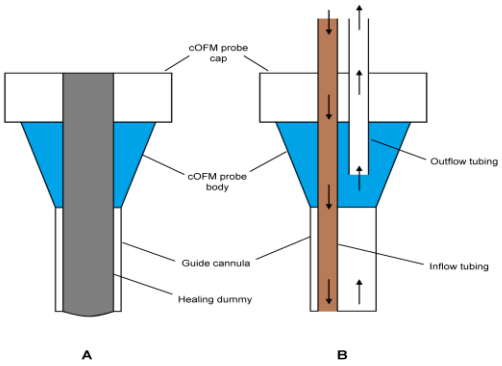

Fig. 4 – Schematic drawing of cOFM probe.

The functional principle of cOFM is depicted in Fig 5. Pump1 push perfusate (1) through the cOFM probe (2), implanted in the frontal lobe of the left hemisphere of a rat brain (3). At the tip of the probe (4) there is exchange between interstitial fluid and perfusate. The resulting mixture of fluids (5) is withdrawn by pump 2 and collected at regular intervals in vials (6).

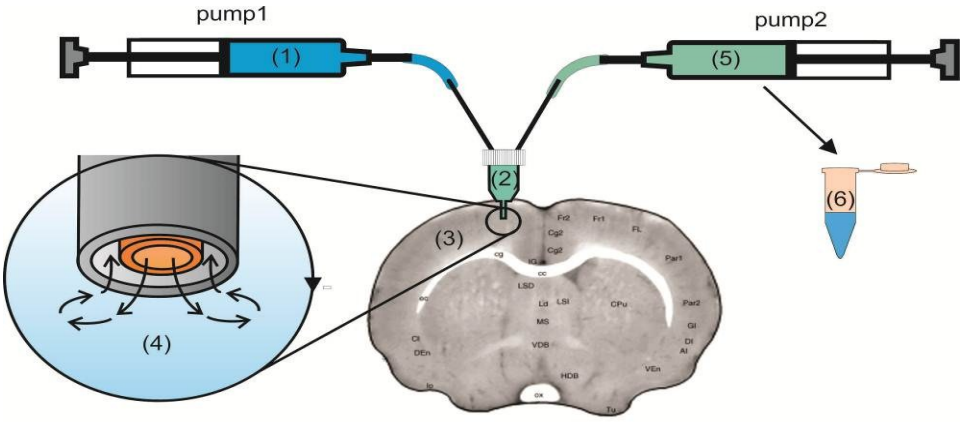

Fig. 5 – cOFM working principle.

2.4. Experimental conditions

A total of 24 rats were divided in four groups. **Group 1** (n = 6) served as a naïve control group without cOFM probe implantation. BBB was intact in both hemispheres. Brain tissue and plasma samples were taken after 1 hour of NaF injection. In **group 2** (n = 6), cOFM dummy probe was implanted and 15 days later brain biopsies and plasma samples were taken after 1 hour of NaF injection. **Group 3** (n = 6) rats were implanted with cOFM dummy probe and after 15 days, on the day of sampling, healing dummy was exchanged with inflow/outflow tubing or measuring unit to allow sampling. Sampling was done with standard cOFM perfusate and started after two and half hours of stabilization period (time after dummy exchange) and hourly sample collection was continued for 5 hours (Fig.6). In **group 4** (n = 6), the same protocol was followed as in group 3 with an exception of perfusate. In group 4, hyperosmolar mannitol solution was used instead of standard cOFM perfusate. During sampling, subjects were anesthetized with inhaled isoflurane (1 % in 0.5 l/min oxygen, Abbott, Canada). A bolus injection of NaF (11 mg/kg in physiological saline) was administered intravenously to all groups. For groups 3 and 4 the bolus was followed by a constant infusion of NaF (11 mg/kg/h in physiological saline) to maintain a steady NaF concentration in the blood.

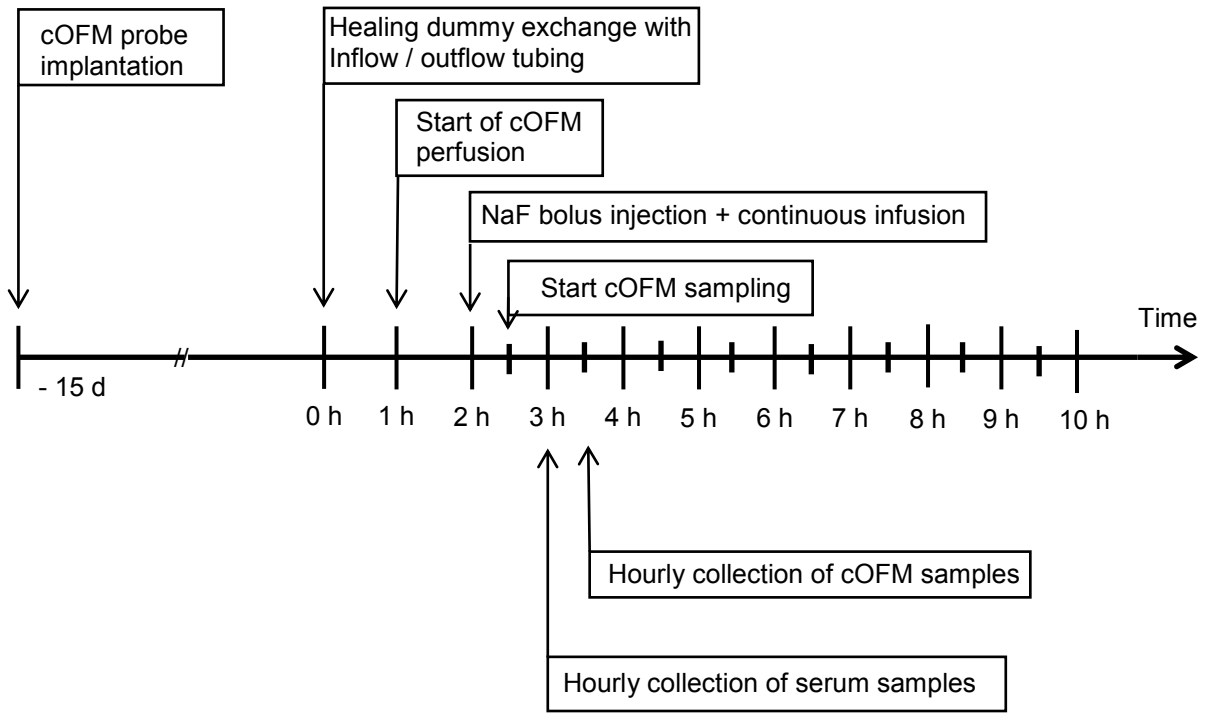

Fig. 6 – Schematic representation of sampling procedure followed for group 3 and 4.

In all groups, brain tissue biopsies 2 mm lateral to the bregma on the left and right hemisphere were taken after 2 min. of transcardial perfusion with PBS. A schematic drawing of the biopsies taken is shown in Fig. 7.

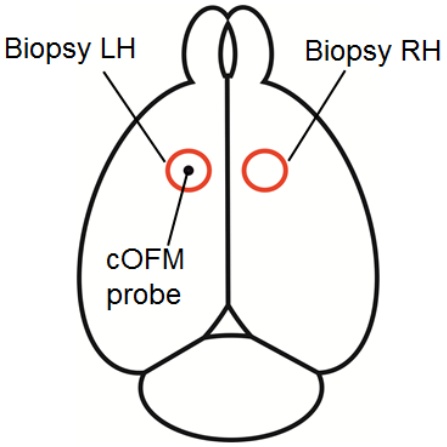

Fig. 7 – Localization of biopsies in rat left and right hemispheres.

2.5. Analytical method

Three different types of samples (cOFM, plasma and brain tissue) were analyzed for NaF.

Sample pretreatment: Protein precipitation was performed for cOFM and plasma samples, whereby 25 µl of sample was mixed with 25 µl of acetonitrile at room temperature. For brain tissue, samples were homogenized in Tris buffer (20 mM containing 1 % Triton X-100, pH 7.4; 2 µl Tris buffer / mg brain tissue) by using a mortar and pestle. After centrifugation (all samples; 5 min at 2,000 g) the supernatant was transferred into a 384-well plate.

NaF analysis: NaF concentration was determined by using a fluorescence microplate reader (Fluostar Optima, BMG labtech, Germany). Detailed information about system settings and linearity ranges are shown in Table 1.

Table 1: Sodium fluorescein system settings and linearity ranges**.**

	System characteristics
detection mode	fluorescence intensity
measurement mode	endpoint, bottom reading
excitation filter	485 nm
emission filter	520 nm
gain setting	95% of highest standard
linearity for cOFM samples (LLOQ – ULOQ)	2.1 – 1,000 ng/ml
linearity for plasma samples (LLOQ – ULOQ)	205 – 100,000 ng/ml
linearity for brain tissue (LLOQ – ULOQ)	4.1 – 1,000 ng/ml

2.6. Statistical analyses

The Kruskal-Wallis rank sum test was performed to compare NaF ratios of left hemisphere (LH) to right hemisphere (RH) in the brain biopsy analysis. The Kruskal-Wallis rank sum test was also used to analyze time and group effects between group 3 (standard perfusate) and group 4 (mannitol), after which a two sided t-test was performed to examine significant differences in Naf concentration between groups at each time point. All statistical analyses were performed with R version 2.13.1, and with the statistical significance set at $p < 0.05$.

Experiment – 3: Histological study of cOFM probe implantation and probe perfusion in surrounding brain tissues.

3.1. Experimental conditions

Animals (n = 36) were divided into three groups with different durations between probe implantation and brain extraction: 3 days (n = 6), 15 days (n = 24) and 30 days (n = 6). Each of the three groups was subdivided evenly into a perfused and a non-perfused group. The perfusion was carried out for 2 hours at days 1, 11 and 15 after cOFM probe implantation and rats were euthanized on days 3, 15 and 30 respectively in order to characterise and compare the morphological changes between perfused and non-perfused animals. In this present experiment, the perfusion session was performed only for 2 h to imitate the experiments of substance measurement by cerebral open flow microperfusion. Existing literature suggest significant morphological changes occur after 3 days and 1 week following microdialysis and ceramic microelectrode arrays (MEAs) implantation (Hascup et al., 2009).

3.2. Surgery and implantation of cOFM probe

cOFM probes were implanted unilaterally in the left frontal lobe of each rat. The surgical procedure was described in detail in section 1.3. For perfusion study, perfusion was carried out for 2 hours at days 1, 11 and 15 after cOFM probe implantation. At the start of the experiment, animals were anaesthetised with Isoflurane (5%) and then anaesthesia was maintained at a very low dose of Isoflurane (1%) for 2 hours. The dummy was replaced with a measuring unit connected with two pumps (Model No.: Aladdin 1000, World Precision Instruments, Sarasota Florida, USA). One pump was engaged to push the artificial brain extracellular fluid at a constant speed of 1 µl/min through the inner tubing, whereas the other was engaged to withdraw the fluid at the same speed (after fluidic exchange with brain ECF) through the outer tubing of the measuring unit. After perfusion, each rat received a subcutaneous injection of cefotaxim (5 mg / 100 g of body weight) and continued for 2 more days in order to prevent any possible infection. These mock measurement sessions were performed to imitate the experiments of monitoring substance transport across BBB by cOFM and to compare the morphological changes between non-perfused and perfused group.

3.3. Histological verification of cOFM probe incision site

On completion of the respective experimentation schedule, each group of rats were deeply anaesthetised with a double dose of FMD injected subcutaneously. The animals were then transcardially perfused with PBS for 20 min. to remove intravascular blood volume in order to avoid unnecessary bleeding during cOFM probe extraction. The cOFM probes were carefully removed and thereafter processed and checked for any adherent tissues with scanning electron microscopy (Fig. 10). Then the skull was opened and the brains were removed and post-fixed in 4% para-formaldehyde overnight. On the following day the tissue was further processed and routinely embedded in paraffin as per standard protocols. Thin coronal sections (4 μm) were made serially throughout the cOFM lesion and at least 5 sections (100 μm apart from each other) were stained with haematoxylin and eosin following standard protocol for gross histological examination.

3.4. Immunohistochemistry

Immunohistochemistry was performed on formalin-fixed, paraffin-embedded tissue sections. Two adjacent slides each were selected for Iba-1 and GFAP staining. Slides for Iba-1 were deparaffinised at 60º C for 30 min and the sections were stained following standard protocol on a Leica Bond^{TM} Max autostainer (Leica Biosystems, Melbourne, Australia). Antigen retrieval was performed with ER1 for 10 min (solution provided by the manufacturer for epitope retrieval). Iba-1 antibody (Cat No.: ab 15690, Abcam, Austria) was used at a concentration of 1:2000 diluted in Bond Primary Antibody (Leica, AR9352). The detection kit used was the Bond^{TM} Polymer Refine Detection (DS9800). For GFAP staining, slides were incubated at 70º C for 1 h and sections were stained following standard technique on a Ventana Benchmark ULTRA autostainer (Ventana Medical Systems, USA). Antigen retrieval was performed with CC1 for 30 min (solution provided by the manufacturer for epitope retrieval). The concentration of GFAP antibody (Cat No.: 258R-24, Cell Marque, USA) was 1:500. For visualization, ultra view Universal DAB Detection Kit (Cat. No.: 760-500, Roche Diagnostics GmbH) was used.

As a positive control for immunohistochemistry, microdialysis membrane was intraparenchymally implanted in the frontl cortex of rats. 15 days following probe implantation, animals were sacrificed and the brains were carefully taken out with the microdialysis membrane inside and fixed in 4% para-formaldehyde overnight. Then the

brain tissue was processed as described earlier and 4 µm sections were cut. Afterwards, the sections were stained for micoglia and astroglia (Fig. 8).

(Standardization of Iba-1 antibody was done by me in the Institute of Pathology. The Leica Bond™ Max autostainer and the Ventana Benchmark ULTRA autostainer were run by Sylvia Schauer and Margit Gogg-Kamerer respectively in Pathology, Medical University of Graz).

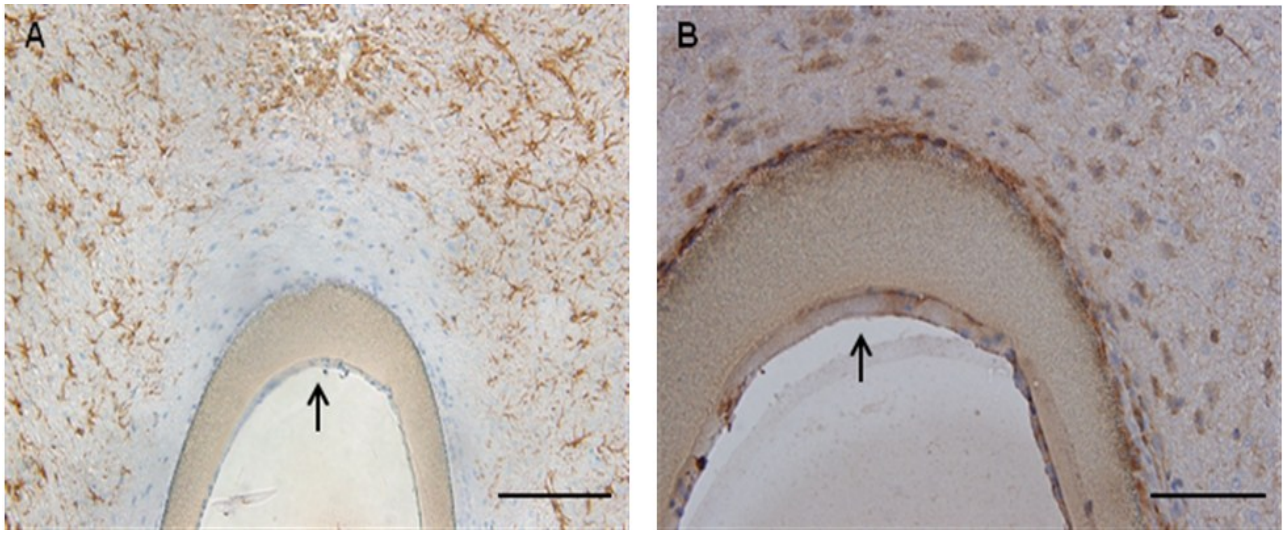

Fig. 8 - Representative images of microdialysis membrane (CMA 12; cut off 20000 Da) implanted in the frontal cortex of Sprague Dawley rats. (A) Increased GFAP+ astroglia surrounding the microdialysis probe 15 days following probe implantation, scale bar = 200 µm. (B) Increased Iba-1+ microglia in close vicinity of the microdialysis probe 15 days after implantation, scale bar = 100 µm. The arrows point towards the inner surface of the microdialysis membrane.

3.5. Light microscopy

Brain sections stained with haematoxylin and eosin (H&E) were examined under light microscope to have an overview of cOFM probe implantation site. Iba-1 and GFAP positive cells were counted at three different distances (0 – 140 µm, 140 – 350 µm, 350 – 700 µm) from the edge of cOFM probe tip under the microscope (Axiocam, Nikon) at magnification of 200X using an optical grid (Fig. 9). Two trained observers counted the cells in three randomly selected squares at each distances and the mean was converted to

cells per mm^2. Cell numbers after decimal point was rounded off to the nearest whole number. Both observers were blinded for the respective groups.

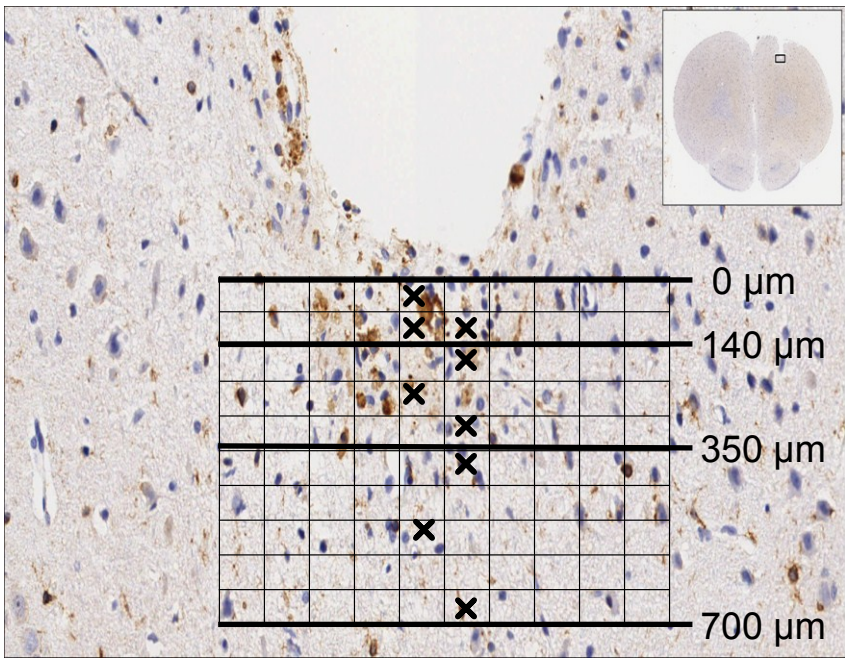

Fig. 9 – Diagrammatic representation of an optical grid. Each small square = 4900 μm^2 under 200X magnification.

3.6. Scanning electron microscopy (SEM) of cOFM probe

cOFM probes were fixed with 2,5% (wt/vol) glutaraldehyde and 2% (wt/vol) paraformaldehyde in 0.1 M cacodylate buffer for 1 h. Samples were rinsed in 0.1 M Cacodylate buffer then post-fixed for 1 h in 2 % (wt/vol) osmium tetroxide and rinsed again in Cacodylate buffer. Then probes were dehydrated in graded series of ethanol. cOFM probes were critical – point dried in super-dry aceton, mounted on aluminium pin and sputter coated and examined under SEM (ZeissDSM 950) (Fig. 10).

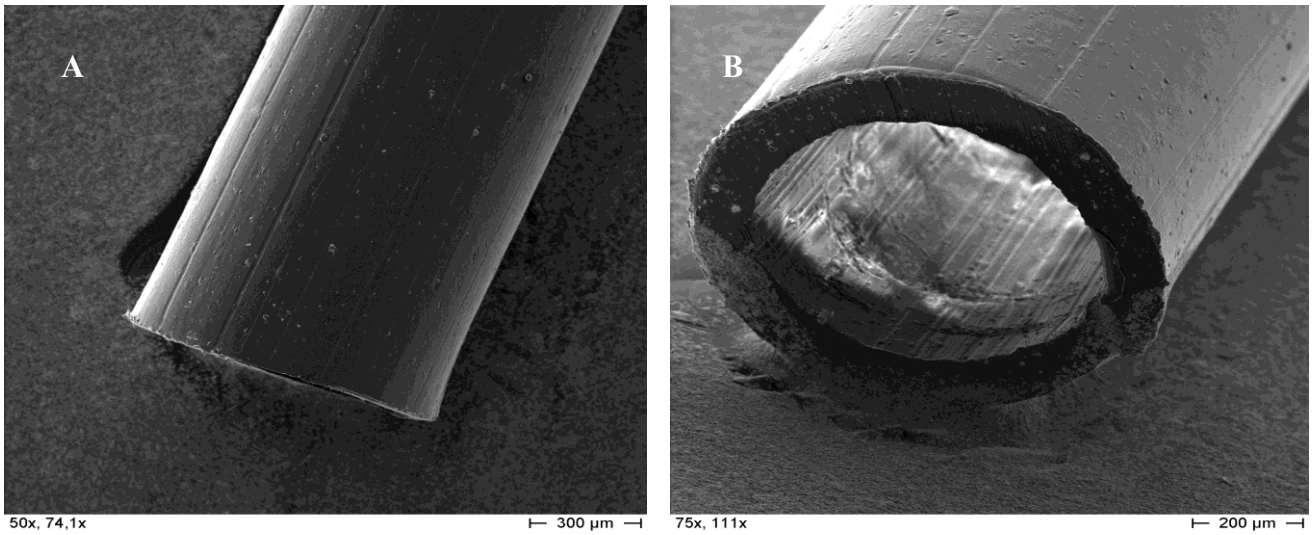

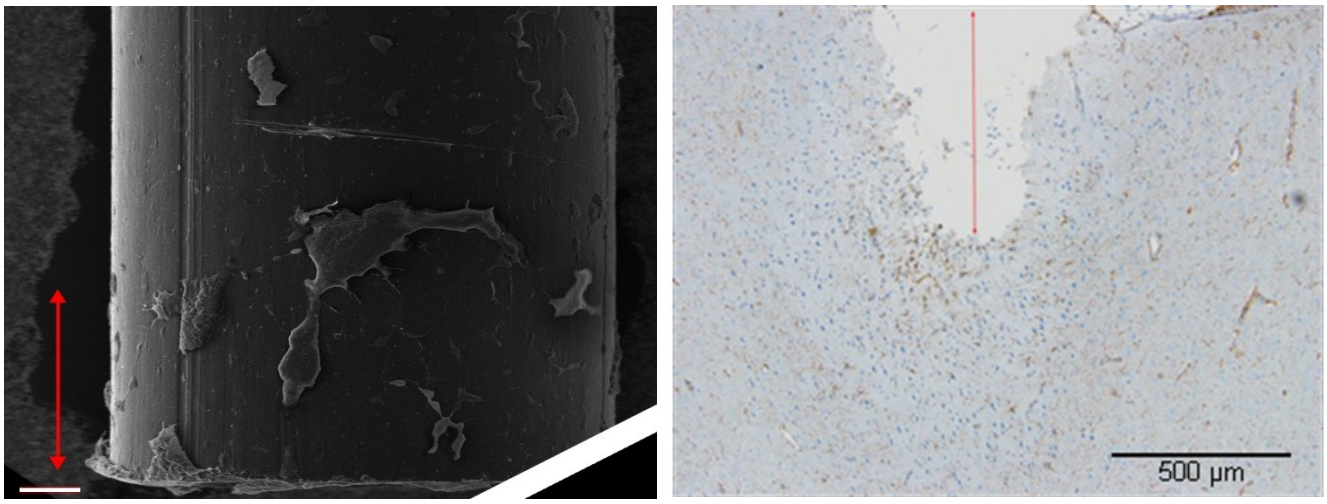

(C) (D)

Fig. 10 – Representative scanning electron microscope (SEM) images of unimplanted cOFM probe (A, B). (C) Represents SEM image of cOFM probe explanted from brain, scale bar = 100 µm. Red arrow indicates the length which was inside in the brain. (D) GFAP staining of the same brain and the implantation track.

(This work was done under Dr. Dagmar Kolb-Lenz in the Core Facility Ultrastructure Analysis, ZMF, Medical University of Graz).

3.7. Statistical analysis

Statistical analyses were performed using the PASW 18.0.0 software (IBM Deutschland GmbH, Ehningen, Germany). All data were expressed as mean ± SD. Two-group comparisons were performed by Student's *t*-test ($\alpha = 0.05$). *T*-test analyses were used to compute *p*-values comparing the cell counts of contralateral (control) hemisphere and cOFM probe implanted hemisphere at different distances such as 0 – 140 µm, 140 – 350 µm and 350 – 700 µm from the edge of cOFM probe tip. Student's t-test was also applied to compare the data between non-perfused and perfused hemispheres at corresponding distances from the edge of the cOFM probe tip. Differences were considered statistically significant for $p < 0.05$.

Results…

BBB re-establishment after cOFM probe implantation

EB was used as a marker to measure BBB permeability to high-molecular-weight substances after cOFM probe implantation in whole, extracted and fixed brains. Macroscopic inspection showed that all brains were free of blood, which indicates that the transcardial flushing procedure was effective (the removal of intravascular blood and EB by transcardial flushing allows clearer measurement of extravascular EB fluorescence, which indicates a leaky BBB).

EB fluorescence measurements in the region of interest (ROI) (2.5 mm circle around the probe) directly after probe insertion showed high fluorescence. The positive control group (taken 2 hours after cOFM probe implantation) showed visible penetration of EB into the brain tissue surrounding the cOFM probe.

Fluorescence of EB in the brain tissue decreased with increasing healing time. Setting EB brain tissue staining to 100% at the point when staining was carried out, staining decreased to 30% after 5 and 7 days and to 15% after 9 days (but still significantly higher than the negative control group ($p \leq 0.02$). After 11 and 15 days, the extracted brains showed fluorescence levels comparable to those of the negative control group (Fig. 11). The standard deviation of the fluorescence measurements decreased with healing time.

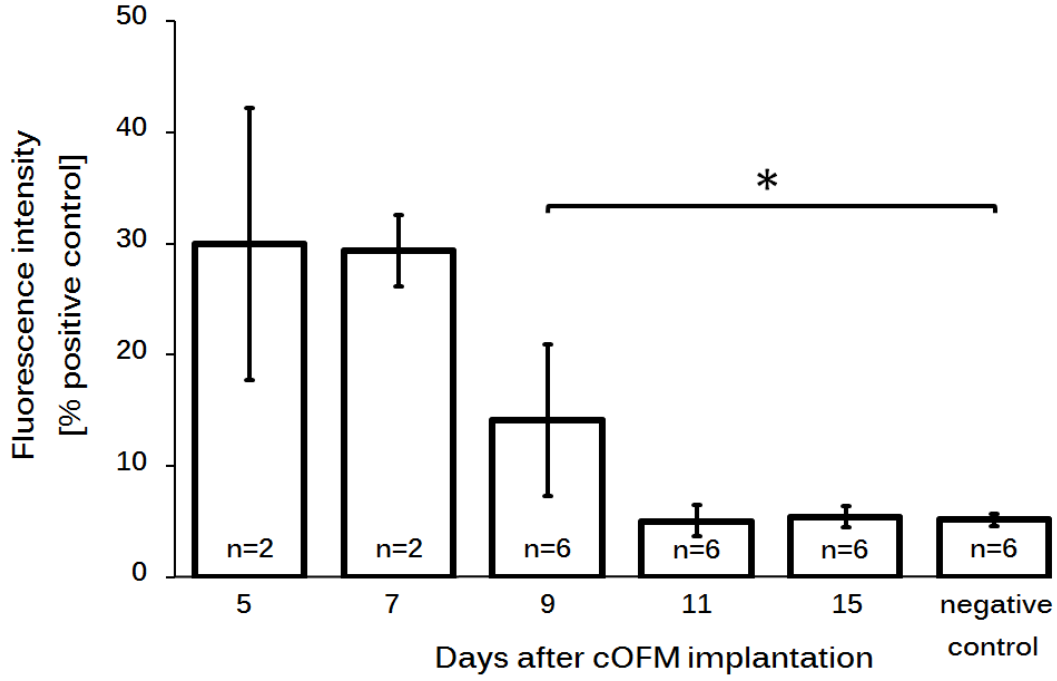

Fig. 11 – BBB permeability for EB after different days of healing mean ± SD.

Characterisation of BBB permeability by brain biopsies

NaF concentrations in brain biopsies from the left hemisphere (LH) containing the probe implantation site were compared to biopsies from the right hemisphere (RH) with intact brain tissue. The NaF (LH) / NaF (RH) ratio offers information on BBB permeability surrounding the probe. Ratios were similar in groups 1 and 2. Group 3, which received standard cOFM perfusate, had a lower NaF ratio than group 1. Group 4, which received cOFM perfusate with hyperosmolar mannitol, had higher ratios (2.1 ± 1.2) than group 1; however, these differences are not statistically significant (Fig.12).

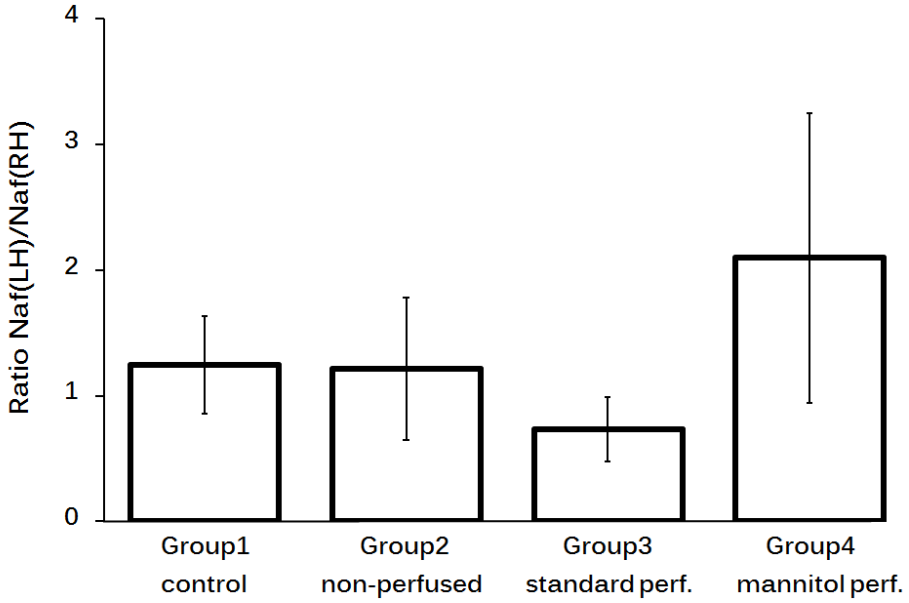

Fig. 12 – The ratios of NaF levels in brain biopsies surrounding the probe (left hemisphere, LH) to the corresponding area on the contralateral hemisphere (right hemisphere, RH) for the four groups mean ± SD.

Continuous monitoring of BBB permeability by cOFM sampling for NaF.

NaF plasma concentration was stable (44 to 112 µg/ml) for all groups over the entire experiment (Fig. 13). NaF concentrations in cOFM samples with standard perfusate (group 3) were about 15 times lower than in cOFM samples with mannitol (group 4). Groups 3 and 4 showed significant differences at each investigated time point ($p \leq 0.002$) (Fig.13).
The same trends were seen by plotting the ratio of cOFM versus plasma NaF concentration. Group 4 has a significantly higher ratio than group 3 at each investigated time point ($p \leq 0.002$).

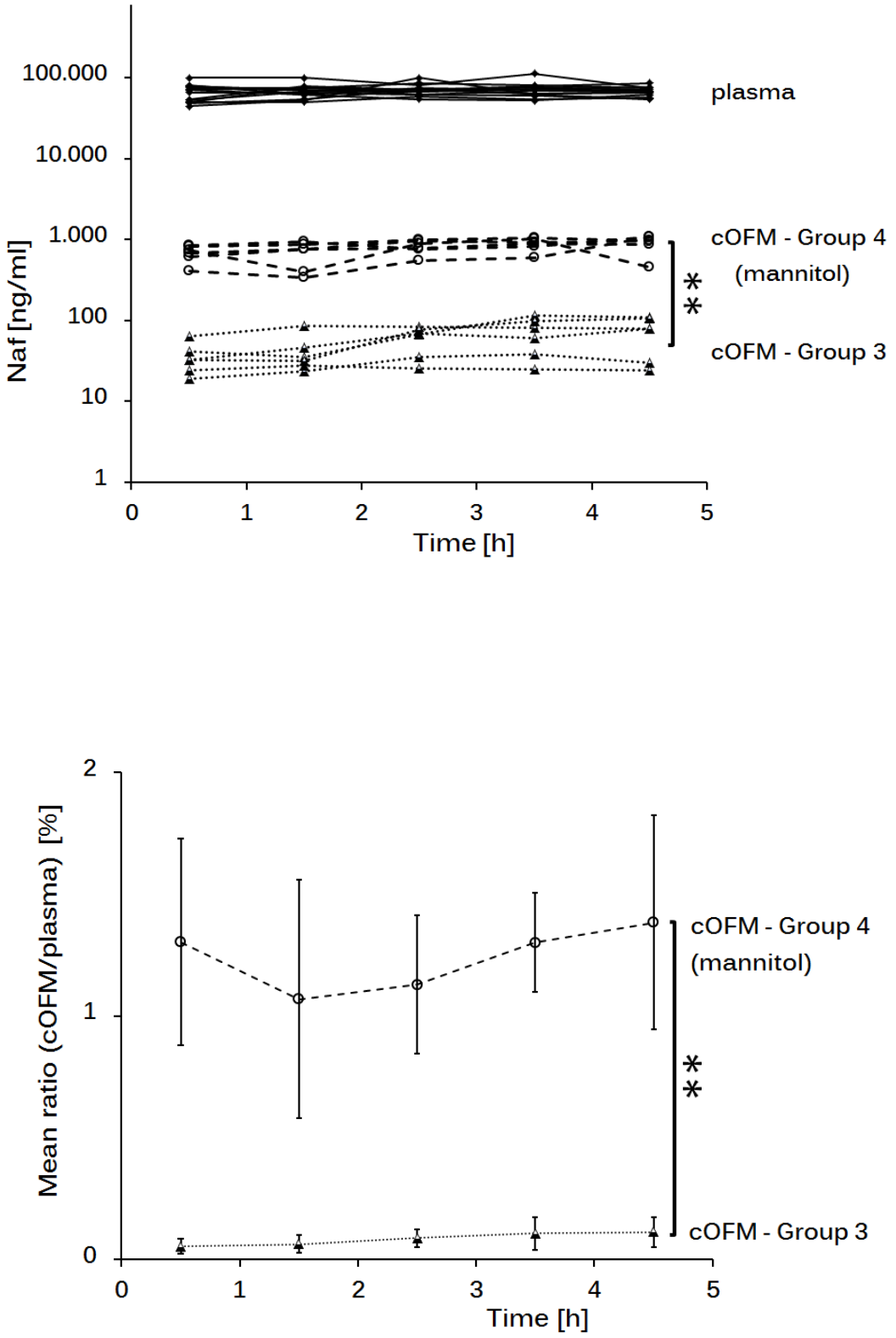

Fig. 13 – Concentration of NaF in cOFM perfusate and plasma samples in groups 3 and 4.

Light microscopy of H&E stained sections

The effect of cOFM probe implantation in rat frontal cortex was assessed at different time points. After 3 days of cOFM probe implantation, residual erythrocytes from implantation trauma were visible in both non-perfused and perfused brain. At this early stage, some edema formation in close vicinity of cOFM probe implantation site was also detected. The extent of edematous zone was similar in non-perfused and perfused brain (Fig.14). Small amounts of tissue debris from the implantation trauma were also detected. Brain sections after 15 days of cOFM probe implantation showed complete resorbtion of erythrocytes and tissue debris. Only a minimal residual edema was detected in non-perfused and perfused brain at this stage. The probe otherwise healed in well without any major tissue reaction (Fig.15). Following 30 days of cOFM probe implantation, the edema formation surrounding the implantation site was completely resorbed (Fig.16). The broken tissue and infrequent erythrocytes in the probe track was the consequence of post-mortem cOFM probe extraction which indicated cOFM probe healed well into the brain tissue at this stage; occasionally some hemosiderophages were also detected.

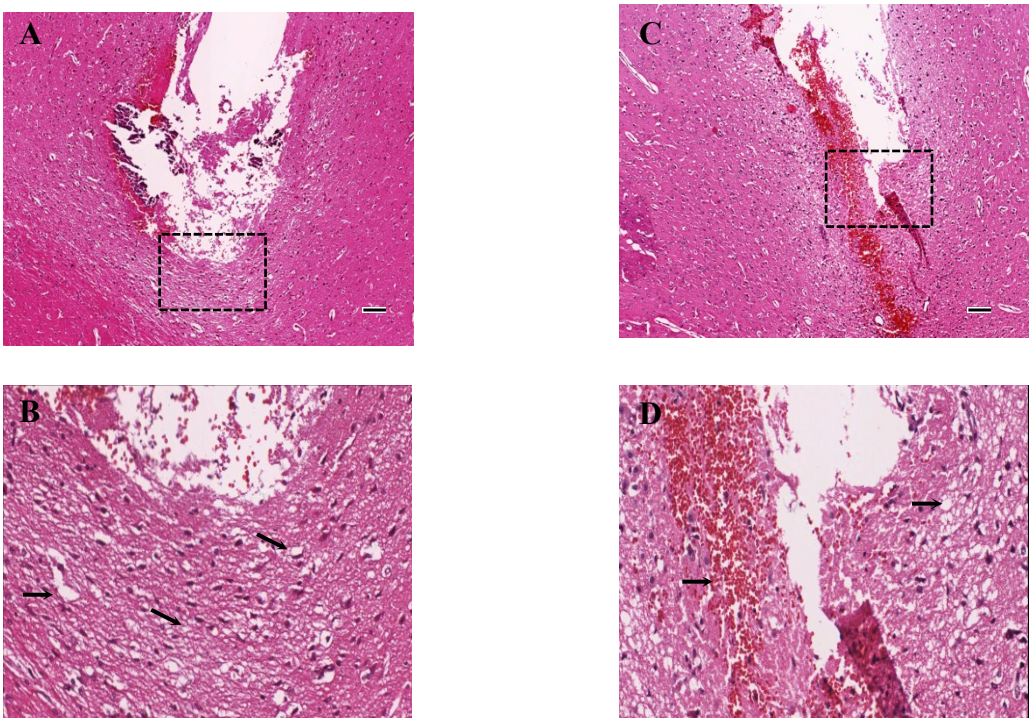

Fig. 14 – Representative images of non-perfused (A, B) and perfused (C, D) rat brain after 3 days of cOFM probe implantation. Small rectangles with broken line in A and C (50x) are shown at higher magnification (200x) in B and D. Small arrows in B and D shows edema and erythrocytes. Scale bar = 100µm.

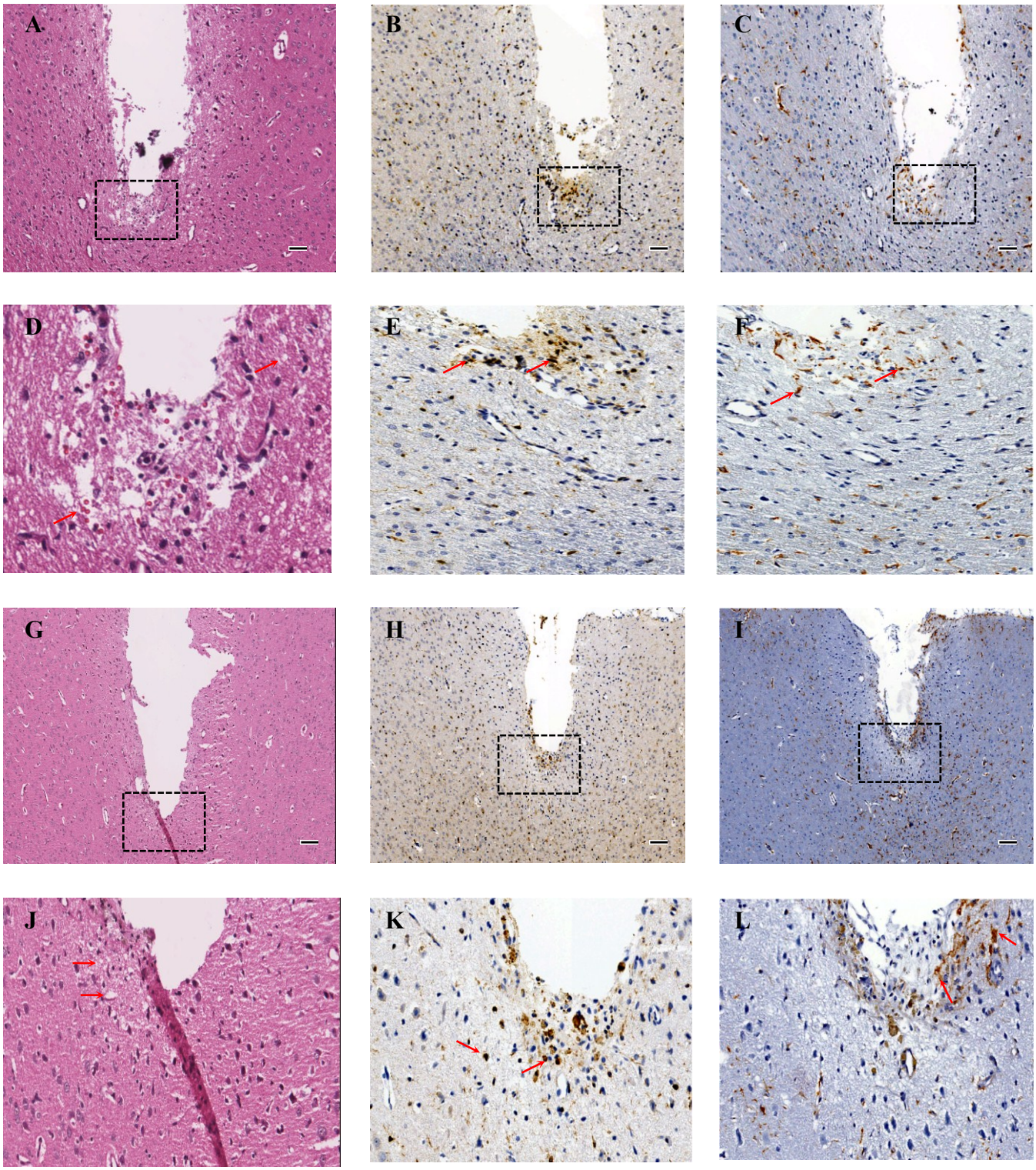

Fig. 15 – Microscopy of the cOFM probe implantation site in the frontal cortex after 15 days. Representative images of non-perfused (A-F) and perfused (G-L) rat brain. Adjacent brain slides were stained with H&E (A, D, G, J), Iba-1 for microglia (B, E, H, K) and GFAP for astrocytes (C, F, I, L). The small rectangles with broken line in A-C and G-I (50x) are shown at higher magnification (200x) in D-F and J-L respectively. At this stage only a minimal residual edema is detectable at H&E staining in both non-perfused and perfused animals. Only a minor microglia (E, K) and astrocyte (F, L) reaction directly adjacent to the cOFM insertion zone is visible. Scale bar = 100µm.

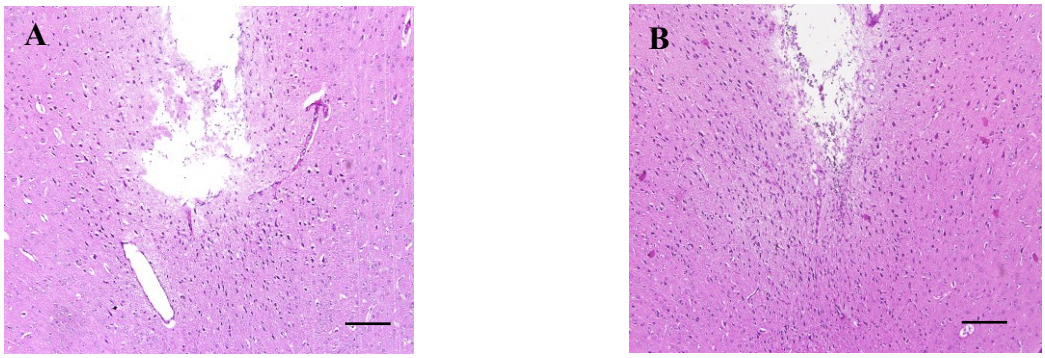

Fig. 16 – Microscopy of cOFM probe implantation site after 30 days. Representative images of non-perfused (A) and perfused (B) brain. Scale bar = 200µm.

Iba-1 immunoreactivity / microglial reaction

Microglia provides first line of defence and activated during CNS injury. It also plays a major role in glial sheath formation. Iba-1 is widely used marker for activated microglia. After 3 days of cOFM probe implantation, Iba-1 immunoreactivity was detected surrounding the cOFM probe implantation site and microglial reaction was slightly more pronounced in perfused animals (Fig.17 A, B). Representative images of Iba-1 reactivity around cOFM probe after 15 days of implantation are shown in Fig.15 (B, E, H, K). Iba-1 cells were counted and expressed per mm^2 as a function of distance from the tip of cOFM probe tissue interface. For details on the counting scheme see methods section 3.6. The basal level of Iba-1+ cells was counted on right hemisphere in both non-perfused (164 ± 54) and perfused (158 ± 61) animals which served as internal control. The number of Iba-1+ cells counted in close proximity (0 – 140 µm) of the implant site was 373 ± 206 in non-perfused and 419 ± 228 in perfused brains (Fig.18). In these region, microglia count in non-perfused and perfused brains were significantly higher ($p < 0.005$ and $p < 0.002$) when compared to the basal level (Tab.2). Similarly, quantification was performed at the distances of 140 – 350 µm and 350 – 700 µm from the tip of cOFM probe tissue interface. The mean cell count per mm^2 was 175 ± 94 and 135 ± 29 in non-perfused and 141 ± 46 and 147 ± 49 in perfused animals (Fig.18). Cell counts in this region show no significant differences when compared to the basal counting levels of the contralateral side (Tab.2). The data obtained from non-perfused and perfused brains were compared with each other and no significant differences were found in Iba-1+ cell counts after 15 days of cOFM probe implantation (Tab.3). After 30 days of cOFM probe implantation, only a minor Iba-1 immunoreactivity was observed at the implantation site (Fig.19 A, B).

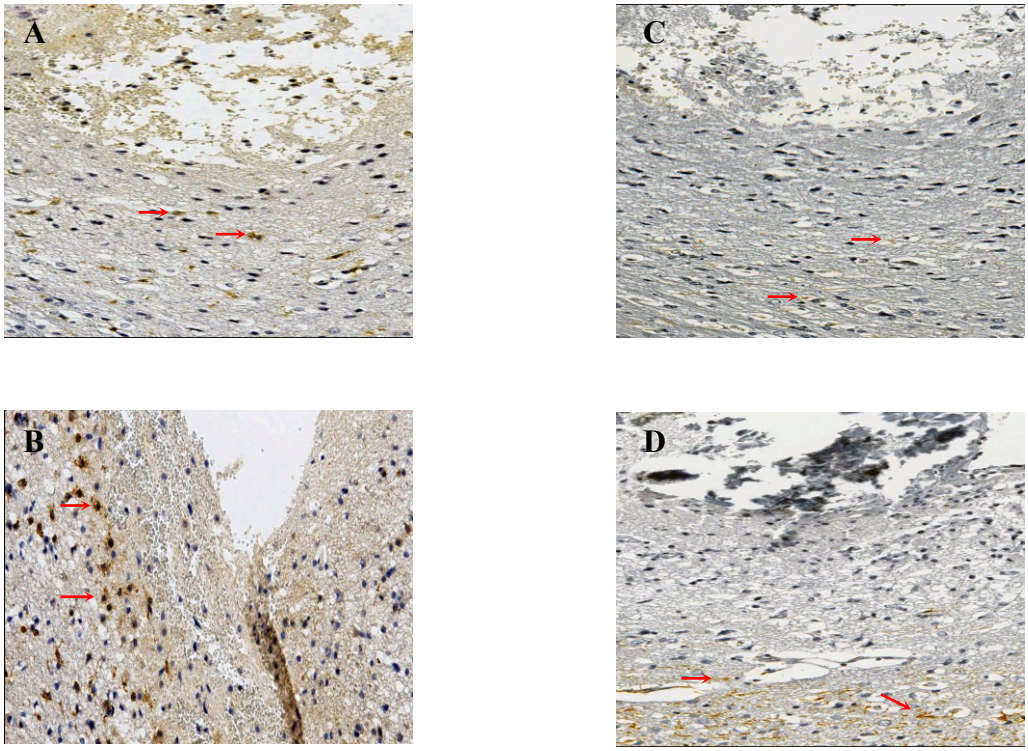

Fig.17. Microscopy of Iba-1 (A, B) and GFAP immunoreactivity (C, D) after 3 days of cOFM probe implantation (200x). Representative images of non-perfused (A, C) and perfused (B, D) rat brains. Arrows in A and B show Iba-1 positive microglia. GFAP positive astrocytes are marked with arrows in C and D.

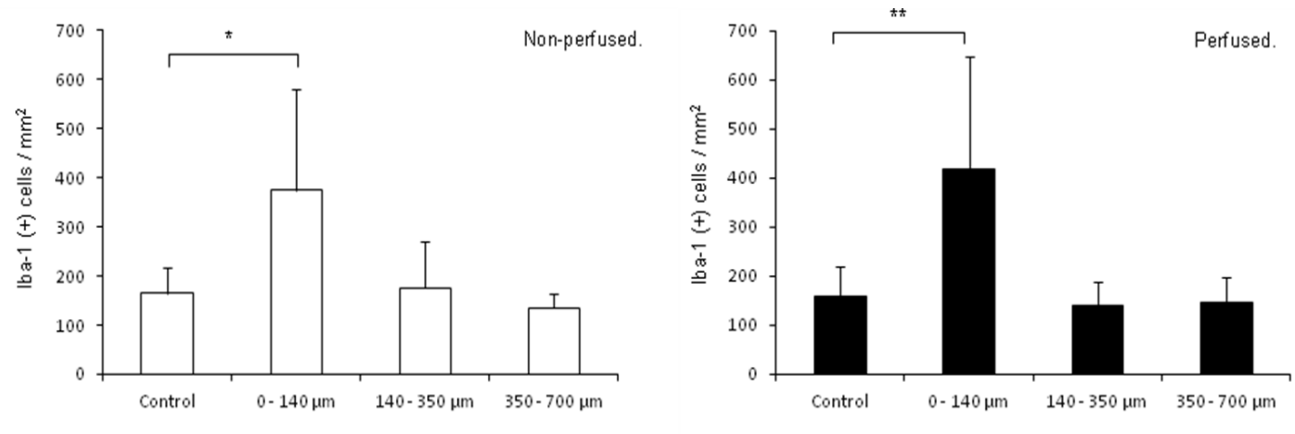

Fig. 18 – Quantification of Iba-1(+) cells after 15 days of cOFM probe implantation.

GFAP immunoreactivity / astroglial reaction

Astrocytes are the major cell types responsible for tissue encapsulation or glial scar formation and GFAP is commonly used to identify reactive astrocytes. After 3 days of cOFM probe implantation, GFAP immunoreactivity was detected surrounding the cOFM probe implantation site. At this early stage, astroglial immunoreaction was slightly pronounced in perfused animals (Fig.17 C, D). Representative images of GFAP reactivity around cOFM probe after 15 days of implantation are shown in Fig.15 (C, F, I, L). GFAP+ cells were counted and expressed per mm^2 as a function of distance from the tip of cOFM probe tissue interface. For details on the counting scheme see methods section 3.6. The basal level of GFAP+ cells per mm^2 were counted on contralateral hemisphere of both non-perfused (209 ± 61) and perfused (215 ± 49) brains as an internal control. Number of GFAP+ astrocytes counted in the direct vicinity (0 – 140 µm) of cOFM probe implant site was 294 ± 124 in non-perfused and 243 ± 114 in perfused animals (Fig.20). Similar quantification was performed at the distances of 140 – 350 µm and 350 – 700 µm from the implant site. The mean cell count in this region was 186 ± 59 and 230 ± 69 in non-perfused and 254 ± 101 and 226 ± 60 in perfused animals (Fig.20). The count was not statistically significant when compared to the contralateral hemisphere (Tab.2). However, GFAP+ cell count in perfused animals always shows a higher value at different distances when compared with non-perfused group. After 15 days of cOFM probe implantation no significant differences were found in GFAP+ cell count between non-perfused and perfused animals (Tab.3). After 30 days of cOFM probe implantation, only a minor astrocytic reaction was seen in both non-perfused and perfused animals (Fig.19 C, D). In none of the animals an astroglial scar developed around the cOFM probe implantation site.

Table 2 – Calculated p - values for Iba-1 (+) and GFAP (+) cells from cOFM probe tip in comparison to the contralateral side.

Duration after cOFM probe implantation	Distance from cOFM probe interface	Iba-1		GFAP	
		Non-perfused	Perfused	Non-perfused	Perfused
15 Days	0 - 140 µm	0.005*	0.002**	0.051	0.446
	140 - 350 µm	0.724	0.442	0.358	0.242
	350 - 700 µm	0.125	0.618	0.437	0.622

* $p < 0.05$

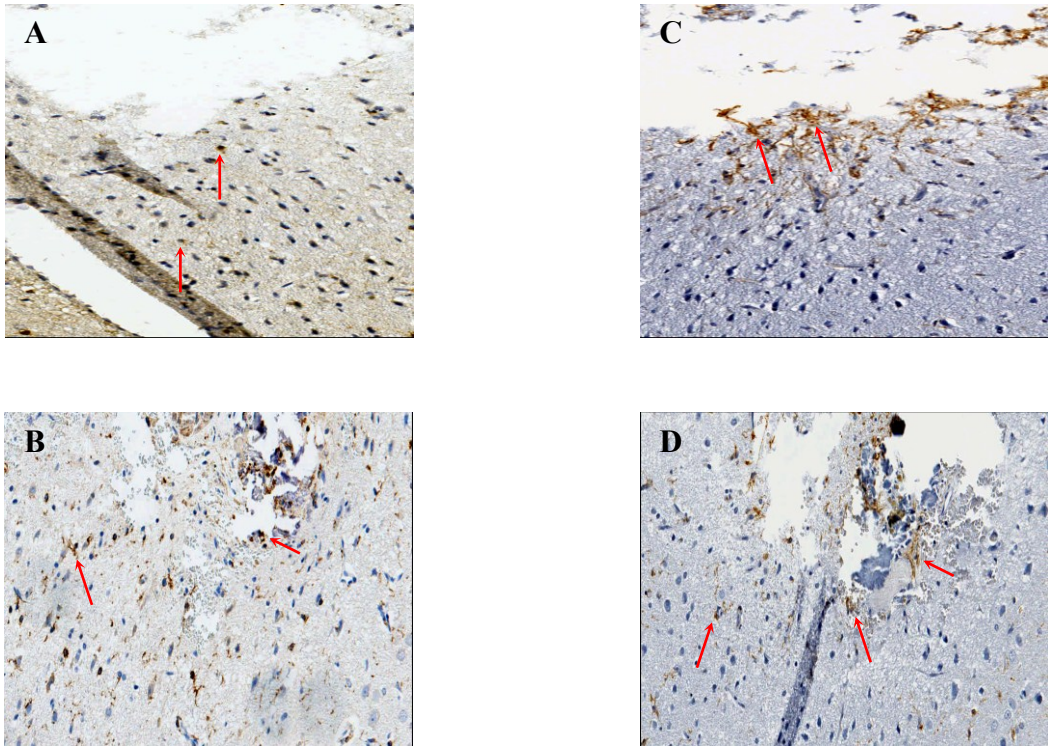

Fig. 19 – Microscopy of Iba-1 (A, B) and GFAP immunoreactivity (C, D) after 30 days of cOFM probe implantation (200x). Representative images of non-perfused (A, C) and perfused (B, D) rat brains. Arrows in A and B show Iba-1 positive microglia. GFAP positive astrocytes are marked with arrows in C and D.

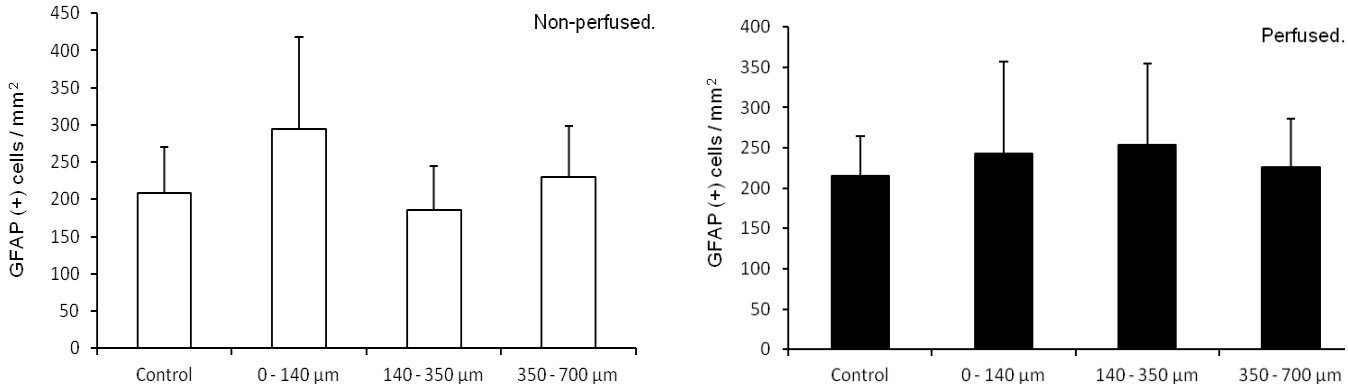

Fig. 20 – Quantification of GFAP positive cells after 15 days of cOFM probe implantation.

Table 3 – Comparison of calculated p - values for Iba-1 (+) and GFAP (+) cells from cOFM probe tip in non-perfused and perfused rat brain.

Duration after cOFM probe implantation	Distance from cOFM probe interface.	Iba-1	GFAP
15 Days	0 - 140 µm	0.616	0.305
	140 - 350 µm	0.276	0.059
	350 - 700 µm	0.486	0.874

Discussions…

cOFM is a continuous in vivo sampling technique that provides access to the interstitial brain fluid. cOFM builds on the strength of microdialysis (MD) but overcomes some limitations associated with using a membrane as an exchange barrier. cOFM puts the perfusate in direct contact with brain interstitial fluid, and thus all substances are sampled regardless of size or lipophilicity.

Like all invasive probe techniques, cOFM causes trauma during probe insertion, which leads to local disruption of the BBB surrounding the cOFM probe. In the case of MD, the time needed for local re-establishment of BBB is still under debate. Earlier MD studies reported intact BBB as early as three hours after probe implantation (Benveniste et al., 1984; Aasmundstad et al., 1995). There are also reports of altered BBB permeability (Westergren et al., 1995; Morgan et al., 1996) up to 24 h following MD probe insertion. A later study reported increased BBB permeability up to 28 days after MD implantation (Groothuis et al., 1998). The same study also described a biphasic elevation of BBB permeability immediately after implantation and two days later, followed by a slow decline in permeability. Marburger et al. suggested that inflammatory damage related to the MD membrane could play a role in delayed BBB re-establishment (Marburger et al. 2000). The seemingly contradictory nature of these findings shows that the determination of BBB permeability after probe insertion is complex and depends on diverse factors such as (i) probe size and materials, (ii) the implantation procedure, (iii) vasoconstriction due to traumatization, which leads to reduced BBB permeability within a few hours of implantation; a hypothesis supported by the observation of decreased local blood flow and decreased glucose metabolism after implantation (Benveniste et al., 1987), and (iv) inflammatory processes. In view of these factors, we anticipated that the determination of BBB permeability after probe insertion may be complex. Therefore, we investigated cOFM insertion trauma and BBB re-establishment in detail.

We took a stepwise approach to measuring BBB intactness, with two established markers: (1) Albumin-bound Evans Blue (EB), which has a total MW of ~66 kDa, does not cross the intact BBB but will stain brain tissue when the BBB is damaged (Manaenko et al. 2011). EB is a marker for structural damage of the vascular system. (2) Sodium fluorescein (NaF) is a low-molecular-weight marker (376 Da) that crosses the intact BBB to a limited extent. Thus, NaF is a sensitive marker even for subtle changes in BBB permeability (Kozler et el., 2003; Lenzsér et al., 2007; Kaya et al., 2011).

To investigate cOFM insertion trauma, EB was injected at the same time as probe insertion (positive control). Insertion trauma caused by cOFM implantation in the positive control group is significant; visible penetration of EB into the brain tissue surrounding the cOFM probe indicates local disruption of the BBB. Visible EB staining was restricted to a maximum diameter of 2 mm around the cOFM probe; therefore the region of interest (ROI) for the image analysis was set to a diameter of 2.5 mm. In the negative control group a cOFM probe was implanted but no EB was injected. In the test groups EB was injected 5, 7, 9, 11 and 15 days after probe insertion. EB staining in brain tissue surrounding the probe decreased with increasing healing time (Fig. 10). Subjects with a healing time of up to 9 days still showed significant differences from the negative control group ($p \leq 0.02$), suggesting that the BBB was not fully healed. After healing times of 11 and 15 days, extracted brains showed fluorescence levels comparable to those of the negative control group, indicating local re-establishment of the BBB. To ensure complete local BBB re-establishment around cOFM probes the time span between cOFM probe insertion and the start of sampling was fixed at 15 days.

To investigate the function of the BBB after its re-establishment we used a second well-established marker for BBB permeability; sodium fluorescein (NaF). NaF was measured in cOFM perfusate, blood and brain tissue samples. In order to compare native brain tissue with brain tissue surrounding the cOFM probe, biopsies were taken. Brain tissue biopsies from the left frontal lobe (LH - probe implantation site) and the contralateral right hemisphere (RH - native) of the same rat were compared. In control group 1, without probe implantation, the LH / RH ratio was 1.2 ± 0.4. The deviation from the expected ratio of 1 (which would indicate similarity of the two hemispheres) may be due to imperfect transcardial flushing leading to residual intravascular NaF. In group 2, cOFM probe was inserted into the left frontal lobe without perfusion. After 15 days the ratio LH / RH (1.2 ± 0.6) was comparable to control group 1, indicating that the BBB surrounding the cOFM probe was intact. In order to check whether perfusion of the cOFM probe influenced the BBB, the probe was perfused with standard perfusate in group 3. The NaF ratio of LH / RH decreased (0.7 ± 0.3) when cOFM sampling was performed. This could be due to NaF being washed out during cOFM sampling. The difference between this group and the untreated control group 1 was not statistically significant. For perfusion of the cOFM probe in group 4 hyperosmolar mannitol was used, which is known to open the BBB (Brown et al. 2004, Bálint et al. 2007, Wang et al. 2007) . The ratio of LH / RH NaF levels in group

4 is higher (2.1 ± 1.2) than in control group 1, indicating increased BBB permeability surrounding the cOFM probe due to the action of the hyperosmolar mannitol. Differences between the four groups are statistically not significant.

Analysis of NaF concentrations in cOFM samples of groups 3 and 4 (Fig. 12) gives similar but statistically significant results. The NaF levels in group 4 (which received hyperosmolar mannitol) were 15 times higher than in group 3 (which received standard perfusate). The increased NaF levels in group 4 indicate a local opening of the BBB. In contrast to results based on brain biopsies, the differences in NaF levels in cOFM samples between groups 3 and 4 are highly significant. NaF levels in cOFM can also be plotted against NaF plasma concentration for the entire duration of the experiment (Fig. 12). Higher NaF levels are observed when using mannitol perfusate over the entire experiment. The measured differences in NaF concentration in the cOFM samples in groups 3 and 4 demonstrate the potential of this technique to detect BBB permeability changes in vivo. This is very important for any in vivo PK or PD experiments for endogenous drug testing. Fluctuations in BBB permeability in such experiments would lead to altered substance-transport rates across the BBB. By using NaF as a standard marker, the degree of BBB permeability can be investigated in each cOFM sample and can be used as a quality control for BBB intactness.

As discussed above, proximate control of BBB permeability provided by continuous BBB monitoring is of fundamental importance for PK studies in the CNS. The combination of substance sampling with cOFM and parallel monitoring of BBB permeability provides powerful insight into the interaction of a drug with the BBB.

For in-vivo collection of substances from a number of complex matrixes microdialysis is widely used in research and clinical practices. However, the technique has some potential drawbacks. The sampling method involves implantation of a small porous hollow fibre (~200 to 500 µm) dialysis membrane into the tissue using a guide needle. The presence of a foreign object in a physiological environment elicits a cascade of inflammatory mechanisms which leads to acute and chronic tissue response. Studies in the brain provide evidences that the implantation of microdialysis probes triggers a generalized injury response including edema (Benveniste et al., 1987; Clap-Lilly et al., 1999; Benveniste et al., 1989) and tissue damage up to 1.4 mm remote from the implant site (Hascup et al.,

2009) and local rise in blood flow strongly influence the recovery of endogenous molecules (Stenken et al., 2010). In this study we assessed the histopathological effects of long-term implanted cOFM probes in the frontal lobe with a special focus on the formation of a glial scar forming a diffusion barrier surrounding the cOFM probe. As a secondary aim we determined tissue reaction following probe perfusion with a physiological fluid, the cOFM perfusate. Tissue reaction due to probe perfusion provides information whether repeated perfusion is possible and therefore an extended experimental setup. Glial scar formation after probe implantation affects substance exchange between brain tissue and the implanted probe and would therefore strongly limit cOFM usability to sample diluted representative brain interstitial fluid. In previous study we have found that BBB is reestablished 15 days after cOFM probe implantation (Birngruber et al., 2013). The current study was thus specifically designed to assess quantitative tissue changes on day 15 after probe implantation focused on the exchange area at the tip of the cOFM probe.

The main components of the glial scar are astrocytes and microglia and therefore the focus of our investigation (Azemi et al., 2011). After 3 days of cOFM probe implantation, Iba-1 immunoreactivity was detected in close proximity of cOFM probe implant site. The perfused brain shows slightly higher microglial reaction than non-perfused brain which is probably due to mechanical forces associated with perfusion. The quantitative analysis of Iba-1 staining on day 15 after cOFM probe implantation revealed only a moderate increase in microglial reaction in the immediate vicinity of the probe tip (< 140 μm). In regions further away from the probe no changes in microglial activation were observed. Similarly, GFAP immunoreactivity was also detected at this early phase which is slightly higher in perfused brain. GFAP staining showed no significant astrocytic reaction along the implantation track at 3, 15 and 30 days. Comparable microdialysis studies have observed a high degree of cell loss, nerve fiber damage, and elevated numbers of astrocytes and microglia up to 300 μm from the probe implantation tracks after 3-14 days (Clapp-Lilly et al., 1999; Borland et al., 2005; Hascup et al., 2009). After a longer implantation time of 30 - 60 days microdialysis probes induced the formation of a 2 mm wide glial scar (De Lange et al., 1995; Benveniste et al., 1987). Compared to the microdialysis probes, cOFM probes caused only very minor tissue reactions and no continuous glial scarring or encapsulation at any time. The formation of a continuous glial scar would impair the function of the probe because it acts as a diffusion barrier between brain tissue and the probe and therefore hampers substance exchange. Methodological investigations showed that the encapsulation

of an implanted probe was found to decreased sensitivity and underestimated extracellular substance concentrations particularly for larger molecules (Bungay et al., 2003). The absence of a glial scar after cOFM implantation probes allows unhindered diffusion and emphasizes the potential of cOFM for long-term sampling of various sized molecules under physiological conditions in brain tissue. Such minor tissue reactions are probably the consequence of cOFM probe design and materials used for the probe. All materials which are in direct contact with brain tissue were chosen with the intention to minimize tissue reaction.

The cOFM guide cannula is made of FEP (fluorinated ethylene propylene), which is very flexible and has a slick and biologically inert surface. The flexibility of the cOFM guide cannula reduces mechanical stress caused by micro-motions of the brain floating in cerebrospinal fluid while the probe is fixed to the skull (Seymour et al., 2007). Brain tissue reactions are considerably increased when rigid implants are anchored to the skull compared to the same probe implanted intraparenchymally without fixation to the skull (Kim et al., 2004). Increasing flexibility of an implanted probe decreases thickness of the glial scar and improves neuronal viability in the close vicinity of the implant (Harris et al., 2011).

Large molecules such as proteins are held responsible for spontaneous adsorption to foreign materials inserted into the body. This adsorption is considered to be the initiator for a cascade of processes which lead to biofouling and finally encapsulation (Dahlin et al., 2012). A limited number of studies addressed this problem by surface modified microdialysis membrane or by dexamethasone-releasing coatings, a highly potent glucocorticoid with anti-inflammatory and immunosuppressive activity (Shain et al., 2003; Spataro et al., 2005; Zhong et al., 2007). The surface modification or dexamethasone coating showed significant improvement in enzymatic degradation of proteins or suppressing gliosis and ischemia respectively but worsen dialysis efficacy and showed limited neuroprotective activity (Dahlin et al., 2012; Jaquins-Gerstl et al., 2011). The slick surface of the cOFM guide cannula avoids adhesion of immunoreactive cells and proteins that access the brain when blood vessels are ruptured and meninges are penetrated during implantation (Abnet et al., 1991; Maxwell et al., 1990).Cell adhesion to rough surfaces or even cell migration into porous structures such as microdialysis membranes (Fitch et al., 1999; Von Grote et al., 2011) were therefore avoided in the cOFM design.

The cOFM healing dummy, a thin steel rod, provides mechanical stability during the implantation process. The tip of the healing dummy is rounded and polished in order to provide a biologically inert surface similar to the guide cannula. The cOFM perfusate is adapted to the actual cerebral interstitial fluid in terms of ion content and pH value in order to avoid chemical stress for the brain. The perfusate flow rate was set to 1 µl/min in order to minimize mechanical shear stress to the tissue. The placement of inflow and outflow tubing warms up the perfusate before it reaches the brain tissue and thus avoids temperature stress (Lange et al., 1997). Perfusion of the cOFM probe had no significant effect on the astrocytic or microglial reaction, with only a slightly higher microglial cell count in the area up to 140 µm around the cOFM probe.

Glial scar formation surrounding the probe is the main limiting factor for long-term implanted sampling systems (Grabb et al., 1998; Thelin et al., 2011). We found that the implantation a cOFM probe did not cause any major tissue reaction during the observed period of 30 days. Moreover, probe perfusion with cOFM perfusate for 2 hours couldn't produce a continuous glial scar surrounding cOFM probe. So, repeated sampling of the same subject is possible over an extended experimental set-up.

CHAPTER – II

Basic aspects of neuroinflammation.

Background…

Compromised BBB integrity is a hallmark feature of neuroinflammatory diseases such as HIV encephalitis, bacterial meningitis and multiple sclerosis (McQuaid et al., 2009; Dallasta et al., 1999; Kim, 2008). Inflammatory reaction in the brain is recently associated with neurodegenerative diseases due to its possible link with multiple sclerosis, Alzheimer disease, Parkinson's disease (O'Callaghan et al., 2008). However, neuroinflammation is a cause or a consequence of neurodegenerative diseases is still an ongoing debate. Usually inflammation is triggered by injurious stimuli which include pathogens, damaged cells, irritants etc. The process is a self-protecting mechanism in order to initiate healing. Inflammation typically involves production and release of cytokines and chemokines. Recently, it has been reported that neuroinflammation involves activation of glial cells which serve as a source as well as targets of proinflammatory cytokines (O'Callaghan et al., 2008).

Tumour necrosis factor alpha (TNF- α) is a pleiotropic proinflammatory cytokine participates in neuroinflammation (Lopez-Ramirez et al., 2012). Microglia are the major source for TNF- α production in CNS. Nishioku et al. have shown elevated TNF- α release from activated microglia causes blood brain barrier dysfunction (Nishioku et al., 2010). It is reported that increased level of TNF- increases blood brain barrier permeability and also stimulates caspase-3 activation leading to brain endothelial cells apoptosis (Nishioku et al., 2010). However, activation of caspases does not always lead to brain endothelial cells apoptosis. It also causes disassembly of tight junction molecules and scaffolding proteins such as claudin-5 and zona occludens-1 respectively (Zehendner et al., 2011).

Interleukin-6 (IL-6) acts as pro-inflammatory and anti-inflammatory cytokine in the body. IL-6 is secreted by T-cells, macrophages and microglia in response to infection, trauma that leads to inflammatory reaction. It can penetrate the BBB and play an important role in cognitive function in normal physiological condition (Baune et al., 2012). It is reported that an association is present between IL-6 level and decreased hippocampal grey matter volume in middle aged adults (Marsland et al., 2008). In-vitro studies have demonstrated that IL-6 improves the survival of different classes of neurons from ischemic injuries and excitotoxic challenges (Baune et al., 2012). It is also reported that IL-6 promote growth of axons and increases the number of synapses (Toulmond et al., 1992; Yamada et al., 1994; Wu et al., 1996, Gadient et al., 1997, Ihara et al., 1996). Moreover, IL-6 has been found to regulate the survival of differentiated neurons along with the development of astrocytes

(Kahn et al., 1994; Murphy et al., 1997). Overall, the above findings suggest that the IL-6 level is associated with neuroinflammation, neurodegeneration and neuroprotection.

Interleukin-10 (IL-10) is a member of anti-inflammatory cytokine family, plays an important role in suppressing proinflammatory cytokines such as TNF- α, IL-1, IL-6 implicated in neuropathic pain (Moore et al., 2001; Chernoff et al., 1995; Conti et al., 2003). It has also been reported that IL-10 downregulates proinflammatory cytokine receptor expression (Sawada et al., 1999). The biological half-life of IL-10 is very short, hence restricts its direct use for treating neuropathic pain. Nevertheless, IL-10 is one of the most important regulators of the immune response.

Introduction…

Neuroinflammation is a devastating condition that results from wide spread acute systemic inflammation and/or direct involvement of the central nervous system such as in bacterial meningitis (Lee et al., 2008; Barichello et al., 2011). The condition is characterized by alteration of blood-brain barrier permeability, leucocytes infiltration, up-regulation of aquaporin-4, activation of microglia, astrocytosis and apoptotic cell death (Alexander et al., 2008). Epidemiological data suggests about 71% of all patients suffering from systemic inflammatory response syndrome with infection in the intensive care unit develops acute irreversible cerebral dysfunction (Semmler et al., 2008).

Increase in blood-brain barrier (BBB) permeability is a hallmark feature of inflammatory conditions of the central nervous system, as detected in bacterial meningitis, multiple sclerosis, stroke and Parkinson's disease (Weiss et al., 2009). Multiple sclerosis - afflicted brains showed greater BBB permeability to activated leucocytes and peripheral inflammatory mediators in the affected areas (Lopez-Ramirez et al., 2012). BBB disruption in neuroinflammation involves production of cytokines and other chemical substances (Aid et al., 2010). These signalling peptides, after being synthesized and secreted from the cells, diffuse into the interstitial fluid of the brain and provide signals to neighbouring cells (Wang et al., 2008). Neuropathological and imaging studies demonstrate that loss of BBB integrity precede neuronal damage in many conditions (Kapurel et al., 2002; Banks et al., 1999; Frank-Cannon et al., 2009). Thus, early detection of compromised BBB function could potentially permit intervention to prevent irreversible brain damage.

To study the deleterious effects of neuroinflammation on CNS function, direct access to the brain interstitial fluid is needed in order to dynamically assess inflammatory markers. Microdialysis is a widely used technique for studying neurotransmitters, metabolites, inflammatory markers or drugs within the brain. In Alzheimer disease microdialysis has been instrumental in establishing the dynamics of amyloid beta production and clearance in vivo. Several studies have been performed using microdialysis as a tool, in order to recover signalling peptides and proteins (Kendrick et al., 1990; Asai et al., 1996; Sjorgen et al., 2002; Winter et al., 2002, Riese et al., 2003; Sopasakis et al., 2004). However, the method suffers several intrinsic drawbacks: The main disadvantage of microdialysis sampling method is the formation of a glial scar with time surrounding the microdialysis probe, hence creating a completely different micro-environment and influence cytokine recovery (Wisniewski et al., 2001; Bungay et al., 2003). A recent microdialysis study showcased

intracerebral cytokines measurement immediately after probe implantation (Takeda et al., 2011). Detection and estimation of cytokines from brain interstitial fluid are difficult because of their chemical nature, low recovery rate and non-specific adsorption to the outlet tubing or microdialysis membrane. Moreover, tissue analysis for mRNA expression levels of these signalling peptides does not always correlate with the protein levels (Lord et al., 2001).

To overcome these inherent disadvantages we have recently developed cerebral open flow microperfusion (cOFM). During an earlier study, we demonstrated that BBB disruption due to cOFM probe implantation in the frontal cortex of rat heals within 15 days. In addition, we showed that cOFM is a promising technique for monitoring transport of substances across the intact BBB (Birngruber et al., 2013). The cOFM probe lacks the membrane used during microdialysis and combines push pull perfusion that allows perfusate to mix directly with brain interstitial fluid, providing access to a wide range of compounds regardless of their size or lipophilicity. Moreover, even minor alterations of BBB permeability can be detected with the help of a suitable low molecular weight marker such as sodium fluorescein (NaF). Of note, the potential contribution of blood (retained in the brain vasculature) to cytokine and chemokine levels in brain can be excluded when applying cOFM (Erikson et al., 2011). During the present study we aimed to characterize the suitability of cOFM to monitor BBB function and the neuroinflammatory response in a rat model.

Aim…

In this study, we adopted a well-characterised rodent model of systemic inflammation induced by lipopolysaccharide (LPS) (Fannin RD et al., 2005) to study neuroinflammation and utilized sodium fluorescein as a marker for BBB permeability. Systemic administration of LPS produces neuroinflammation which includes BBB disruption (Watkins et al. 1995), release of cytokine (Reyes et al. 1999, Verma et al. 2006), increase in immune cell adherence and passage (De Vries et al. 1994, Persidsky et al. 1997) and alteration of transport systems (Banks et al 2008, Minami 1998, Nonaka 2005, Xiao et al. 2001). Using cOFM, we investigated blood brain barrier permeability in neuroinflammation over a prolonged period and monitored the dynamic time profile changes of some cytokines such as tumour necrosis factor alpha (TNF-alpha), interleukin-6 (IL-6) and interleukin-10 (IL-10) in brain and serum.

Materials and methods…

Animals

All animal protocols used in this study were approved by the Austrian Ministry of Science and Research Ref.II/10b, Vienna. A total of 38 adult male Sprague Dawley rats (Harlan Laboratories, Udine, Italy) weighing approximately 350 – 450 g were used for the study. The animals were housed in a 12 h light / dark cycle with food and water available *ad libitum*. Animals were allowed at least 1 week after transportation to acclimatise to the environment prior to any surgical procedure. Appropriate animal care such as cleaning of cage, bedding etc. was provided by the resource staffs at the animal care facility centre (Institute for Biomedical Research, Medical University of Graz, Austria).

cOFM probe

The cOFM probe consists of a 20Ga guide tube (Perfluorethylenpropylen – FEP) and two 25Ga inflow/outflow tubing with a low adhesion surface (Polytetrafluorethylen – PTFE). After fabrication, cOFM probes were sterilized by storage in ethanol and then packaged aseptically. During implantation, a healing dummy was placed in the guide tube allowing tissue regeneration and preventing tissue migration into guide tube (Fig.1A). On the day of perfusion, the healing dummy was replaced by inflow/outflow tubing (Fig.1B) and cOFM perfusate was pushed into brain tissue and withdrawn at a flow rate of 1 µl/min.

cOFM perfusate

cOFM standard perfusate was composed to match brain extracellular fluid in order to avoid chemical stress for the BBB (modified from McNay and Sherwin, 2004). Perfusate composition: 123 mM NaCl, 0.4 mM MgCl2 (purity ≥ 98%), 0.7 mM CaCl2 (purity ≥ 93%), 4.3 mM KCl, 1.3 mM NaH_2PO4, 21 mM Na_2HPO4, 4 mM glucose. All reagents were dissolved in sterile water (Aqua bidest, Fresenius Kabi, Austria). In order to remove possible bacterial contamination the perfusate was filtered through a 0.22 µm sterile filter (Thermo Fisher Scientific, Germany). All following steps were carried out under sterile conditions.

Surgery and implantation of cOFM probe

For cOFM probe implantation, the rats were anaesthetised with a combination (2:2:1) of Fentanyl® (0.05 mg/ml; Janssen-Cilag Pharma, Austria), Midazolam® (5 mg/ml; Janssen-Cilag Pharma, Austria) and Domitor® (0.1 mg/ml, Pfizer Corporation, Austria). A dose of 0.15 ml/100gm of body weight was given subcutaneously. The rats were prepared for

surgery by shaving the head and placed in a stereotactic frame (KOPF Instruments, USA). The surgical area of the scalp was disinfected using 70% ethanol and a 2 cm midline incision was made to expose the skull. cOFM probes were implanted unilaterally in the left prefrontal cortex navigating bregma (2 mm left from midline, 0 mm anterior to bregma and 1.5 mm below the dura) under anaesthesia as described above. A hole of 1 mm diameter for cOFM probe was made on the skull with the help of a dental drill with great care without harming the dura mater. Afterwards, the dura mater was carefully punctured with fine forceps. Two more holes of same diameter were made posteriorly (3.5 – 4 mm) on the skull to fix the anchor screws. The cOFM probe was inserted slowly in the brain with the help of a manipulator arm (Kopf, USA) and glued together with the anchor screws already placed on the skull with dental cement (i–CEM, Heraeus Kulzer GmbH) and hardened by UV-irradiation. The manipulator arm was then carefully screwed off and detached from the cOFM probe. The surgical procedure was completed within 30 min after initial induction with Isoflurane for each rat. Following surgery, rats were individually housed in specially designed cages under same conditions. After surgery, the animals received a mixture of Anexate® (0.1 mg/ml; Roche Austria GmbH) and Antisedan® (0.5 mg/ml; Pfizer Corporation, Austria) (5: 0.1). For two days after surgery a daily dose of antibiotic Claforan® (5 mg/100gm; Sanofi-aventis GmbH, Wien) and Rimadyl® (Carprofen 50 mg/ml; Pfizer Corporation, Austria) were injected subcutaneously.

Systemic inflammation

To produce acute systemic inflammation rats were injected i.p. with 5 mg/kg lipopolysaccharide (LPS; Escherichia coli 0111:B4, Sigma-Aldrich GmbH, Wien, Austria) after collection of a baseline cOFM sample. LPS was dissolved in 0.5 ml pyrogen-free sterile normal saline (0.9%) just before use and injected intraperitoneally. Control animals received the same volume of pyrogen-free normal saline.

Determination of BBB integrity 15 days following cOFM probe implantation

BBB integrity was tested 15 days after cOFM probe implantation as described in section 2.4.

Determination of BBB permeability in LPS treated rats

cOFM probe implantation into the frontal lobe of the left hemisphere of the rat brain was performed as described above. Fifteen days post surgery the healing dummy was

exchanged with inflow and outflow tubing to allow sampling. Perfusion was started one hour after healing-dummy exchanged. Sampling was started two and half hours after healing-dummy exchange, and was performed hourly for seven hours (Fig.6). During sampling, subjects were anesthetized with inhaled isoflurane (1 % in 0.5 l/min oxygen, Abbott, Canada). A bolus injection of NaF (11 mg/kg in physiological saline) was administered in the femoral vein 1h after perfusion started followed by a constant infusion of NaF (11 mg/kg/h in physiological saline) in order to maintain a steady NaF concentration in the blood. In the LPS treated group (n = 6), animals were injected i.p. 5 mg/kg LPS after collection of a baseline cOFM sample in order to establish the basal NaF penetration into the brain whereas the control group (n = 6) received same volume of normal pyrogen free saline.

Cytokine measurement

TNF-alpha, IL-6 and IL-10 were measured in the cOFM perfusate and in serum. cOFM samples were directly stored at -80^0 C until further use. Blood was collected from femoral vein and mixed with commercially available blood clot enhancer (S-Monovette; Sarstedt, Nümbrecht, Germany). After 30 minutes, centrifugation was performed for 10 min at 1000xg and serum was removed and stored in low adhesion polypropylene tube at -80^0 C until further analysis. Levels of cytokines were measured using commercially available multiplexed cytokine analysis kit (RCYTO-80K) as recommended by the manufacturer (Millipore GmbH, Austria). The limit of detection of the assays was 4.44 pg/ml for TNF-alpha, 9.8 pg/ml for IL-6, and 5.41 pg/ml for IL-10.

(This measurement was done by the analytical team, Joanneum Research).

Statistical analysis

Statistical analysis was performed using PASW statistics 19 (SPSS, USA). A Shapiro-Wilk test was used to examine normal distribution. A Mann-Whitney U Test was performed to determine the level of significance for the BBB permeability study and brain cytokine analysis. We used the one-sample Wilcoxon signed-rank test for serum cytokine analysis. p values < 0.05 were considered significant.

Results…

Determination of BBB integrity

In a first round of experiments BBB integrity was tested in cOFM probe implanted rats (n = 6) 15 days post implantation. NaF concentration in brain biopsies from left hemisphere (LH) containing the probe insertion site were compared to biopsies from the right hemisphere (RH) with intact brain tissues. The ratio of NaF concentrations in brain biopsies in cOFM probe implanted left hemisphere (LH) and the corresponding right hemisphere (RH) was compared to that of unimplanted (naïve) rats (n = 6). No significant difference was found between unimplanted (1.25 ± 0.16) and implanted (1.21 ± 0.23) groups (Fig. 21).

Next we time-dependently monitored alterations of BBB function in vivo in response to a single systemic LPS bolus by quantitating NaF accumulation in the cOFM perfusate. These analyses revealed that in response to LPS the NaF concentration in the cOFM perfusate was elevated over baseline after 2 h (Fig. 22). At the end of the experiment (6 h) NaF concentrations in the cOFM perfusate was 3.5-fold higher in LPS treated rats (311.5 ng/ml vs. 87.8 ng/ml; LPS vs. saline). These data clearly demonstrate that cOFM is well suited to detect alterations of BBB permeability in living animals.

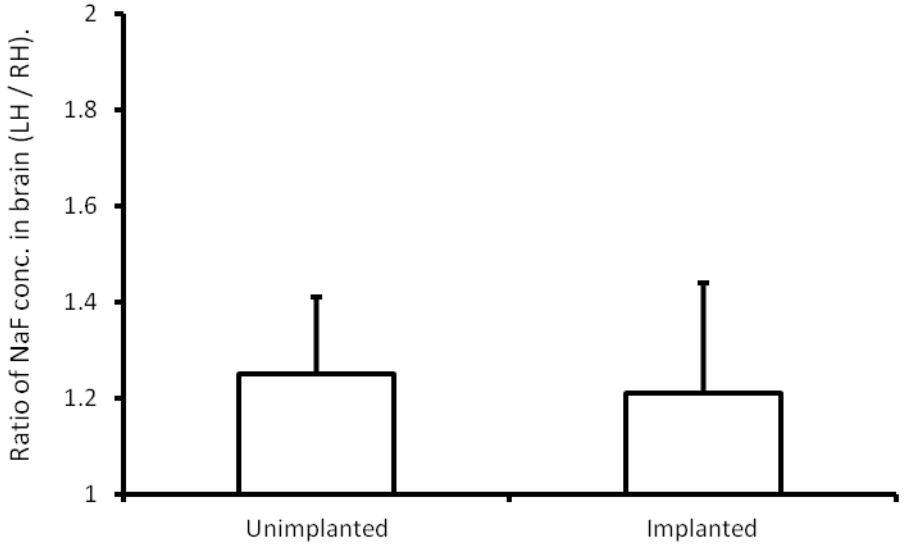

Fig. 21 – Concentration of NaF in brain biopsies in unimplanted and 15 days following cOFM probe implanted group.

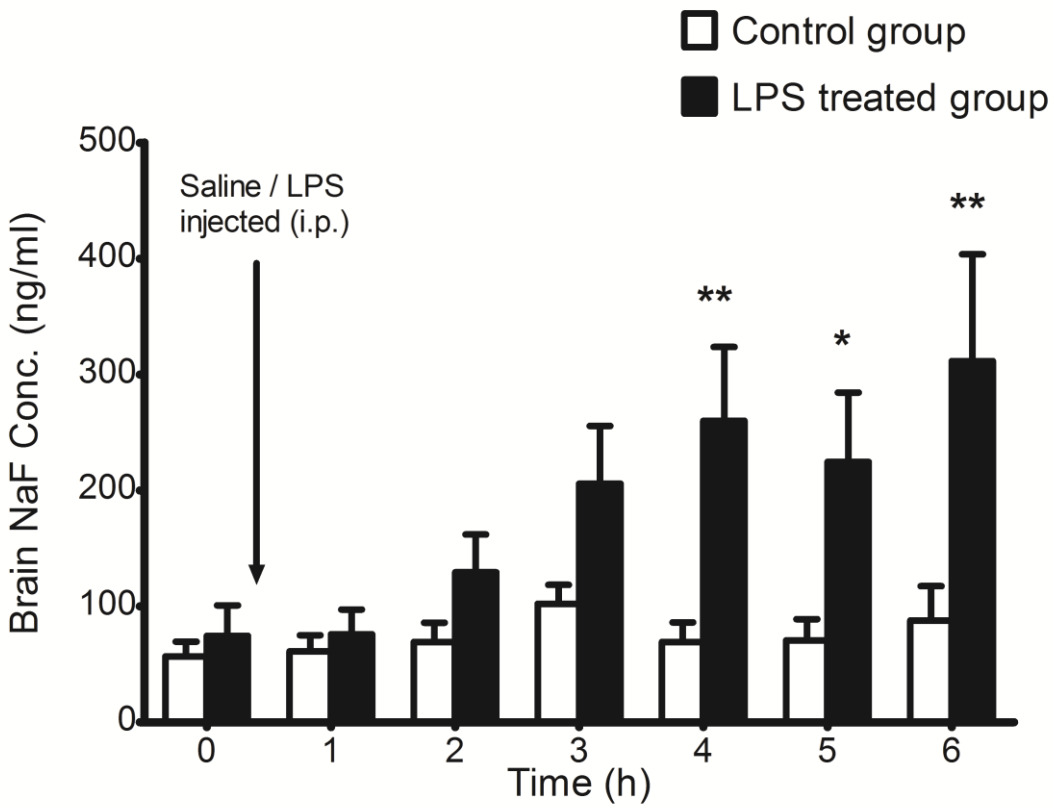

Fig. 22 – LPS induced changes in BBB permeability (* $p < 0.05$, ** $p < 0.01$).

Measurement of TNF-alpha in the brain and serum

Intraperitoneal injection of LPS resulted in an increase in TNF-alpha concentration after 2 h in the frontal cortex, with a significant increase 3 to 6 hours after LPS administration (12.08 cf. 8.33 ng/ml; $p < 0.05$ (Fig. 23). In the control group (saline injected; $n = 7$), the concentration of TNF-alpha was very low (< 0.004 ng/ml) throughout the experiments. On the other hand, a sharp increase of TNF-alpha serum concentrations was detected 2 h after LPS administration, reaching the highest concentration at 3 h (246-fold higher than in brain). In contrast to the brain, TNF-alpha concentration in the serum decreased 58-fold (about 2% of maximum serum TNF-alpha concentration) 6 h post LPS administration (Fig. 24).

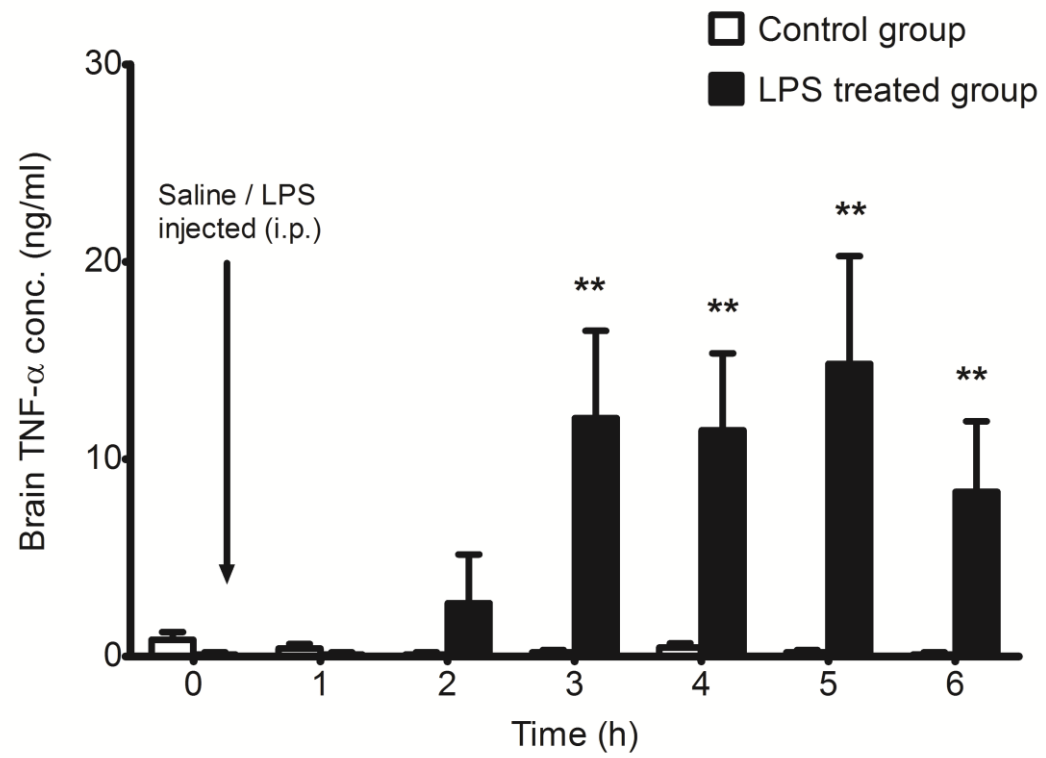

Fig. 23 - LPS induced changes in intracerebral concentration of TNF-α, (** $p < 0.01$).

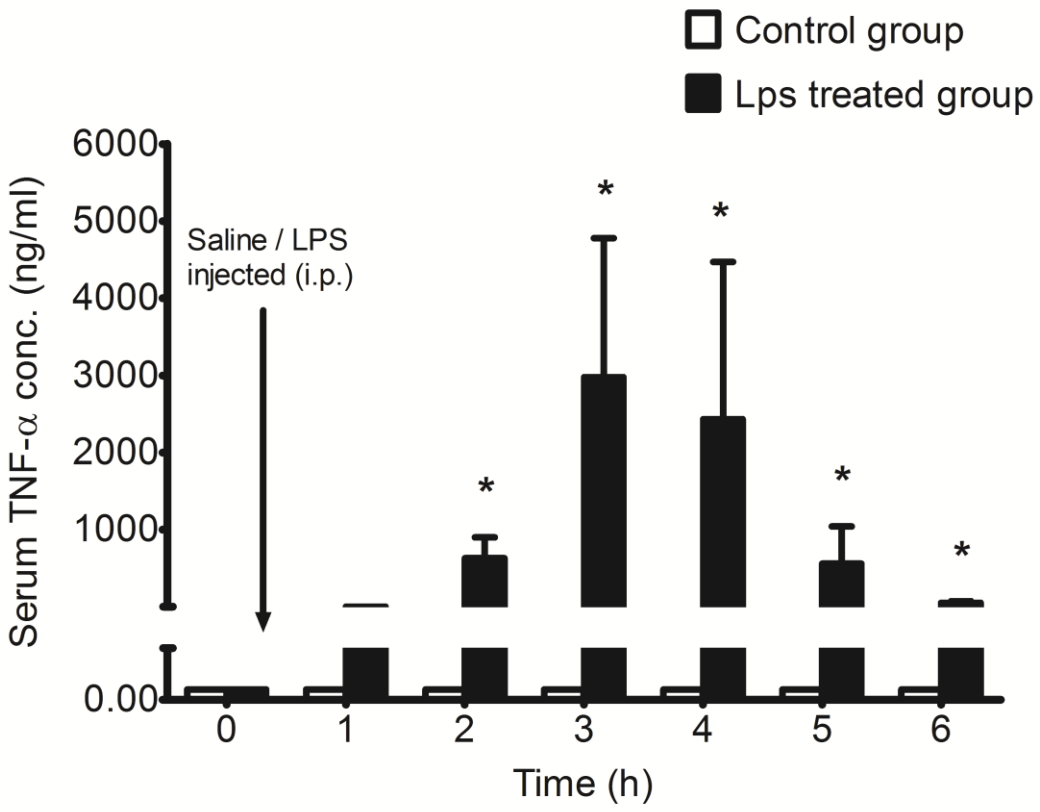

Fig. 24 - LPS induced changes in serum concentration of TNF-α, (* $p < 0.05$).

Measurement of IL-6 in the brain and serum

We observed a gradual increase in intracerebral concentration of IL-6 at later (4 – 6 h) time points post LPS application. The IL-6 concentration was significantly higher ($p < 0.05$) in the cOFM sample than in the control 5 hours after LPS administration (Fig. 25). A similar time-dependent increase of IL-6 concentration was observed in the serum; however, in contrast to brain, the level of IL-6 showed a marked decline at 6 h (Fig. 26).

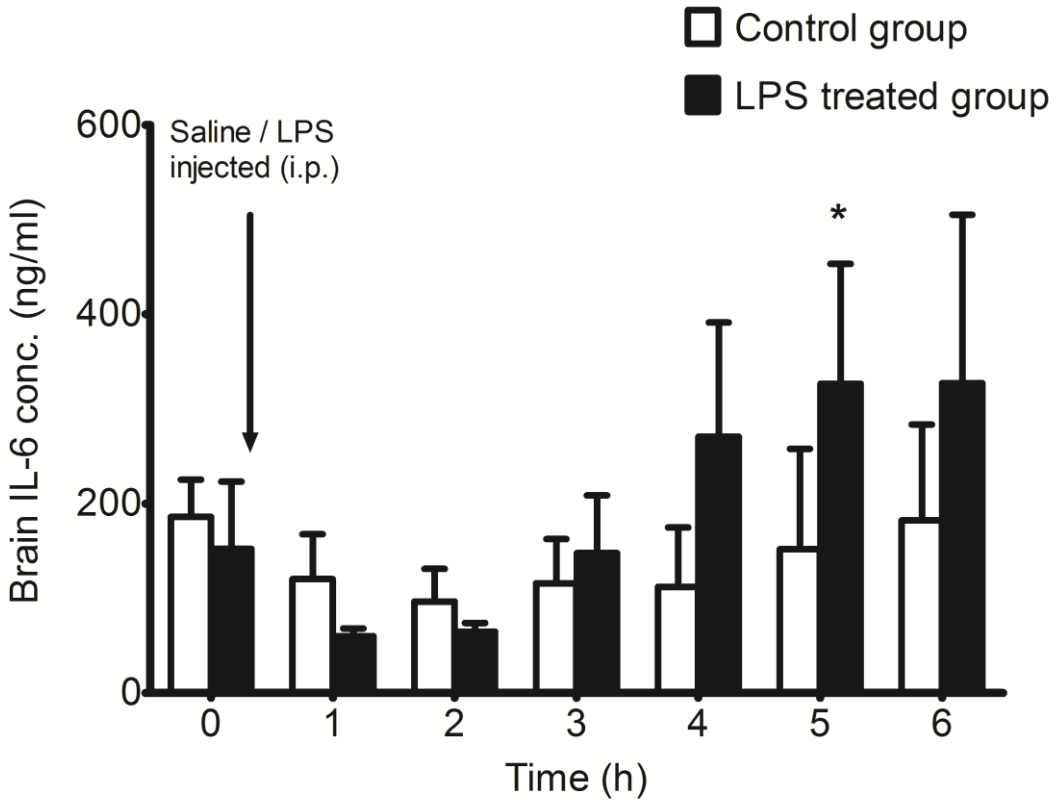

Fig. 25 - LPS induced changes in intracerebral concentration of IL-6, (* $p < 0.05$).

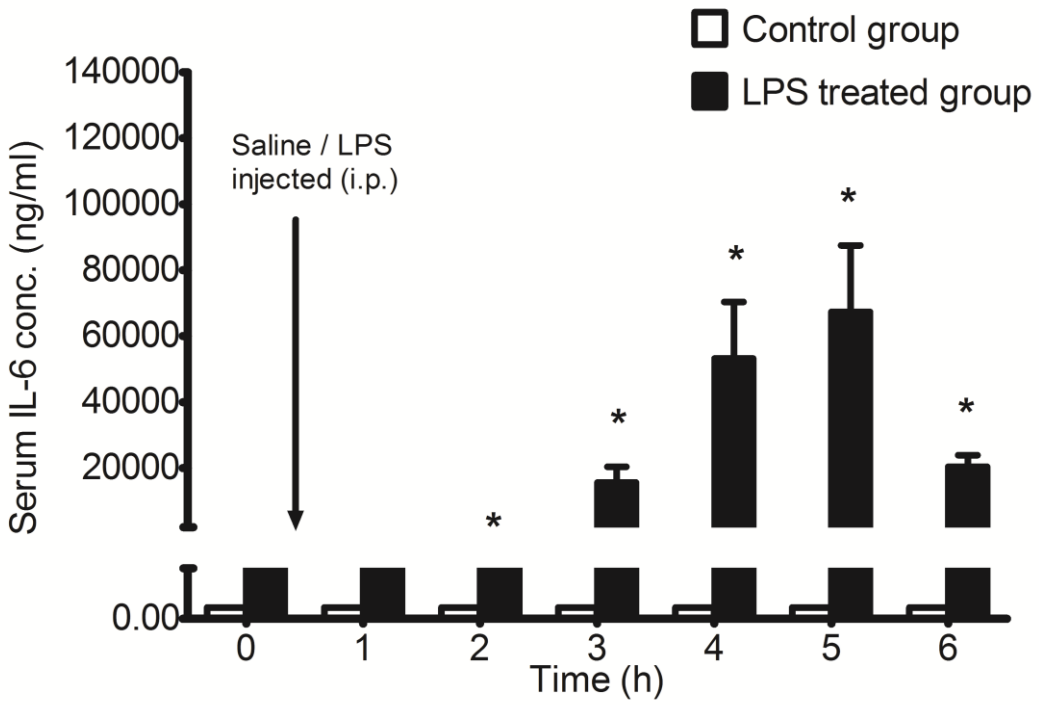

Fig. 26 - LPS induced changes in serum concentration of IL-6, (* $p < 0.05$).

Measurement of IL-10 in brain and serum

It was also interesting to see whether the synthesis of anti-inflammatory cytokine IL-10 was affected in response to systemic LPS. The intracerebral concentration of IL-10 was significantly higher ($p < 0.05$) at 4 and 5 hours post LPS injection, showing a constant increase with time (Fig. 27). In contrast, elevated IL-10 levels were detected in the serum after 2 h with a peak after 4 hours followed by a gradual decline (Fig. 28). These results reveal dynamic changes in the levels of intracerebral cytokines in an early phase of neuroinflammation triggered by acute systemic inflammation.

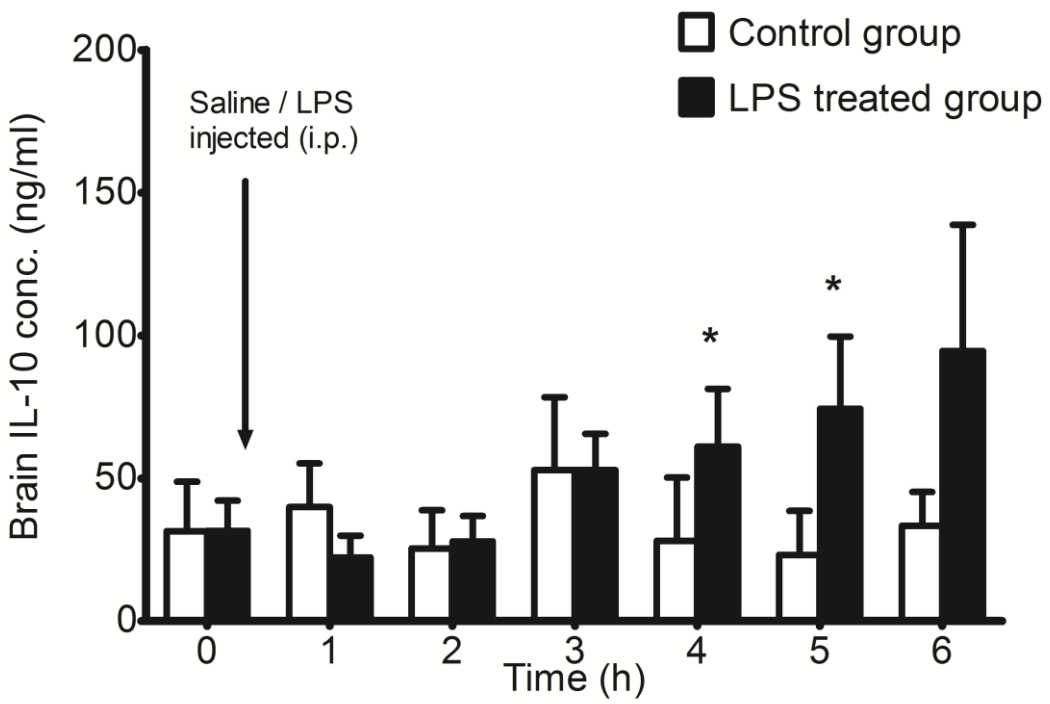

Fig. 27 - LPS induced changes in intracerebral concentration of IL-10, (* $p < 0.05$).

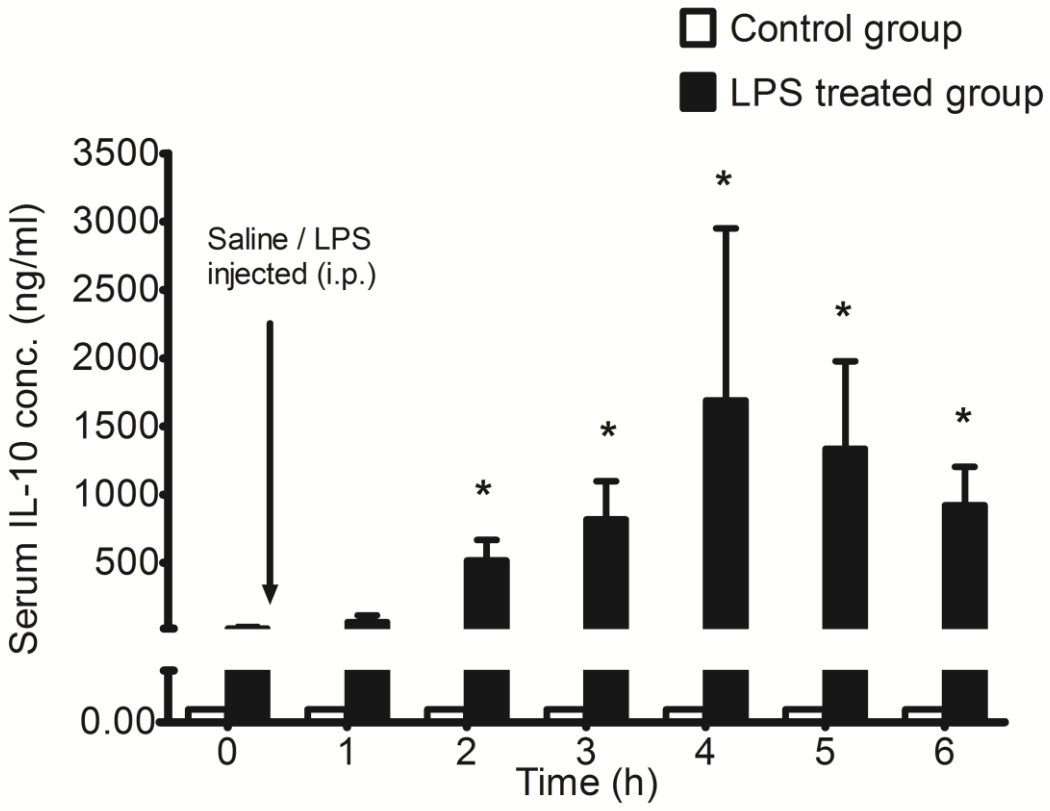

Fig. 28 - LPS induced changes in serum concentration of IL-10, (* $p < 0.05$).

Discussion…

BBB hyper-permeability may lead to neurotoxicity and is implicated in the pathophysiology of neuroinflammation (Weiss et al., 2009). Data obtained during the present study provide in vivo evidence that cOFM is a convenient experimental tool to time-dependently monitor BBB function and the neuroinflammatory response in living animals. Using this newly established technology we found that peripheral LPS administration induced severe BBB dysfunction (monitored by NaF accumulation in the cOFM samples), and was accompanied by increased production of pro- (TNF-alpha and IL-6) and anti-inflammatory (IL-10) cytokines in brain interstitial fluid. Furthermore we showed that TNF-alpha concentrations in brain extracellular fluid and serum increased rapidly, whereas IL-6 and IL-10 production lagged behind approximately 1 h.

cOFM perfusate closely resembles the brain extracellular fluid, therefore compatible with a wide array of analytical techniques and on-line analysis can produce near real-time results with high temporal resolution providing benefits for pharmacokinetic studies in neurosciences. Of note, the concentration of intracerebral cytokines in cOFM samples was 1000-fold higher as compared to conventional microdialysis studies indicating superior recovery. In addition, cOFM overcomes some of the inherent disadvantages of microdialysis. Nevertheless, as in microdialysis, implantation of cOFM probes is invasive and causes injury to brain tissue with local BBB disruption. To clarify this issue we have time dependently measured BBB function after cOFM probe implantation (NaF was used as reporter molecule). These experiments revealed that BBB function re-established 15 d post probe implantation, which is in line with one of our previous reports (Birngruber et al., 2013).

In response to a single injection of LPS we have observed significant breakdown of BBB function as indicated by increased NaF concentrations in the cOFM perfusate. Since we have not analysed the tight junction architecture or signalling events the mechanisms that induce BBB dysfunction are not clear. Although LPS only minimally penetrates the intact BBB (Rosenberg, 2002) signal transduction via Toll-like receptors on brain endothelial cells (Nagyoszi et al., 2010) can elicit downstream events that are implicated in the disruption of the tight-junction architecture. Upon activation, RhoA, nuclear factor kappa B, Phosphoinositide 3-kinase, myosin light chain kinase, protein kinase C or the MAPK members have been shown to participate in these pathophysiological processes (Schreibelt et al., 2007; Üllen et al., 2013; Dohgu et al., 2011; He et al., 2011). Ultimately output of

these signalling cascades can impact on barrier function by directly affecting tight junction architecture proteins or by mediating indirect effects on junctional complexes via cytoskeletal arrangements (Stamatovic et al., 2008).

In addition to the structural barrier that is formed by brain microvascular endothelial cells, the BBB also fulfils an important biochemical barrier function. This is achieved through polarized expression of highly specific transport systems on brain endothelial cells (Zlokovic, 2008). Many of these specific transport systems show altered function under inflammatory conditions suggesting that inflammation can affect disease progression via the BBB. Along the same line, transport of insulin, leptin, amyloid beta or TNF-alpha is affected by peripheral LPS administration (Xiao et al., 2001; Nonaka et al., 2004; Jaeger et al., 2009; Osburg et al., 2002). Although the underlying mechanisms are not completely understood, cytokines and chemokines are presumed to play a central role in these processes. Rosenberg et al. demonstrated that endotoxin-induced vascular endothelial permeability is due to the release of cytokines, free radicals, matrix-metalloproteinases, nitric oxide and products of the arachidonic acid cascade (Rosenberg et al., 1993; Rosenberg, 2002).

During the present study, we monitored LPS-induced BBB disruption in individual animals over a period of 6 h and measured the kinetics of TNF-alpha, IL-6 and IL-10 production in serum and brain by cOFM after a single LPS injection. In this regard, it is important to note that cytokine profiles that develop during the inflammatory response heavily depend on the LPS injection paradigm (Erickson et al., 2011). In terms of time dependency, we found that the inflammatory response in brain resolves more slowly than the peripheral response, which is in line with previous observations (Erickson et al., 2011; Qin et al., 2007). This might be due to different Toll-like receptor signaling in the brain (Chakravarty et al., 2005) and the periphery (Steiner et al., 2006) as well as minimal penetration of LPS across the BBB (Banks et al., 2010).

Under normal physiological conditions, the basal level of TNF-alpha remains low, but TNF-alpha concentration increases in acute inflammation, trauma and autoimmune diseases (Pan et al., 2001). In LPS-treated group, brain TNF-alpha concentrations started to increase 2 h post LPS injection which coincides with the time course of BBB dysfunction indicating a relationship between TNF-alpha production and BBB function. This is

supported by a previous report demonstrating that BBB disruption in sepsis is mediated by TNF-alpha signalling through TNFR1 (Alexander et al., 2008). In addition, it was shown that TNF-alpha is responsible for increased BBB permeability in E.coli induced meningitis (Tsao et al., 2001). In an MPTP-induced mouse model of Parkinson disease it was shown that TNF-alpha knockout also significantly attenuated BBB dysfunction (Zhao et al., 2007). However, it is noteworthy that LPS from different sources can affects BBB function differently, despite equally increased serum TNF-alpha levels (Jin et al., 2013).

In the present study we noticed that the increase in serum TNF-alpha was transient and decreased dramatically at 6 h. In contrast, brain TNF-alpha remained elevated throughout the experiment indicating slower resolution of the inflammatory response in the brain, findings that are in line with results obtained in LPS mouse models (Erickson et al., 2011; Qin et al., 2007).

In addition, we observed delayed intracerebral production of IL-6 in response to peripheral LPS challenge. This could indicate indirect stimulation of intracerebral IL-6 production via TNF-alpha. Results from a chemokine network analysis in an LPS mouse model are in support of this notion (Erickson et al., 2011). Along the same line, an earlier study demonstrated that LPS-induced production of IL-6 in brain was mediated by TNF (Ghezzi et al., 2000). It was also shown that TNF-alpha and IL-1 induce release of IL-6 by lymphocytes, glial cells and neurons (Godbout et al., 2004). Moreover, immunohistochemical studies on brain sections revealed an early appearance of TNF-alpha and IL-1beta positive cells followed by IL-6 positive cells in excitotoxic brain lesion (Acarin et al., 2000). Therefore, it is plausible that a synergistic action between TNF-alpha and IL-6 contributes to a self-propelling neuroinflammatory environment.

The decrease in concentration of proinflammatory cytokines in the serum after LPS administration was probably due to the gradual increase in anti-inflammatory IL-10. This fact is supported by an earlier observation that IL-10 can suppress synthesis of proinflammatory cytokines such as TNF-alpha, IL-6, and IL-1, by targeting circulating immune cells, liver and spleen (Jancálek et al., 2010; Harden et al., 2013) and can down-regulate receptors for proinflammatory cytokines (Sawada et al., 1999). We observed a slight increase in serum IL-10 as early as 1 h after LPS injection. In contrast, we found that the brain concentration of IL-10 gradually increased and remained significantly elevated

until the end of the experiment. Generally, an increase in anti-inflammatory cytokines levels results in the subsequent decline of proinflammatory cytokines with time, as we documented in this study. Therefore, it remains unclear why intracerebral TNF-alpha and IL-6 levels remained high despite the higher intracerebral concentration of IL-10. It was previously reported that a single intraperitoneal injection of LPS provoked a rapid increase of TNF-alpha that lasted for months (Qin et al., 2007). Therefore, it seems that the production of anti-inflammatory cytokines such as IL-10 in brain is insufficient to attenuate TNF-alpha production. In addition it was shown that IL-10 mRNA in the cortex had returned to baseline levels 8 hours after a single LPS injection (Henry et al., 2009). Moreover, the biological half-life of IL-10 is very short (Jancálek et al., 2010; Li et al. 1999). Studying all of them including other factors which might play a role in LPS induced BBB disruption over an extended period of time was beyond the scope of this present study.

In summary, we have performed a time-dependent cytokine analysis (TNF-alpha, IL-6 and IL-10) in the frontal cortex of the rat brain in response to a single peripheral administration of lipopolysaccharide (LPS) by using the newly developed technique, cOFM. We monitored BBB function by using sodium fluorescein as low-molecular-weight reporter in the cOFM sample. Our data clearly demonstrate that cOFM is well suited for detecting alterations of BBB permeability in living animals, and monitoring changes in brain cytokine levels during the neuroinflammatory response.

References…

Aasmundstad TA, Mørland J, Paulsen RE (1995). Distribution of morphine 6-glucuronide and morphine across the blood-brain barrier in awake, freely moving rats investigated by in vivo microdialysis sampling. J Pharmacol Exp Ther **275**(1):435–441.

Abbott NJ (2002). Astrocyte-endothelial interactions and blood-brain barrier permeability. J Anat 200(6):629-638.

Abbruscato TJ, Lopez SP, Mark KS, Hawkins BT, Davis TP (2002). Nicotine and cotinine modulate cerebral microvascular permeability and protein expression of ZO-1 through nicotinic acetylcholine receptors expressed on brain endothelial cells. J Pharm Sci **91**(12):2525–2538.

Abnet K, Fawcett JW, Dunnett SB (1991). Interactions between meningeal cells and astrocytes in vivo and in vitro. Brain Res Dev Brain Res **59**(2):187–196.

Acarin L, Gonzalez B, Castellano B (2000). Neuronal, astroglial and microglial cytokine expression after an excitotoxic lesion in the immature rat brain. Eur J Neurosci **12**(10): 3505-3520.

Adibhatla RM, Hatcher JF (2008). Tissue plasminogen activator (tPA) and matrix metalloproteinases in the pathogenesis of stroke: therapeutic strategies. CNS Neurol Disord Drug Targets **7**(3):243-253.

Aid S, Silva AC, Candelario-Jalil E, Choi SH, Rosenberg GA, Bosetti F (2010). Cyclooxygenase-1 and -2 differentially modulate lipopolysaccharide-induced blood-brain barrier disruption through matrix metalloproteinase activity. J Cereb Blood Flow Metab **30**(2):370-380.

Alexander JJ, Jacob A, Cunningham P, Hensley L, Quigg RJ (2008). TNF is a key mediator of septic encephalopathy acting through its receptor, TNF receptor-1. Neurochem Int **52**(3):447-456.

Ao X, Stenken JA (2006). Microdialysis sampling of cytokines. Methods **38**(4): 331-341.

Asai S, Kohno T, Ishii Y, Ishikawa K (1996). A newly developed procedure for monitoring of extracellular proteins using a push-pull microdialysis. Anal Biochem **237**(2):182-187.

Armulik A, Genovè G, Mäe M, Nisancioqlu MH, Wallgard E, Niaudet C et al. (2010). Pericytes regulate the blood-brain barrier. Nature **468**(7323):557-561.

Azemi E, Lagenaur CF, Cui XT (2011). The surface immobilization of the neural adhesion molecule L1 on neural probes and its effect on neuronal density and gliosis at the probe/tissue interface. Biomaterials **32**(3):681–692.

Bálint Z, Krizbai IA, Wilhelm I, Farkas AE, Párducz A, Szegletes Z, et al (2007). Changes induced by hyperosmotic mannitol in cerebral endothelial cells: an atomic force microscopic study. Eur Biophys J **36**(2):113–120.

Banks WA (1999). Physiology and pathology of the blood-brain barrier: implications for microbial pathogenesis, drug delivery and neurodegenerative disorders. J Neurovirol **5**(6): 538-555.

Banks WA, Robinson SM (2010). Minimal penetration of lipopolysaccharide across the murine blood-brain barrier. Brain Behav Immun **24**(1): 102-109.

Barichello T, dos Santos I, Savi GD, Simões LR, Silvestre T, Comim CM, et al. (2010). TNF-alpha, IL-1beta, IL-6, and cinc-1 levels in rat brain after meningitis induced by Streptococcus pneumoniae. J Neuroimmunol **221**(1-2):42-45.

Barichello T, Pereira JS, Savi GD, Generoso JS, Cipriano AL, Silvestre C, et al. (2011). A kinetic study of the cytokine/chemokines levels and disruption of blood-brain barrier in infant rats after pneumococcal meningitis. J Neuroimmunol **233**(1-2):12-17.

Bauer H-C, Traweger A, and Bauer H (2004) Proteins of the tight junction in the blood-brain barrier, in Blood-Spinal Cord and Brain Barriers in Health and Disease (Sharma HS and Westman J eds) pp 1–10, Elsevier, San Diego.

Baune BT, Konrad C, Grotegerd D, Suslow T, Birosova E, Ohrmann P et al., (2012). Interleukin-6 gene (IL-6): a possible role in brain morphology in the healthy adult brain. J Neuroinflammation **9**:125.

Bazzoni G, Martinez-Estrada OM, Mueller F, Nelboeck P, Schmid G, Bartfai T et al. (2000). Homophilic interaction of junctional adhesion molecule. J Biol Chem **275**(40): 30970-30976.

Benveniste H, Drejer J, Schousboe A, Diemer NH (1984). Elevation of the extracellular concentrations of glutamate and aspartate in rat hippocampus during transient cerebral ischemia monitored by intracerebral microdialysis. J Neurochem **43**(5):1369–1374.

Benveniste H, Drejer J, Schousboe A, Diemer NH (1987). Regional cerebral glucose phosphorylation and blood flow after insertion of a microdialysis fiber through the dorsal hippocampus in the rat. J Neurochem **49**(3):729–734.

Benveniste H, Hansen AJ, Ottosen NS (1989). Determination of brain interstitial concentrations by microdialysis. J Neurochem **52**(6):1741-1750.

Bernoud N, Fenart L, Benistant C, Pageaux JF, Dehouck MP, Moliere P et al. (1998). Astrocytes are mainly responsible for the polyunsaturated fatty acid enrichment in blood-brain barrier endothelial cells in vitro. J Lipid Res **39**(9):1816-1824.

Berry M, Maxwell WL, Logan A, Mathewson A, McConnell P, Ashhurst DE, et al. (1983). Deposition of scar tissue in the central nervous system. Acta Neurochir Suppl (Wien) **32**:31-53.

Betanzos A, Huerta M, Lopez-Bayghen E, Azuara E, Amerena J, Gonzalez-Mariscal L (2004). The tight junction protein ZO-2 associates with Jun, Fos and C/EBP transcription factors in epithelial cells. Exp Cell Res **292**(1):51–66.

Biran R, Martin DC, Tresco PA (2005). Neuronal cell loss accompanies the brain tissue response to chronically implanted silicon microelectrode arrays. Exp Neurol **195**(1):115-126.

Birngruber T, Ghosh A, Perez-Yarza V, Kroath T, Ratzer M, Pieber TR et al. (2013). cOFM: a novel in vivo technique to continuously measure substance transport across the intact blood-brain barrier. Clin Exp Pharmacol Physiol **40**(12):864-871.

Bodenlenz M, Schaupp L, Druml T, Sommer R, Wutte A, Schaller HC, et al. (2005). Measurement of interstitial insulin in human adipose and muscle tissue under moderate hyperinsulinemia by means of direct interstitial access. Am J Physiol Endocrinol Metab **289**(2):E296-E300.

Bodenlenz M, Höfferer C, Magnes C, Schaller-Ammann R, Schaupp L, Feichtner F, et al. (2012). Dermal PK/PD of a lipophilic topical drug in psoriatic patients by continuous intradermal membrane-free sampling. Eur J Pharm Biopharm **81**(3):635-641.

Bolton SJ, Anthony DC, Perry VH (1998) Loss of the tight junction proteins occludin and zonula occludens-1 from cerebral vascular endothelium during neutrophil-induced blood-brain barrier breakdown in vivo. Neuroscience **86**(4):1245–1257.

Borland LM, Shi G, Yang H, Michael AC (2005). Voltammetric study of extracellular dopamine near microdialysis probes acutely implanted in the striatum of the anesthetized rat. J Neurosci Methods 146(2):149–158.

Braet K, Paemeleire K, D'Herde K, Sanderson MJ, and Leybaert L (2001). Astrocyte-endothelial cell calcium signals conveyed by two signalling pathways. Eur J Neurosci **13**(1):79–91.

Brightman MW, Reese TS (1969). Junctions between intimately apposed cell membranes in the vertebrate brain. J Cell Biol **40**(3):648–677.

Brown RC, Egleton RD, Davis TP (2004). Mannitol opening of the blood-brain barrier: regional variation in the permeability of sucrose, but not 86Rb+ or albumin. Brain Res **1014**(1-2):221–227.

Brown RC, Davis TP (2005) Hypoxia/aglycemia alters expression of occludin and actin in brain endothelial cells. Biochem Biophys Res Commun **327**(4):1114–1123.

Bungay PM, Morrison PF, Dedrick RL (1990). Steady-state theory for quantitative microdialysis of solutes and water in vivo and in vitro. Life Sciences **46**(2):105-119.

Bungay PM, Newton-Vinson P, Isele W, Garris PA, Justice JB (2003). Microdialysis of dopamine interpreted with quantitative model incorporating probe implantation trauma. J Neurochem **86**(4):932–946.

Burmeister JJ, Gerhardt GA (2001). Self-referencing ceramic-based multisite microelectrodes for the detection and elimination of interferences from the measurement of L-glutamate and other analytes. Anal Chem **73**(5):1037-1042.

Cardoso FL, Brites D, Brito MA (2010). Looking at the blood-brain barrier: molecular anatomy and possible investigation approaches. Brain Res Rev **64**(2):328-363.

Carvey PM, Hendey B, Monahan AJ (2009). The bool-brain barrier in neurodegenerative disease: a rhetorical perspective. J Neurochem **111**(2):291-314.

Chakravarty S, Herkenham M (2005). Toll-like receptor 4 on nonhematopoietic cells sustains CNS inflammation during endotoxemia, independent of systemic cytokines. J Neurosci **25**(7):1788-1796.

Chefer VI, Thompson AC, Zapata A, Shippenberg TS (2009). Overview of brain microdialysis. Curr Protoc Neurosci **7**(7.1):1-34.

Chernoff AE, Granowitz EV, Shapiro L, Vannier E, Lonnemann G, Angel JB et al., (1995). A randomized, controlled trial of IL-10 in humans. Inhibition of inflammatory cytokine production and immune responses. J Immunol **154**(10):5492–5499.

Citi S, Sabanay H, Kendrick-Jones J, Geiger B (1989). Cingulin: characterization and localization. J Cell Sci **93**(Pt 1):107–122.

Clapp-Lilly KL, Roberts RC, Duffy LK, Irons KP, Hu Y, Drew KL (1999). An ultrastructural analysis of tissue surrounding a microdialysis probe. J Neurosci Methods **90**(2): 129-142.

Conti P, Kempuraj D, Kandere K, Di Gioacchino M, Barbacane RC, Castellani ML, et al., (2003). IL-10, an inflammatory/inhibitory cytokine, but not always. Immunol Lett **86**(2):123–129.

Dahlin AP, Hjort K, Hillered L, Sjödin MOD, Bergquist J, Wetterhall M (2012). Multiplexed quantification of proteins adsorbed to surface-modified and non-modified microdialysis membranes. Anal Bioanal Chem **402**(6):2057–2067.

Dallasta LM, Pisarov LA, Esplen JE, Werley JV, Moses AV, Nelson JA et al., (1999). Blood-brain barrier tight junction disruption in human immunodeficiency virus-1 encephalitis. Am J Pathol **155**(6):1915-1927.

de Boer AG, Gaillard PJ (2006). Blood-brain barrier dysfunction and recovery. J Neural Transm **113**(4):455-462.

de Lange EC, Danhof M, Zurcher C, De Boer AG, Breimer DD (1995). Repeated microdialysis perfusions: periprobe tissue reactions and BBB permeability. Brain Res **702**(1-2):261–265.

de Lange EC, Danhof M, de Boer AG, Breimer DD (1997). Methodological considerations of intracerebral microdialysis in pharmacokinetic studies on drug transport across the blood-brain barrier. Brain Res Brain Res Rev **25**(1):27-49.

de Robertis E, Gerschenfeld HM (1961). Submicroscopic morphology and function of glial cells. Int Rev Neurobiol **3:**1–65.

Dejana E, Lampugnani MG, Martinez-Estrada O, and Bazzoni G (2000). The molecular organization of endothelial junctions and their functional role in vascular morphogenesis and permeability. Int J Dev Biol **44**(6):743–748.

Del Maschio A, De Luigi A, Martin-Padura I, Brockhaus M, Bartfai T, Fruscella P, et al. (1999). Leukocyte recruitment in the cerebrospinal fluid of mice with experimental meningitis is inhibited by an antibody to junctional adhesion molecule (JAM). J Exp Med **190**(9):1351–1356.

Dohgu S, Fleegal-DeMotta MA, Banks WA (2011). Lipopolysaccharide-enhanced transcellular transport of HIV-1 across the blood-brain barrier is mediated by luminal microvessel IL-6 and GM-CSF. J Neuroinflammation **8**:167.

Dore-Duffy P (2008). Pericytes: pluripotent cells of the blood brain barrier. Curr Pharm Des **14**(16):1581-1593.

Ehrlich P (1885). Das sauerstufbudurfnis des organismus, in Eine Farbenanalytische Studie, Hirschwald, Berlin.

Ehrlich P (1904). Ueber die beziehungen von chemischer constitution, verteilung und pharmakologischer wirkung, in Gesammelte Arbeiten zur Immunitaetsforschung, pp 574, Hirschwald, Berlin.

Ellmerer M, Schaupp L, Sendlhofer G, Wutte A, Brunner GA, Trajanoski Z, et al. (1998) Lactate metabolism of subcutaneous adipose tissue studied by open flow microperfusion. J Clin Endocrinol Metab **83**(12):4394–4401.

Erickson MA, Banks WA (2011). Cytokine and chemokine responses in serum and brain after single and repeated injections of lipopolysaccharide: multiplex quantification with path analysis. Brain Behav Immun **25**(8):1637-1648.

Fannin RD, Auman JT, Bruno ME, Sieber SO, Ward SM, Tucker CJ (2005). Differential gene expression profiling in whole blood during acute systemic inflammation in lipopolysaccharide-treated rats. Physiol Genomics **21**(1):92-104.

Fanning AS, Jameson BJ, Jesaitis LA, Anderson JM (1998). The tight junction protein ZO-1 establishes a link between the transmembrane protein occludin and the actin cytoskeleton. J Biol Chem **273**(45):29745–29753.

Farkas E, Luiten PG (2001). Cerebral microvascular pathology in aging and Alzheimer's disease. Prog Neurobiol **64**(6):575–611.

Fenstermacher J, Gross P, Sposito N, Acuff V, Pettersen S, and Gruber K (1988). Structural and functional variations in capillary systems within the brain. Ann NY Acad Sci **529:**21–30.

Fiacco TA, Agulhon C, McCarthy KD (2009). Sorting out astrocyte physiology from pharmacology. Annu Rev Pharmacol Toxicol **49**:151-174.

Fischer S, Wobben M, Marti HH, Renz D, Schaper W (2002). Hypoxia-induced

hyperpermeability in brain microvessel endothelial cells involves VEGF-mediated changes in the expression of zonula occludens-1. Microvasc Res **63**(1):70–80.

Fitch MT, Doller C, Combs CK, Landreth GE, Silver J (1999). Cellular and molecular mechanisms of glial scarring and progressive cavitation: in vivo and in vitro analysis of inflammation-induced secondary injury after CNS trauma. J Neurosci **19**(19):8182-8198.

Frank-Cannon TC, Alto LT, McAlpine FE, Tansey MG (2009). Does neuroinflammation fan the flame in neurodegenerative diseases? Mol Neurodegener **4**:47.

Fricker G, Miller DS (2004). Modulation of drug transporters at the blood–brain barrier. Pharmacology **70**(4): 169–176.

Friedemann U (1942). Blood-brain barrier. Physiol Rev **22:**125–145.

Fromm, M.F (2003). Importance of P-glycoprotein for drug disposition in humans. Eur J Clin Invest **33** (Suppl. 2): 6–9.

Fromm MF (2004). Importance of P-glycoprotein at blood–tissue barriers. Trends Pharmacol Sci **25**(8): 423–429.

Furuse M, Fujita K, Hiiragi T, Fujimoto K, Tsukita S (1998). Claudin-1 and -2: novel integral membrane proteins localizing at tight junctions with no sequence similarity to occludin. J Cell Biol **141**(7):1539–1550.

Furuse M, Sasaki H, Tsukita S (1999). Manner of interaction of heterogeneous claudin species within and between tight junction strands. J Cell Biol **147**(4):891–903.

Gadient RA, Otten UH (1997). Interleukin-6 (IL-6)–a molecule with both beneficial and destructive potentials. Prog Neurobiol **52**(5):379–390.

Gao B, Meier PJ (2001). Organic anion transport across the choroid plexus. Microsc Res Tech **52**(1): 60–64.

Ghezzi P, Sacco S, Agnello D, Marullo A, Caselli G, Bertini R (2000). Lps induces IL-6 in the brain and in serum largely through TNF production. Cytokine **12**(8):1205-1210.

Godbout JP, Johnson RW (2004). Interleukin-6 in the aging brain. J Neuroimmunol **147**(1-2):141-4.

Goldmann EE (1913). Vitalfarbung am zentralnervensystem. Abhandl Konigl preuss Akad Wiss **1:**1–60.

Gonzalez-Mariscal L, Betanzos A, Avila-Flores A (2000). MAGUK proteins: structure and role in the tight junction. Semin Cell Dev Biol **11**(4):315–324.

Grabb MC, Sciotti VM, Gidday JM, Cohen SA, Van Wylen DG (1998). Neurochemical and morphological responses to acutely and chronically implanted brain microdialysis probes. J Neurosci Methods 82(1):25-34.

Groothuis DR, Ward S, Schlageter KE, Itskovich a C, Schwerin SC, Allen CV, et al. (1998). Changes in blood-brain barrier permeability associated with insertion of brain cannulas and microdialysis probes. Brain Res **803**(1-2):218–230.

Gumbiner B, Lowenkopf T, Apatira D (1991). Identification of a 160-kDa polypeptide that binds to the tight junction protein ZO-1. Proc Natl Acad Sci USA **88**(8):3460–3464.

Hagenbuch B, Meier PJ (2004). Organic anion transporting polypeptides of the OATP/SLC21 family: phylogenetic classification as OATP/SLCO superfamily, new nomenclature and molecular/functional properties. Pflugers Arch **447**(5): 653–665.

Harden LM, Rummel C, Luheshi GN, Poole S, Gerstberger R, Roth J (2013). Interleukin-10 modulates the synthesis of inflammatory mediators in the sensory circumventricular organs: implications for the regulation of fever and sickness behaviors. J Neuroinflammation **10**:22.

Harris JP, Capadona JR, Miller RH, Healy BC, Shanmuganathan K, Rowan SJ et al. (2011). Mechanically adaptive intracortical implants improve the proximity of neuronal cell bodies. J Neural Eng **8**(6):066011.

Hascup ER, af Bjerkèn S, Hascup KN, Pomerleau F, Huettl P, Strömberg I et al. (2009). Histological studies of the effects of chronic implantation of ceramic-based microelectrode arrays and microdialysis probes in rat prefrontal cortex. Brain Res **1291**:12-20.

Hatzfeld M (2005). The p120 family of cell adhesion molecules. Eur J Cell Biol **84**(2-3):205-214.

Hawkins BT, Abbruscato TJ, Egleton RD, Brown RC, Huber JD, Campos CR, et al (2004). Nicotine increases in vivo blood-brain barrier permeability and alters cerebral microvascular tight junction protein distribution. Brain Res **1027**(1-2): 48–58.

Hawkins BT, Davis TP (2005). The blood-brain barrier/neurovascular unit in health and disease. Pharmacol Rev **57**(2): 173-185.

He F, Peng J, Deng XL, Yang LF, Wu LW, Zhang CL., et al. (2011). RhoA and NF-κB are involved in lipopolysaccharide-induced brain microvascular cell line hyperpermeability. Neuroscience **188**:35-47.

Heiskala M, Peterson PA, Yang Y (2001). The roles of claudin superfamily proteins in paracellular transport. Traffic **2**(2):93–98.

Helmy A, Carpenter KL, Hutchison PJ (2007). Microdialysis in the human brain and its potential role in the development and clinical assessment of drugs. Curr Medicinal Chem **14**(14):1525-1537.

Henry CJ, Huang Y, Wynne AM, Godbout JP (2009). Peripheral lipopolysaccharide (LPS) challenge promotes microglial hyperactivity in aged mice that is associated with exaggerated induction of both pro-inflammatory IL-1beta and anti-inflammatory IL-10 cytokines. Brain Behav Immun **23**(3):309-317.

Hillman J, Aneman O, Anderson C, Sjogren F, Saberg C, Mellergard P (2005). A microdialysis technique for routine measurement of macromolecules in the injured human brain. Neurosurgery **56**(6):1264-1268.

Hirase T, Staddon JM, Saitou M, Ando-Akatsuka Y, Itoh M, Furuse M, et al (1997). Occludin as a possible determinant of tight junction permeability in endothelial cells. J Cell Sci **110**(Pt 14):1603–1613.

Holmgaard R, Benfeldt E, Nielsen JB, Gatschelhofer C, Sorensen JA, Höfferer C, et al. (2012). Comparison of open-flow microperfusion and microdialysis methodologies when sampling topically applied fentanyl and benzoic acid in human dermis ex vivo. Pharm Res **29**(7):1808-1820.

Howarth AG, Hughes MR, Stevenson BR (1992). Detection of the tight junction associated protein ZO-1 in astrocytes and other nonepithelial cell types. Am J Physiol **262**(2 Pt 1):C461–C469.

Huber JD, Hau VS, Borg L, Campos CR, Egleton RD, Davis TP (2002). Blood brain barrier tight junctions are altered during a 72-h exposure to lambda-carrageenan-induced inflammatory pain. Am J Physiol Heart Circ Physiol **283**(4): H1531–H1537.

Ihara S, Iwamatsu A, Fujiyoshi T, Komi A, Yamori T, Fukui Y (1996). Identification of interleukin-6 as a factor that induces neurite outgrowth by PC12 cells primed with NGF. J Biochem **120**(5):865–868.

Islas S, Vega J, Ponce L, Gonzalez-Mariscal L (2002) Nuclear localization of the tight junction protein ZO-2 in epithelial cells. Exp Cell Res **274**(1):138–148.

Itoh M, Nagafuchi A, Yonemura S, Kitani-Yasuda T, Tsukita S (1993). The 220-kD protein colocalizing with cadherins in non-epithelial cells is identical to ZO-1, a tight junction-associated protein in epithelial cells: cDNA cloning and immunoelectron microscopy. J Cell Biol **121**(3):491–502.

Jaeger LB, Dohgu S, Sultana R, Lynch JL, Owen JB, Erickson MA, et al. (2009). Lipopolysaccharide alters the blood-brain barrier transport of amyloid beta protein: a mechanism for inflammation in the progression of Alzheimer's disease. Brain Behav Immun **23**(4):507-517.

Jancálek R, Dubový P, Svízenská I, Klusáková I (2010). Bilateral changes of TNF-alpha and IL-10 protein in the lumbar and cervical dorsal root ganglia following a unilateral chronic constriction injury of the sciatic nerve. J Neuroinflammation **7**:11.

Jaquins-Gerstl A, Shu Z, Zhang J, Liu Y, Weber SG, Michael AC (2011). Effect of dexamethasone on gliosis, ischemia, and dopamine extraction during microdialysis sampling in brain tissue. Anal Chem **83**(20):7662-7667.

Jin L, Nation RL, Li J, Nicolazzo JA (2013). Species-Dependent Blood-brain Barrier Disruption of Lipopolysaccharide: Amelioration by Colistin in vitro and in vivo. Antimicrob Agents Chemother **57**(9):4336-4342.

Kahn MA, De Vellis J (1994). Regulation of an oligodendrocyte progenitor cell line by the interleukin-6 family of cytokines. Glia **12**(2):87–98.

Kapural M, Krizanac-Bengez Lj, Barnett G, Perl J, Masaryk T, Apollo D, et al., (2002). Serum S-100beta as a possible marker of blood-brain barrier disruption. Brain Res **940**(1-2):102-104.

Karumbaiah L, Norman SE, Rajan NB, Anand S, Saxena T, Betancur M, et al (2012). The upregulation of specific interleukin (IL) receptor antagonists and paradoxical enhancement of neuronal apoptosis due to electrode induced strain and brain micromotion. Biomaterials **33**(26):5983-5996.

Kawano H, Kimura-Kuroda J, Komuta Y, Yoshioka N, Li HP, Kawamura K et al. (2012). Cell Tissue Res 349(1):169-180.

Kaya M, Ahishali B (2011). Assessment of permeability in barrier type of 1 endothelium in brain using 2 tracers: Evans blue, sodium fluorescein, and horseradish peroxidase. Methods Mol Biol **763**:369–382.

Kendrick KM (1990). Microdialysis measurement of in vivo neuropeptide release. J Neurosci Methods **34**(1-3):35-46.

Kim RB (2003). Organic anion-transporting polypeptide (OATP) transporter family and drug disposition. Eur J Clin Invest **33** (Suppl. 2):1–5.

Kim Y-T, Hitchcock RW, Bridge MJ, Tresco PA (2004). Chronic response of adult rat brain tissue to implants anchored to the skull. Biomaterials 25(12):2229–2237.

Kim KS (2008). Mechanisms of microbial traversal of the blood-brain barrier. Nat Rev Microbiol **6**(8):625-634.

Kniesel U, Wolburg H (2000). Tight junctions of the blood-brain barrier. Cell Mol Neurobiol **20**(1):57–76.

Kojima T, Yamamoto T, Murata M, Chiba H, Kokai Y, and Sawada N (2003). Regulation of the blood-biliary barrier: interaction between gap and tight junctions in hepatocytes. Med Electron Microsc **36**(3):157–164.

Kottegoda S, Shaik I, Shippy SA (2002). Demonstration of low flow push-pull perfusion. J Neurosci Methods **121**(1):93-101.

Kozler P, Pokorný J (2003). Altered blood-brain barrier permeability and its effect on the distribution of Evans blue and sodium fluorescein in the rat brain applied by intracarotid injection. Physiological Research **52**(5):607–614.

König K, Rickels E, Heissler HE, Zumkeller M, Samii M (2001). Artificial elevation of brain tissue glycerol by administration of a glycerol-containing agent. Case report. J Neurosurg **94**(4):621-623.

Kubota K, Furuse M, Sasaki H, Sonoda N, Fujita K, Nagafuchi A, Tsukita S (1999). Ca(2^+)-independent cell-adhesion activity of claudins, a family of integral membrane proteins localized at tight junctions. Curr Biol **9**(18):1035–1038.

Lee G, Dallas S, Hong M, Bendayan R (2001). Drug transporters in the central nervous system: brain barriers and brain parenchyma considerations. Pharmacol Rev **53**(4): 569–596.

Lee JW, Lee YK, Yuk DY, Choi DY, Ban SB, Oh KW et al. (2008) Neuro-inflammation induced by lipopolysaccharide causes cognitive impairment through enhancement of beta-amyloid generation. J Neuroinflammation **5**:37.

Lenzsér G, Kis B, Snipes JA, Gáspár T, Sándor P, Komjáti K, et a (2007). Contribution of poly (ADP ribose) polymerase to postischemic blood-brain barrier damage in rats. J Cereb Blood Flow Metab **27**(7):1318–1326.

Lewandowsky M (1900). Zur lehre von der cerebrospinalflussigkeit. Z Klin Med **40:**480–494.

Lin JH (2004). How significant is the role of P-glycoprotein in drug absorption and brain uptake? Drugs Today (Barc.) **40**(1): 5–22.

Lippoldt A, Kniesel U, Liebner S, Kalbacher H, Kirsch T, Wolburg H, et al. (2000). Structural alterations of tight junctions are associated with loss of polarity in stroke-prone spontaneously hypertensive rat blood-brain barrier endothelial cells. Brain Res **885**(2):251–261.

Lopez-Ramirez MA, Fischer R, Torres-Badillo CC, Davies HA, Logan K, Pfizenmaier K et al. (2012). Role of caspases in cytokine-induced barrier breakdown in human brain endothelial cells. J Immunol **189**(6):3130-3139.

Lord R, Goto S, Pan T, Chiang K, Chen C, Sunagawa M (2001). Peak protein expression of IL-2 and IFN-gamma correlate with the peak rejection episode in a spontaneously tolerant model of rat liver transplantation. Cytokine **13**(3):155-161.

Manaenko A, Chen H, Kammer J, Zhang JH, Tang J (2011). Comparison Evans Blue injection routes: Intravenous versus intraperitoneal, for measurement of blood-brain barrier in a mice hemorrhage model. J Neurosci Methods **195**(2):206–210.

Marburger A, Sohr R, Reum T, Morgenstern R (2000). Comparison by microdialysis of striatal L-DOPA after its systemic administration in rats with probes implanted acutely or through a guide cannula. J Neurosci Methods **102**(2):127–132.

Mark KS, Davis TP (2002). Cerebral microvascular changes in permeability and tight junctions induced by hypoxia-reoxygenation. Am J Physiol Heart Circ Physiol **282**(4):H1485–H1494.

Marsland AL, Gianaros PJ, Abramowitch SM, Manuck SB, Hariri AR (2008). Interleukin-6 covaries inversely with hippocampal grey matter volume in middle-aged adults. Biol Psychiatry **64**(6):484–490.

Martin-Padura I, Lostaglio S, Schneemann M, Williams L, Romano M, Fruscella P, Panzeri C, Stoppacciaro A, Ruco L, Villa A, et al. (1998). Junctional adhesion molecule, a novel member of the immunoglobulin superfamily that distributes at intercellular junctions and modulates monocyte transmigration. J Cell Biol **142**(1): 117–127.

Maxwell WL, Follows R, Ashhurst DE, Berry M (1990). The response of the cerebral hemisphere of the rat to injury. I. The mature rat. Philos Trans R Soc Lond B Biol Sci **328**(1250):501-513.

McCarthy PT, Madangopal R, Otto KJ, Rao MP (2009). Titanium-based multi-channel, micro-electrode array for recording neural signals. Conf Proc IEEE Eng Med Biol Soc **2009**:2062-2065.

McQuaid S, Cunnea P, McMahon J, Fitzgerald U (2009). The effects of blood-brain barrier disruption on glial cell function in multiple sclerosis. Biochem Soc Trans **37**(Pt 1):329-331.

Miller G. (2002). Drug targeting. Breaking down barriers. *Science (New York, N.Y.)*, **297**(5584), 1116-1118.

Mitala CM, Wang Y, Borland LM, Jung M, Shand S, Watkins S (2008). Impact of microdialysis probes on vasculature and dopamine in the rat striatum: a combined fluorescence and voltammetric study. J Neurosci Methods **174**(2):177-185.

Moore KW, de Waal Malefyt R, Coffman RL, O'Garra A (2001). Interleukin-10 and the interleukin-10 receptor. Annu Rev Immunol **19**:683–765.

Morcos Y, Hosie MJ, Bauer HC, Chan-Ling T (2001). Immunolocalization of occludin and claudin-1 to tight junctions in intact CNS vessels of mammalian retina. J Neurocytol **30**(2):107–123.

Morgan ME, Singhal D, Anderson BD (1996). Quantitative assessment of blood-brain barrier damage during microdialysis. J Pharmacol Exp Ther **277**(2):1167–1176.

Murphy M, Dutton R, Koblar S, Cheema S, Bartlett P (1997). Cytokines which signal through the LIF receptor and their actions in the nervous system. Prog Neurobiol **52**(5):355–378.

Myres RD (1986). Development of push-pull systems for perfusion of anatomically distinct regions of the brain of the awake animal. Ann N Y Acad Sci **473**:21-41.

Nagafuchi A (2001). A molecular architecture of adherens junctions. Curr Opin Cell Biol **13**(5):600-603.

Nishioku T, Matsumoto J, Dohgu S, Sumi N, Miyao K, Takata F et al. (2010). Tumour necrosis factor-alpha mediates the blood-brain barrier dysfunction induced by activated microglia in mouse brain microvascular endothelial cells. J Pharmacol Sci **112**(2):251-254.

Nitta T, Hata M, Gotoh S, Seo Y, Sasaki H, Hashimoto N, et al. (2003). Size-selective loosening of the blood-brain barrier in claudin-5-deficient mice. J Cell Biol **161**(3):653–660.

Nonaka N, Hileman SM, Shioda S, Vo TQ, Banks WA (2004). Effects of lipopolysaccharide on leptin transport across the blood-brain barrier. Brain Res **1016**(1):58-65.

O'Callaghan JP, Sriram K, Miller DB (2008). Defining Neuroinflammation. Ann N Y Acad Sci. **1139**:318-330.

Oldendorf WH, Cornford ME, and Brown WJ (1977). The large apparent work capability of the blood-brain barrier: a study of the mitochondrial content of capillary endothelial cells in brain and other tissues of the rat. Ann Neurol **1**(5):409–417.

Osburg B, Peiser C, Dömling D, Schomburg L, Ko YT, Voigt K (2002). Effect of endotoxin on expression of TNF receptors and transport of TNF-alpha at the blood-brain barrier of the rat. Am J Physiol Endocrinol Metab **283**(5):E899-908.

Pan W, Kastin AJ (2001). Upregulation of the transport system for TNFalpha at the blood-brain barrier. Arch Physiol Biochem **109**(4):350-353.

Pardridge WM (2005). The blood-brain barrier and neurotherapeutics. NeuroRx **2**(1):1–2.

Persidsky Y, Ramirez SH, Haorah J, Kanmogne GD (2006). Blood-brain barrier: structural components and function under physiologic and pathologic conditions. J Neuroimmune Pharmacol **1**(3):223-236.

Polikov VS, Tresco PA, Reichert WM (2005). Response of brain tissue to chronically implanted neural electrodes. J Neurosci Methods **148**(1):1-18.

Qin L, Wu X, Block ML, Liu Y, Breese GR, Hong JS, et al (2007). Systemic LPS causes chronic neuroinflammation and progressive neurodegeneration. Glia **55**(5):453-462.

Reese TS, Karnovsky MJ (1967). Fine structural localization of a blood-brain barrier to exogenous peroxidase. J Cell Biol **34**(1):207–217.

Reyes TM, Fabry Z, Coe CL (1999). Brain endothelial cell production of a neuroprotective cytokine, interleukin-6, in response to noxious stimuli. Brain Res **851**(1-2):215–220.

Riese J, Boecker S, Hohenberger W, Klein P, Haupt W (2003). Microdialysis: a new technique to monitor perioperative human peritoneal mediator production. Surg Infect (Larchmt) **4**:11-15.

Rosenberg GA, Estrada E, Kelley RO, Kornfeld M (1993). Bacterial collagenase disrupts extracellular matrix and opens blood-brain barrier in rat. Neurosci Lett **160**(1):117-119.

Rosenberg GA (2002). Matrix metalloproteinases in neuroinflammation. Glia **39**:279-291.

Rosenbloom AJ, Sipe DM, Weedn VW (2005). Microdialysis of proteins: performance of the CMA/20 13 probe. J Neurosci Methods **148**(2):147–153.

Rosenbloom AJ, Ferris R, Sipe DM, Riddler SA, Connolly NC, Abe K, et al (2006). In vitro and in vivo 10 protein sampling by combined microdialysis and ultrafiltration. J Immunol. Methods **309**(1-2):55–68.

Sawada M, Suzumura A, Hosoya H, Marunouchi T, Nagatsu T (1999). Interleukin-10 inhibits both production of cytokines and expression of cytokine receptors in microglia. J Neurochem **72**(4):1466–1471.

Schachtrup C, Ryu JK, Helmrick MJ, Vagena E, Galanakis DK, Degen JL et al. (2010). Fibrinogen triggers astrocyte scar formation by promoting the availability of active TGF-beta after vascular damage. J Neurosci **30**(17):5843-5854.

Schaupp L, Ellmerer M, Brunner GA, Wutte A, Sendlhofer G, Trajanoski Z, et al. (1999). Direct access to interstitial fluid in adipose tissue in humans by use of open-flow microperfusion. Am J Physiol **276**(2 Pt 1): E401-E408.

Schreibelt G, Kooij G, Reijerkerk A, van Doorn R, Gringhuis SI, van der Pol S., et al. (2007). Reactive oxygen species alter brain endothelial tight junction dynamics via RhoA, PI3 kinase, and PKB signaling. FASEB J **21**(13):3666-3676.

Schulze C, Firth J (1993). A immunohistochemical localization of adherens junction components in blood-brain barrier microvessels of the rat. J Cell Sci **104**(Pt 3)**:**773–782.

Scopelliti PE, Borgonovo A, Indrieri M, Giorgetti L, Bongiorno G, Carbone R, et al. (2010). The effect of surface nanometre-scale morphology on protein adsorption. PLoS One **5**:e11862.

Sedlakova R, Shivers RR, and Del Maestro RF (1999). Ultrastructure of the bloodbrain barrier in the rabbit. J Submicrosc Cytol Pathol **31**(1):149–161.

Semmler A, Hermann S, Mormann F, Weberpals M, Paxian SA, Okulla T et al. (2005). Sepsis causes neuroinflammation and concomitant decrease of cerebral metabolism. J Neuroinflammation **5**:38.

Seymour JP, Kipke DR (2007). Neural probe design for reduced tissue encapsulation in CNS. Biomaterials **28**(25):3594-3607.

Shain W, Spataro L, Dilgen J, Haverstick K, Retterer S, Isaacson M, et al. (2003). Controlling cellular reactive responses around neural prosthetic devices using peripheral and local intervention strategies. IEEE Trans Neural Syst Rehabil Eng **11**(2):186-188.

Shin H, Hsueh YP, Yang FC, Kim E, Sheng M (2000). An intramolecular interaction between Src homology 3 domain and guanylate kinase-like domain required for channel clustering by postsynaptic density-95/SAP90. J Neurosci **20**(10):3580–3587.

Simard M, Arcuino G, Takano T, Liu QS, and Nedergaard M (2003). Signaling at the

gliovascular interface. J Neurosci **23**(27):9254–9262.

Singh AK, Jiang Y (2004). How does peripheral lipopolysaccharide induce gene expression in the brain of rats? Toxicology **201**(1-3):197-207.

Sjogren F, Svensson C, Anderson C (2002). Technical prerequisites for in vivo microdialysis determination of interleukin-6 in human dermis. Br J Dermatol **146**(3):375-382.

Sopasakis VR, Sandqvist M, Gustafson B, Hammarstedt A, Schmelz M, Yang X, et al., (2004). High local concentrations and effects on differentiation implicate interleukin-6 as a paracrine regulator. Obes Res **12**(3):454-460.

Spataro L, Dilgen J, Retterer S, Spence AJ, Isaacson M, Turner JN, et al. (2005). Dexamethasone treatment reduces astroglia responses to inserted neuroprosthetic devices in rat neocortex. Exp Neurol **194**(2):289-300.

Stahl M, Bouw R, Jackson A, Pay V (2002). Human microdialysis. Curr Pharmaceutical Biotechnol 3(2):165-178.

Stamatovic SM, Keep RF, Andjelkovic AV (2008). Brain endothelial cell-cell junctions: how to 'open' the blood brain barrier. Curr Neuropharmacol **6**(3):179-192.

Steiner AA, Chakravarty S, Rudaya AY, Herkenham M, Romanovsky AA (2006). Bacterial lipopolysaccharide fever is initiated via Toll-like receptor 4 on hematopoietic cells. Blood **107**(10):4000-4002.

Stenken JA, Church MK, Gill CA, Clough GF (2010). How minimally invasive is microdialysis sampling ? A cautionary note for cytokine collection in human skin and other clinical studies. AAPS J **12**(1):73-78.

Stensaas SS, Stensaas LJ (1978). Histopathological evaluation of materials implanted in the cerebral cortex. Acta Neuropathol **41**(2):145-155.

Stevenson BR, Siliciano JD, Mooseker MS, Goodenough DA (1986) Identification of ZO-1: a high molecular weight polypeptide associated with the tight junction (zonula occludens) in a variety of epithelia. J Cell Biol **103**(3):755–766.

Stice P, Gilletti A, Panitch A, Muthuswamy J (2007). Thin microelectrodes reduce GFAP expression in the implant site in rodent somatosensory cortex. J Neural Eng **4**(2):42-53.

Sun H, Dai, H, Shaik N, Elmquist WF (2003). Drug efflux transporters in the CNS. Adv Drug Deliv Rev **55**(1):83–105.

Szarowski DH, Andersen MD, Retterer S, Spence AJ, Isaacson M, Craighead HG et al (2003). Brain responses to micro-machined silicon devices. Brain Res **983**(1-2):23-35.

Takeda S, Sato N, Ikimura K, Nishino H, Rakugi H, Morishita R (2011). Novel microdialysis method to assess neuropeptides and large molecules in free-moving mouse. Neuroscience **186**:110-119.

Tagami M, Nara Y, Kubota A, Fujino H, and Yamori Y (1990). Ultrastructural changes in cerebral pericytes and astrocytes of stroke-prone spontaneously hypertensive rats. Stroke **21**(7):1064–1071.

Tao-Cheng JH, Nagy Z, Brightman MW (1987). Tight junctions of brain endothelium in vitro are enhanced by astroglia. J Neurosci **7**(10):3293–3299.

Thelin J, Jörntell H, Psouni E, Garwicz M, Schouenborg J, Danielsen N et al. (2011). Implant size and fixation mode strongly influence tissue reactions in the CNS. PLoS One **6**(1):e16267.

Toulmond S, Vige X, Fage D, Benavides J (1992). Local infusion of interleukin-6 attenuates the neurotoxic effects of NMDA on rat striatal cholinergic neurons. Neurosci Lett **144**(1-2):49–52.

Toyofuku T, Yabuki M, Otsu K, Kuzuya T, Hori M, Tada M (1998). Direct association of the gap junction protein connexin-43 with ZO-1 in cardiac myocytes. J Biol Chem **273**(21):12725–12731.

Trajanoski Z, Brunner GA, Schaupp L, Ellmerer M, Wach P, Pieber TR, et al. (1997). Open-flow microperfusion of subcutaneous adipose tissue for on-line continuous ex vivo measurement of glucose concentration. Diabetes Care **20**(7):1114–1121.

Traweger A, Fuchs R, Krizbai IA, Weiger TM, Bauer HC, Bauer H (2002). The tight junction protein ZO-2 localizes to the nucleus and interacts with the heterogeneous nuclear ribonucleoprotein scaffold attachment factor-B. J Biol Chem **278**(4):2692–2700.

Tsao N, Hsu HP, Wu CM, Liu CC, Lei HY (2001). Tumour necrosis factor-alpha causes an increase in blood-brain barrier permeability during sepsis. J Med Microbiol **50**(9): 812-821.

Tschirgi RD (1962). Blood-brain barrier: fact or fancy? Fed Proc **21:**665–671.

Turner JN, Shain W, Szarowski DH, Andersen M, Martins S, Isaacson M et al. (1999). Cerebral astrocyte response to micromachined silicon implants. Exp Neurol **156**(1):33-49.
Upton RN (2007). Cerebral uptake of drugs in humans. Clin Exp Pharmacol Physiol **34**(8):695–701.

Üllen A, Singewald E, Konya V, Fauler G, Reicher H, Nusshold C., et al. (2013). Myeloperoxidase-derived oxidants induce blood-brain barrier dysfunction in vitro and in vivo. PLoS One **8**(5):e64034.

Verma S, Nakaoke R, Dohgu S, Banks WA (2006). Release of cytokines by brain endothelial cells: a polarized response to lipopolysaccharide. Brain Behav Immun **20**(5):449–455.

Von Grote EC, Venkatakrishnan V, Duo J, Stenken JA (2011). Long-term subcutaneous microdialysis sampling and qRT-PCR of MCP-1, IL-6 and IL-10 in freely moving rats. Mol Biosyst **7**(1):150-161.

Vorbrodt AW, Dobrogowska DH (2003). Molecular anatomy of intercellular junctions in brain endothelial and epithelial barriers: electron microscopist's view. Brain Res Brain Res Rev **42**(3):221–242.

Wang M, Etu J, Joshi S (2007). Enhanced disruption of the blood 1 brain barrier by intracarotid mannitol injection during transient cerebral hypoperfusion in rabbits. J Neurosurg Anesthesiol **19**(4):249–256.

Wang X, Lennartz MR, Loegering DJ, Stenken JA (2008). Multiplexed cytokine detection of interstitial fluid collected from polymeric hollow tube implants—a feasibility study. Cytokine **43**(1):15-19.

Watkins LR, Maier SF, Goehler LE (1995). Cytokine-to-brain communication: a review & analysis of alternative mechanisms. Life Sci **57**(11):1011–1026.

Weiss N, Miller F, Cazaubon S, Couraud PO (2009). The blood-brain barrier in brain homeostasis and neurological diseases. Biochim Biophys Acta **1788**(4):842-857.

Weksler BB, Subileau EA, Perrière N, Charneau P, Holloway K, Leveque M et al. (2005). Blood-brain barrier specific properties of a human adult brain endothelial cell line. FASEB J **19**(13):1872-1874.

Westergren I, Nyström B, Hamberger A, Johansson BB (1995). Intracerebral dialysis and the blood brain barrier. J Neurochem **64**(1):229–234.

Winslow BD, Tresco PA (2010). Quantitative analysis of the tissue response to chronically implanted microwire electrodes in rat cortex. Biomaterials **31**(7):1558-1567.

Winter CD, Iannotti F, Pringle AK, Trikkas C, Clough GF, Church MK (2002). A microdialysis method for the recovery of IL-1beta, IL-6 and nerve growth factor from human brain in vivo. J Neurosci Methods **119**(1):45-50.

Wisniewski N, Klitzman B, Miller B, Reichert WM (2001). Decreased analyte transport through implanted membranes: differentiation of biofouling from tissue effects. J Biomed Mater Res **57**(4):513-521.

Witt KA, Mark KS, Hom S, Davis TP (2003). Effects of hypoxia-reoxygenation on rat blood-brain barrier permeability and tight junctional protein expression. Am J Physiol Heart Circ Physiol **285**(6):H2820–H2831.

Wolburg H, Lippoldt A (2002). Tight junctions of the blood-brain barrier: development, composition and regulation. Vascul Pharmacol **38**(6):323–337.

Wolburg H, Wolburg-Buchholz K, Kraus J, Rascher-Eggstein G, Liebner S, Hamm S, et al. (2003). Localization of claudin-3 in tight junctions of the blood-brain barrier is selectively lost during experimental autoimmune encephalomyelitis and human glioblastoma multiforme. Acta Neuropathol **105**(6):586–592.

Wolburg H, Noell S, Mack A, Wolburg-Buchholz K, Fallier-Becker P (2009). Brain endothelial cells and the glio-vascular complex. Cell Tissue Res **335**(1):75-96.

Wu YY, Bradshaw RA (1996). Induction of neurite outgrowth by interleukin-6 is accompanied by activation of Stat3 signaling pathway in a variant PC12 cell (E2) line. J Biol Chem **271**(22):13023–13032.

Wu Z, Zhang J, Nakanishi H (2005). Leptomeningeal cells activate microglia and astrocytes to induce IL-10 production by releasing pro-inflammatory cytokines during systemic inflammation. J Neuroimmunol **167**(1-2): 90-98.

Xaio H, Banks WA, Niehoff ML, Morley JE (2001). Effect of LPS on the permeability of the blood-brain barrier to insulin. Brain Res **896**(1-2):36-42.

Yamada M, Hatanaka H (1994). Interleukin-6 protects cultured rat hippocampal neurons against glutamate-induced cell death. Brain Res **643**(1-2):173–180.

Yamagata K, Tagami M, Nara Y, Mitani M, Kubota A, Fujino H et al. (1997). Astrocyte-conditioned medium induces blood-brain barrier properties in endothelial cells. Clin Exp Pharmacol Physiol **24**(9-10):710-713.

Zehendner CM, Librizzi L, de Curtis M, Kuhlmann CR, Luhmann HJ (2011). Caspase-3 contributes to ZO-1 and Cl-5 tight-junction disruption in rapid anoxic neurovascular unit damage. PLoS ONE **6**(2):e16760.

Zhao C, Ling Z, Newman MB, Bhatia A, Carvey PM (2007). TNF-alpha knockout and minocycline treatment attenuates blood-brain barrier leakage in MPTP-treated mice. Neurobiol Dis **26**(1): 36-46.

Zheng W, Aschner M, Ghersi-Egea JF (2003). Brain barrier systems: a new frontier in metal neurotoxicological research. Toxicol Appl Pharmacol **192**(1):1-11.

Zhong Y, Enomoto K, Tobioka H, Konishi Y, Satoh M, Mori M (1994). Sequential decrease in tight junctions as revealed by 7H6 tight junction-associated protein during rat hepatocarcinogenesis. Jpn J Cancer Res **85**(4):351–356.

Zhong Y, Bellamkonda RV (2007). Dexamethasone-coated neural probes elicit attenuated inflammatory response and neuronal loss compared to uncoated neural probes. Brain Res **1148**:15-27.

Zlokovic BV (2008). The blood-brain barrier in health and chronic neurodegenerative disorders. Neuron **57**(2):178-201.

Appendix

Publications

Research articles:

Birngruber T*, **Ghosh A***, Perez-Yarza V, Kroath T, Ratzer M, Pieber TR, Sinner F (2013). Cerebral open flow microperfusion: A new *in vivo* technique for continuous measurement of substance transport across the intact blood-brain barrier. Clin Exp Pharmacol Physiol **40**(12):864-871. [* *Equal contribution*].

Birngruber T*, **Ghosh A***, Hochmeister S, Asslaber M, Kroath T, Pieber TR, Sinner F (2013). Long-term implantation of cOFM probe causes minimal tissue reaction in the brain. PLoS One (In press). [* *Equal contribution*].

Ghosh A, Birngruber T, Sattler W, Sinner F, Pieber TR (2013). Functional assessment of blood-brain barrier integrity and neuroinflammatory response using cerebral Open Flow Microperfusion (cOFM) [Communicated].

Abstracts published / Poster Presentations:

Ghosh A, Birngruber T, Sinner F, Pieber TR. cOFM: a histological study. 100th Indian Science Congress, January 3 – 7, 2013, Kolkata, India [Invited Oral Presentation].

Birngruber T, **Ghosh A**, Hochmeister S, Kroath T, Pieber TR, Sinner F. cOFM for cerebral monitoring causes no significant brain tissue reaction. 7th Microdialysis Symposium 2013 - Inserm - Université de Poitiers [Poster].

Birngruber T, **Ghosh A**, Perez-Yarza VA, Kroath T, Ratzer M, Pieber TR, Sinner F. cOFM: a novel in-vivo technique to continuously measure substance transport across the intact blood-brain barrier. Gordon Research Conference, Barriers of the CNS, June 16-17, 2012 Colby-Sawyer College, New London, NH, USA [Poster].

Ghosh A, Birngruber T, Sinner F, Pieber TR. cOFM: a novel technique to explore extracellular milieu in brain. 99th Indian Science Congress, January 3 – 7, 2012, Bhubaneswar, India [Oral Presentation].

Birngruber T, **Ghosh A**, Perez-Yarza VA, Kroath T, Ratzer M, Pieber TR, Sinner F. cerebral Open-Flow Microperfusion (cOFM) an innovation in drug testing in-vivo. Conference on Cerebral Vascular Biology, 21 – 25 June, 2011, Leiden, the Netherlands [Poster].

Birngruber T**, Ghosh A**, Perez-Yarza VA, Kroath T, Ratzer M, Pieber TR, Sinner F. cerebral Open-Flow Microperfusion (cOFM) eine innovative Methode zur Messung des Substanztransports über die BBB. Herrenalber Transport Tage, 30.5. – 1.6.2011, Bad Herrenalb, Germany.